UNIWERSYTET ŚLĄSKI
W KATOWICACH

Instytut Fizyki
im. Augusta Chełkowskiego

ZAKŁAD BIOFIZYKI I FIZYKI MOLEKULARNEJ

PRACA DOKTORSKA:

Metody poprawy fizycznej stabilności amorficznej formy ezetimibu

mgr inż. Justyna Knapik

PROMOTOR PRACY:
Prof. zw. dr hab. Marian Paluch

PROMOTOR POMOCNICZY PRACY:
Dr Katarzyna Grzybowska

KATOWICE 2016

Serdecznie dziękuję mojemu Promotorowi Profesorowi Marianowi Paluchowi za poświęcony czas na niezwykle interesujące oraz inspirujące dyskusję, które zaszczepiły we mnie pasję do nauki oraz motywowały do ciągłego rozwijania i pogłębiania wiedzy.

Dziękuję Promotorowi pomocniczemu Doktor Katarzynie Grzybowskiej za życzliwość i cenne uwagi.

Chciałabym również podziękować moim Koleżankom i Kolegom z laboratorium dielektrycznego, w szczególności Dr Żanecie Wojnarowskiej, za wsparcie, miłą atmosferę pracy, owocne dyskusje oraz czas, który mi poświęcili.

SPIS TREŚCI

1 WSTĘP

Jak podaje Światowa Organizacja Zdrowia (WHO, ang. *World Health Organization*) choroby układu krążenia są obecnie najczęstszą przyczyną zgonów na świecie[1]. Ponieważ powodem większości z nich jest zwężanie się światła tętnic wywołane nagromadzeniem lipoprotein, głównie frakcji LDL (ang. *low-density lipoprotein*), w błonie wewnętrznej naczyń krwionośnych, bardzo istotne wydaje się poszukiwanie nowych lub ulepszanie już istniejących leków obniżających poziom LDL, czyli „złego" cholesterolu, we krwi[2,3]. Jednym z leków nowej generacji na wspomniane dolegliwości jest ezetimib (EZB)[4]. Lek ten gromadzi się w enterocytach oraz hepatocytach, gdzie blokuje wchłanianie cholesterolu LDL poprzez wiązanie go z białkiem NPC1L1 (*Niemann-Pick C1 like 1*)[5]. W rezultacie mniej cholesterolu przedostaje się do krwioobiegu, obniżając prawdopodobieństwo wystąpienia zawału lub udaru. Dzięki swojemu działaniu, bez wątpienia ezetimib można zakwalifikować do grupy bardzo istotnych farmaceutycznie substancji. Należy jednak podkreślić, że lek ten charakteryzuje się wyjątkowo niską rozpuszczalnością w wodzie (84 mg/l)[6]. Słaba rozpuszczalność ezetimibu w wodzie wpływa na jego niską dostępność biologiczną równą 35%[7]. Aby więc poprawić efektywność działania ezetimibu, czyli innymi słowy zwiększyć jego biodostępność, należy poprawić jego rozpuszczalność w wodzie.

Najnowsze doniesienia naukowe wskazują, że jedną z efektywniejszych metod poprawy rozpuszczalności, niemal nierozpuszczalnych w wodnie leków, jest ich amorfizacja[8,9,10,11]. Metoda ta polega na wytworzeniu materiału, który w przeciwieństwie do swojego krystalicznego odpowiednika, nie posiada daleko zasięgowego uporządkowania[12]. Brak uporządkowania sprawia, że substancja amorficzna charakteryzuje się wyższą energią swobodną Gibbsa od swojego krystalicznego odpowiednika, co bezpośrednio wpływa na jej lepszą rozpuszczalność, a tym samym i wyższą biodostępność. W przypadku materiału nieposiadającego dalekozasięgowego uporządkowania lepszą rozpuszczalność uzyskuje się jednak kosztem obniżenia jego fizycznej stabilności[13]. Nadmiar energii, który z jednej strony jest zaleta sprawia, że amorficzny układ jest termodynamicznie niestabilny. Bezpostaciowy materiał dążąc do oddania nadmiaru energii i osiągnięcia najniższego stanu energetycznego, prędzej lub później powraca do swojej krystalicznej formy, tracąc jednocześnie korzystne własności wynikające z nieuporządkowania[14,15,16]. Fakt ten wyjaśnia, dlaczego farmaceutyki w formie amorficznej są o wiele mniej powszechne na rynku w porównaniu do swoich krystalicznych odpowiedników charakteryzujących się gorszą biodostępnością. Zrozumiałe jest, że dla dobra pacjentów amorficzne materiały muszą przejść dodatkowe testy związane z

badaniem ich fizycznej stabilności[17]. Minimalny czas fizycznej stabilności, jaki jest wymagany od substancji leczniczej w formie amorficznej, aby mogła zostać wprowadzona do sprzedaży, wynosi trzy lata.

Zdecydowana większość leków w stanie amorficznym nie spełnia wspomnianego kryterium, dlatego niezwykle istotne wydaje się poszukiwanie jak najodpowiedniejszych metod prowadzących do poprawy ich fizycznej stabilności[18]. W celu znalezienia odpowiedniego rozwiązania warto na początek przyjrzeć się czynnikom, które mogą wpływać na fizyczną stabilność materiałów nieposiadających daleko zasięgowego uporządkowania. Jest ich wiele, m.in. metoda amorfizacji, zawartość wody w próbce, powierzchnia właściwa, entropia konfiguracyjna, obecność zanieczyszczeń, tautomerów czy też dodatkowych związków w układzie[19,20,21,22]. Jednak to ruchliwość molekularna jest aktualnie uznawana za najważniejszy czynnik wpływający na fizyczną stabilność amorficznych materiałów[23,24,25]. Z tej przyczyny najbardziej obiecującymi metodami prowadzącymi do hamowania re-krystalizacji bezpostaciowych farmaceutyków wydają się metody prowadzące do spowolnienia ich dynamiki molekularnej.

Wysoka wartość temperatury przejścia szklistego niektórych polimerów używanych w przemyśle farmaceutycznym spowodowała, że substancji tych zaczęto używać do stabilizacji amorficznych form leków[26]. To właśnie ta grupa materiałów jest obecnie najczęściej stosowana do hamowania re-krystalizacji farmaceutyków w formie amorficznej[27,28,29]. Polimery, które charakteryzują się wysoką wartością przejścia szklistego są w stanie podnieść T_g mieszaniny[30]. Wzrost T_g skutkuje spowolnieniem dynamiki molekularnej leku znajdującego się w mieszaninie, zatem możliwe jest wydłużenie czasu fizycznej stabilności substancji zmieszanej z polimerem. Innym mechanizmem odpowiedzialnym za poprawę fizycznej stabilności amorficznych leków przez polimerowy dodatek może być tworzenie się specyficznych oddziaływań pomiędzy cząsteczkami stabilizowanego materiału a samym stabilizatorem. Niejednokrotnie pokazano, że specyficzne oddziaływania występujące pomiędzy lekiem, a polimerem, takie jak wiązania wodorowe, mogą znacząco spowalniać dewitryfikację substancji leczniczej nawet bez zmiany jego dynamiki molekularnej[31,32]. Lepszą fizyczną stabilność układów składających się z łatwo krystalizującego amorficznego leku oraz polimeru przypisuje się również samej budowie wspomnianego stabilizatora. Mianowicie, długie polimerowe łańcuchy mogą stanowić pewnego rodzaju zawadę steryczną dla cząsteczek farmaceutyku, utrudniając im tym samym formowanie kryształu.

Jak niedawno pokazano, alternatywnym, dobrze rokującym sposobem poprawy fizycznej stabilności amorficznych leków jest łączenie ich z substancjami o znacznie

mniejszej od polimerów masie cząsteczkowej, takimi jak na przykład: acetylowane cukry, aminokwasy, czy też inne substancje lecznicze[33,34,35,36,37,38]. W takich układach za główny mechanizm stabilizacji uznaje się specyficzne oddziaływania międzycząsteczkowe (m.in. wiązania wodorowe). Jednak w zależności od ilości oraz typu użytego stabilizatora nie wyklucza się również, że dodatkowe cząsteczki mogą pełnić rolę antyplastyfikatora czy też zawad sterycznych dla stabilizowanej substancji. Na szczególną uwagę zasługuje fakt, że wytwarzając jedną tabletkę zawierającą w swoim rdzeniu dwie amorficzne substancje czynne leku można poza samą poprawą fizycznej stabilności leków znajdujących się w mieszaninie, również:

- uzyskać lepszy efekt terapeutyczny (dwie substancje czynne leku podane na raz),
- zredukować koszty związane z wytwarzaniem tabletek (jedna linie produkcyjna, jedno opakowanie, łatwiejsza dystrybucja),
- poprawić prasowalność – tabletkowanie (mniej substancji pomocniczych w rdzeniu tabletki),
- zwiększyć biodostępność obu leków (obie substancje w formie amorficznej),
- zredukować ilość przyjmowanych przez pacjentów tabletek, co bezpośrednio wiąże się z poprawą komfortu pacjentów.

Poza wspomnianymi metodami stabilizacji amorficznych farmaceutyków, które bazują na zmianie dynamiki molekularnej układu albo miedzy cząsteczkowych oddziaływaniach, istnieją również naukowe doniesienia o próbach stabilizacji amorficznych farmaceutyków poprzez ograniczanie ich objętości do skali nanometrycznej[39,40]. Umieszczając amorficzny lek wewnątrz porów znajdujących się na przykład w krzemionkowych materiałach, istnieje możliwość nawet całkowitego zahamowania jego re-krystalizacji[41]. Powodem tak imponującej poprawy fizycznej stabilności łatwo krystalizującego amorficznego materiału wypełniającego pory jest uniemożliwienie powstania zarodków krystalizacji substancji znajdującej się wewnątrz porów[42]. Zgodnie z klasyczną teoria nukleacji, zarodek krystalizacji może powstać jedynie po osiągnięciu wielkości krytycznej[43]. Stosując więc materiały posiadające pory o promieniu mniejszym od krytycznego promienia zarodka krystalizacji łatwo re-krystalizującego leku, można całkowicie wyeliminować proces jego krystalizacji, co w konsekwencji oznacza całkowitą stabilizację amorficznego farmaceutyku.

Celem niniejszej pracy doktorskiej było sprawdzenie czy skala czasowa związana z procesem relaksacji strukturalnej koreluje się z czasem fizycznej stabilności amorficznej formy ezetimibu. Ponadto podjęto skuteczne próby znalezienia efektywnej metody prowadzącej do ustabilizowania tej formy ezetimibu.

Rezultaty prowadzonych badań zostały opublikowane, jako ciąg trzech tematycznie spójnych artykułów, w prestiżowym czasopiśmie naukowym *Molecular Pharmaceutics*, którego współczynnik oddziaływania (IF) wynosi aktualnie 4.384:

A1. Knapik J., Wojnarowska Z., Grzybowska K., Hawelek L., Sawicki W., Wlodarski K., Markowski J., Paluch M. *Physical Stability of the Amorphous Anticholesterol Agent (Ezetimibe): The Role of Molecular Mobility*. Mol. Pharmaceutics 2014, 11, 4280−4290.

A2. Knapik J., Wojnarowska Z., Grzybowska K., Jurkiewicz K., Tajber L., Paluch M. *Molecular Dynamics and Physical Stability of Coamorphous Ezetimib and Indapamide Mixtures.* Mol. Pharmaceutics 2015, 12, 3610−3619.

A3. Knapik J., Wojnarowska Z., Grzybowska K., Jurkiewicz K., Stankiewicz A., Paluch M. *Stabilization of the Amorphous Ezetimibe Drug by Confining Its Dimension.* Mol. Pharmaceuticals 2016, 13, 1308–1316.

Treść wyżej wymienionych publikacji naukowych, które stanowią podstawę rozprawy doktorskiej, można znaleźć w rozdziale 3.

Poza problematyką pracy doktorskiej pozostaje 13 współautorskich artykułów naukowych, które nie zostały włączone do rozprawy, ale świadczą o mojej aktywności naukowej:

B1. Hensel-Bielowka S., Wojnarowska Z., Knapik J., Paluch M., *New insight into relaxation dynamics of an epoxy/hydroxyl functionalized polybutadiene from dielectric and mechanical spectroscopy studies.* Colloid Polym Sci 2014, 292, 1853-1862.

B2. Wojnarowska Z., Knapik J., Díaz M., Ortiz A., Ortiz I., Paluch M. *Conductivity Mechanism in Polymerized Imidazolium – Based Protic Ionic Liquid [HSO3-BVIm][OTf]: Dielectric relaxation studies.* Macromolecules 2014, 47, 4056-4065.

B3. Hensel-Bielowka S., Ngai K.L., Swiety-Pospiech A., Hawelek L., Knapik J., Sawicki W., Paluch M. *On the molecular origin of secondary relaxations In amorphous Proti ionic conductor chlorpromazine hydrochloride – High pressure dielectric studies.* J. Non-Cryst. Solids 2014, 407, 81-87.

B4. Wojnarowska Z., Paluch K. J., Shoifet E., Schick C., Tajber L., Knapik J., Wlodarczyk P., Grzybowska K., Hensel-Bielowka S., Verevkin S.P., Paluch M. *Molecular Origin of Enhanced Proton Conductivity in Anhydrous Ionic Systems.* J. Am. Chem. Soc. 2014, 137, 1157–1164.

B5. Tripathy S. N., Wojnarowska Z., Knapik J., Shirota H., Biswas R., Paluch M. *Glass transition dynamics and conductivity scaling in ionic deep eutectic solvents: The case of (acetamide + lithium nitrate/sodium thiocyanate) melts*. J. Chem. Phys. 2015, 142, 184504.

B6. Wlodarski K., Sawicki W., Haber K., Knapik J., Wojnarowska Z., Paluch M., Lepek P., Hawelek L., Tajber L. *Physicochemical properties of tadalafil solid dispersions - impact of polymer on the apparent solubility and dissolution rate of tadalafil.* Eur. J. Pharm. Biopharm. 2015, 94, 106-115.

B7. Rams-Baron M., Wojnarowska Z., Grzybowska K., Dulski M., Knapik J., Jurkiewicz K., Smolka W., Sawicki W., Ratuszna A., Paluch M. *Towards a better understanding of the physical stability of amorphous anti-inflammatory agents: the role of molecular mobility and molecular interaction patterns.* Mol. Pharmaceutics 2015, 12, 3628−3638.

B8. Wojnarowska Z., Rams-Baron M., Knapik J., Ngai K. L., Kruk D., Paluch M. *Dynamic properties of glass-formers governed by the frequency dispersion of the structural α-relaxation: examples from prilocaine.* J. Phys. Chem. B 2015, 119, 12699−12707.

B9. Grzybowska K., Grzybowski A., Wojnarowska Z., Knapik J., Paluch M. *Ionic liquids and their bases: Striking differences in the dynamic heterogeneity near the glass transition.* Scientific Reports 2015, 5, 16876.

B10. Wojnarowska Z., Knapik J., Jacquemin J., Berdzinski S., Strehmel V., Sangoro J. R., Paluch M. *Effect of Pressure on Decoupling of Ionic Conductivity from Segmental Dynamics in Polymerized Ionic Liquids.* Macromolecules 2015, 48 (23), 8660–8666.

B11. Paluch M., Knapik J., Wojnarowska Z., Grzybowski A., Ngai K. L. *Universal Behavior of Dielectric Responses of Glass Formers: Role of Dipole-Dipole Interactions.* PRL 2016, 116, 025702.

B12. Wojnarowska Z., Knapik J., Rams-Baron M., Jedrzejowska A., Paczkowska M., Krause A., Cielecka-Piontek J., Jaworska M., Lodowski P., Paluch M. *Amorphous*

Protic Ionic Systems as Promising Active Pharmaceutical Ingredients: The Case of the Sumatriptan Succinate Drug. Mol. Pharmaceutics 2016, 13, 1111−1122.

B13. Knapik J., Wojnarowska Z., Grzybowska K., Tajber L., Mesallati H., Paluch K.J., Paluch M. *Molecular dynamics and physical stability of amorphous nimesulide drug and its binary drug-polymer systems.* Mol. Pharmaceutics 2016, DOI: 10.1021/acs.molpharmaceut.6b00115

Rezultaty moich badań były również prezentowane na poniżej wymienionych międzynarodowych konferencjach naukowych:

- *9th World Meeting on Pharmaceutics, Biopharmaceutics and Pharmaceutical Technology* (2014) Lizbona, Portugalia;
- *CONFERENCE AMPTEC 2014 Advanced Materials and Pharmaceutical Technologies* (2014) Lille, Francja;
- *8th International Conference on Broadband Dielectric Spectroscopy and its applications* (2014) Wisła, Polska;
- *2nd Workshop on Stability of Amorphous Pharmacauticals* (2015) Piza, Włochy;
- *10th World Meeting on Pharmaceutics, Biopharmaceutics and Pharmaceutical Technology* (2016) Glasgow, UK;
- *51st AAPS Arden conference: Contemporary Perspectives on Developing Amorphous Pharmaceuticals* (2016) Baltimore, USA.

Przeprowadzone na potrzeby niniejszej pracy doktorskiej badania finansowane były w ramach programu OPUS 3 Narodowego Centrum Nauki pt. *Otrzymywanie i fizykochemiczne badania nad substancjami leczniczymi w formie amorficznej w zakresie optymalizacji rozpuszczalności, procesu tabletkowania oraz trwałości* otrzymanego na podstawie decyzji numer: DEC-2012/05/B/NZ7/03233 oraz SYMFONIA 3 Narodowego Centrum Nauki pt. *Wpływ procesów fizycznych oraz substancji pomocniczych na charakterystykę właściwości substancji leczniczych trudno rozpuszczalnych w wodzie* o numerze UMO-2015/16/W/NZ7/00404.

2 OMÓWIENIE ARTYKUŁÓW NAUKOWYCH

2.1 Przygotowanie amorficznego ezetimibu oraz badanie jego fizycznej stabilności

Główną motywacją podjętych badań była chęć polepszenia biodostępności ezetimibu. W tym celu przekształcono krystaliczny, trudno rozpuszczalny w wodzie ezetimib, do postaci amorficznej. Jako metodę amorfizacji wybrano witryfikację, polegającą na szybkim przechłodzeniu uprzednio stopionego krystalicznego materiału. Temperaturę topnienia (T_m = 436 K), jak również temperaturę przejścia szklistego (T_g = 334 K) ezetimibu wyznaczono przy pomocy skaningowej kalorymetrii różnicującej (DSC – and. *Differerential Scaning Calorymetry*). [A1 Rysunek 1]. Aby upewnić się, że przygotowane przy pomocy wyżej opisanego sposobu próbki są całkowicie amorficzne, zbadano je metodą dyfrakcji rentgenowskiej (XRD – ang. *X-ray diffrection*). Otrzymane dyfraktogramy, ze względu na brak charakterystycznych dla krystalicznych materiałów ostrych pików Braggowskich, są dowodem pełnej amorfizacji badanej substancji leczniczej [A1 Rysunek 2].

Ponieważ amorficzne materiały mają tendencję do krystalizacji, w kolejnym kroku zajęto się badaniem fizycznej stabilności amorficznej formy badanego leku przeciw cholesterolowego. Powszechnie uważa się, że ruchliwość molekularna układów nieuporządkowanych jest głównym czynnikiem decydującym o fizycznej stabilności próbki, dlatego w przypadku ezetimibu została ona gruntownie zbadana przy pomocy szerokopasmowej spektroskopii dielektrycznej (BDS – and. *Broadband Dielectric Spectroscopy*). Technika ta, dzięki badaniu efektów związanych z oddziaływaniem zewnętrznego zmiennego pola elektrycznego z badanym materiałem, umożliwia obserwowanie występujących w nim procesów relaksacyjnych w szerokim zakresie częstotliwości, temperatur, a nawet ciśnień. Analizując widma strat dielektrycznych *ε''(f)* ezetimibu, zauważono, że badana substancja posiada aż cztery procesy relaksacyjne [A1 Rysunki 3, 9, 10]. Poza relaksacją strukturalną α, odzwierciedlającą kooperatywne ruchy całych molekuł, ezetimib ujawnia również trzy drugorzędowe procesy relaksacyjne, którym przypisuje się pochodzenie wewnątrz molekularne. Dwa spośród nich są dobrze widoczne na widmach zarejestrowanych poniżej przejścia szklistego i zostały oznaczone przy pomocy greckich liter β i γ. Natomiast, podejrzewa się, że trzeci drugorzędowy proces relaksacyjny ezetimibu jest ukryty pod tzw. skrzydłem nadmiarowym. Dodatkowo na widmach strat dielektrycznych ezetimibu zarejestrowanych powyżej T_g zaobserwowano gwałtowny spadek intensywności α-procesu przy T > 383 K, który jest manifestacją zimnej krystalizacji

ezetimibu [A1 Rysunek 3]. Oznacza to, że amorficzna forma badanego leku przeciw cholesterolowego przechowywana w temperaturach powyżej przejścia szklistego z łatwością powraca do swojej krystalicznej formy. Aby zbadać kinetykę procesu krystalizacji ezetimibu w cieczy przechłodzonej oraz, aby wyznaczyć jego energię aktywacji, wykonano serię czasowo zależnych, izotermicznych eksperymentów przy pomocy spektroskopii dielektrycznej [A1 Rysunki 5, 6]. Na podstawie wspomnianych pomiarów wykonanych dla siedmiu różnych temperatur wyznaczono pozorną energię aktywacji krystalizacji ezetimibu w cieczy przechłodzonej – E_a = 127.5 kJ/mol [A1 Rysunek 7].

W związku z tym, że standardowo leki przechowuje się w temperaturze pokojowej, czyli w przypadku ezetimibu prawie 40 stopni poniżej T_g, w kolejnym etapie badań podjęto próbę określenia czasu fizycznej stabilności testowanego leku, jeśli przechowuje się go w temperaturze równej 298 K. Ponieważ uważa się, że dynamika molekularna nieuporządkowanego układu ma kluczowy wpływ na jego fizyczną stabilność, to często minimalny czas fizycznej stabilności amorficznych leków utożsamia się z czasem relaksacji strukturalnej[44]. Do oszacowania czasu strukturalnej relaksacji ezetimibu przechowywanego w T = 298 K, to znaczy głęboko w szkle, użyto metody polegającej na skonstruowaniu tzw. master plotów. Procedura ta polega na horyzontalnym nasunięciu widma strat dielektrycznych $\varepsilon''(f)$ z dobrze widocznym α-procesem, czyli z obszaru cieczy przechłodzonej, na widma, w których jedynie prawe zbocze strukturalnej relaksacji jest widoczne. Należy podkreślić, że ta procedura jest prawidłowa tylko i wyłącznie wtedy, gdy kształt α-procesu nie zmienia się z temperaturą – czyli dokładnie tak, jak ma to miejsce w przypadku ezetimibu [A1 Rysunek 4]. Korzystając ze wspomnianej metody oszacowano, że badany lek przechowywany w temperaturze pokojowej powinien być stabilny przez około 20 dni. Ponieważ, przewidziany czas, po jakim amorficzny ezetimib może zacząć re-krystalizować, nie jest zbyt długi zdecydowano się zweryfikować poprawność użytej metody i eksperymentalnie wyznaczyć czas fizycznej stabilności ezetimibu przechowywanego w temperaturze 298 K. W tym celu przeprowadzono długoterminowe pomiary stabilności amorficznej formy badanego leku przy pomocy XRD. Dyfraktogramy otrzymane podczas wspomnianego eksperymentu dowiodły, że użyta metoda bardzo trafnie przewiduje fizyczną stabilność amorficznej formy ezetimibu. Jak pokazano na rysunku zamieszczonym przy abstrakcie artykułu A1, ezetimib przechowywany w temperaturze pokojowej zaczyna re-krstalizować po około dwóch tygodniach od momentu jego amorfizacji.

Uważa się, że czasy relaksacji strukturalnej amorficznych materiałów przechowywanych w temperaturach poniżej ich T_g można również wyznaczyć przy pomocy zmodyfikowanego

równania Adama – Gibbsa bazującego na dynamice molekularnej układów w cieczy przechłodzonej[45]. Dlatego też, w artykule A1 zdecydowano się sprawdzić, czy wspomniany model będzie w stanie trafnie przewidzieć czas fizycznej stabilności ezetimibu przechowywanego w T = 298 K. Jak pokazano na rysunku 8 w artykule A1, zgodnie z modelem Adama – Gibbsa, badany farmaceutyk powinien być fizycznie stabilny w temperaturze 298 K przez ponad 275 dni. Ten wynik wskazuje, że w przypadku ezetimibu zmodyfikowane równanie Adama – Gibbsa nie jest w stanie prawidłowo przewidzieć czasu jego fizycznej stabilności.

Wszystkie metody użyte do określenia czasu fizycznej stabilności amorficznego ezetimibu przechowywanego w temperaturze pokojowej wykazały, że badany lek przeciw cholesterolowy nie spełnia minimalnego czasu stabilności, jaki jest wymagany od amorficznych farmaceutyków przed wprowadzeniem ich na rynek (tj. 3-ech lat). W związku z tym w kolejnych etapach badań zajęto się poszukiwaniem jak najefektywniejszej metody prowadzącej do poprawy fizycznej stabilności amorficznej formy ezetimibu.

2.2 Stabilizacja amorficznego ezetimibu przy pomocy polimeru

Obecnie najczęściej stosowaną metodą poprawy fizycznej stabilność amorficznych farmaceutyków jest tworzenie binarnego układu składającego się z substancji leczniczej oraz polimeru. Ponieważ stosowane do stabilizacji leków polimery bardzo często charakteryzują się wysoką wartością T_g, są w stanie spowolnić dynamikę molekularną niestabilnego w formie amorficznej farmaceutyku, co w konsekwencji prowadzi do zahamowania jego silnej tendencji do re-krystalizacji. Duża skuteczność polimerów w stabilizacji substancji leczniczych w formie amorficznej była przyczyną podjęcia próby ustabilizowania amorficznego ezetimibu przy pomocy polimeru o nazwie Soluplus. Wspomniany polimer jest obecnie bardzo często stosowany w przemyśle farmaceutycznym. Został on stworzony specjalnie do polepszania rozpuszczalności słabo rozpuszczalnych w wodzie leków. Dlatego też, spodziewano się, że stosując Soluplus do stabilizacji amorficznej formy ezetimibu, również biodostępność badanego leku przeciw cholesterolowego zostanie znacznie polepszona.

W celu sprawdzenia jak 20% dodatek Soluplusu wpłynął na dynamikę molekularną ezetimibu, badano przygotowaną kompozycję przy pomocy spektroskopii dielektrycznej. Analizując widma strat dielektrycznych *ε"(f)* tej mieszaniny, zauważono, że Soluplus, zgodnie z oczekiwaniem, spowalnia dynamikę molekularną badanego leku. Co więcej,

podczas pomiarów nie zaobserwowano, aby badany układ re-krystalizował – brak drastycznego spadku w $\Delta\varepsilon_\alpha$ mierzonej próbki [A1 Rysunek 13].

Aby przewidzieć jak długo amorficzny ezetimib z 20% polimerowym dodatkiem będzie stabilny w temperaturze pokojowej użyto, jak w przypadku czystego ezetimibu, metody bazującej na konstrukcji tzw. master plotów. Zgodnie z przeprowadzonymi przewidywaniami badana mieszanina składająca się z ezetimibu i Soluplusu przechowywana w temperaturze pokojowej powinna być stabilna w formie amorficznej przez minimum cztery lata. Biorąc pod uwagę fakt, że czysty ezetimib przechowywany w T = 298 K jest stabilny jedynie przez dwa tygodnie od momentu jego amorfizacji, bez wątpienie można stwierdzić, że zastosowanie 20% polimerowego dodatku imponująco polepsza fizyczną stabilność amorficznej formy badanego leku. Na uwagę zasługuje również fakt, iż przewidziany czas stabilności ezetimibu ustabilizowanego Soluplusem jest dłuższy od wymaganego czasu fizycznej stabilności komercyjnie stosowanych leków, co jedynie podkreśla słuszność stosowania Soluplusu do stabilizacji amorficznego ezetimibu. Aby sprawdzić czy amorficzna forma ezetimibu ustabilizowana polimerem charakteryzuje się lepszą rozpuszczalnością w wodzie od swojej krystalicznej, dotychczas sprzedawanej formy, przeprowadzono pomiary rozpuszczalność wymienionych materiałów. Jak się okazało amorficzny ezetimib z 20% dodatkiem Soluplusu charakteryzuje się niesamowicie wysoką, bo ponad sześciokrotnie większą rozpuszczalnością w wodzie od swojego czystego, krystalicznego odpowiednika.

2.3 Stabilizacja amorficznego ezetimibu przy pomocy innego leku

Niejednokrotnie pokazano, że łatwo krystalizujące amorficzne farmaceutyki można stabilizować nie tylko poprzez dodanie do nich polimerów, ale również substancji o znacznie mniejszej masie molowej tj. acetykowane cukry, amonokwasy, czy też inne aktywne formy leków. Ze względu na fakt, że wysoki poziom cholesterolu bardzo często towarzyszy nadciśnieniu tętniczemu, zdecydowano się spróbować ustabilizować amorficzną formę ezetimibu przy pomocy indapamidu – leku często stosowanego w celu obniżania ciśnienia tętniczego. Podkreślić należy, że stosowanie obu wymienionych farmaceutyków jednocześnie jest medycznie uzasadnione, dodatkowo wymienione leki zaleca się przyjmować w taki sam sposób – raz dziennie – co jedynie podnosi potencjał wspomnianej mieszaniny leków.

Będące tematem artykułu A2 podwójnie amorficzne układy składające się z ezetimibu i indapamidu przygotowano w pięciu różnych stosunkach molowych (EZB 10:1 IDP, EZB 5:1 IDP, EZB 2:1 IDP, EZB 1:1 IDP oraz EZB 1:2 IDP) poprzez szybkie przechłodzenie

uprzednio stopionej fizycznej mieszaniny dwóch materiałów. Własności termiczne świeżo przygotowanych układów badano przy pomocy skaningowej kalorymetrii różnicującej [A1 Rysunek 1]. Na otrzymanych termogramach mieszanin zawierających EZB i IDP widoczny jest jedynie charakterystyczny dla przejścia szklistego skok ciepła właściwego, który wraz ze wzrostem zawartości IDP przesuwa się w kierunku wyższych temperatur. Brak egzotermicznego piku odzwierciedlającego re-krystalizcję dowodzi, że nawet niewielka ilość indapamidu (8.8 %) jest w stanie polepszyć fizyczną stabilność amorficznej formy ezetimibu. Zaobserwowane spowolnienie re-krystalizacji ezetimibu po dodaniu do niego indapamidu może być wynikiem efektu antyplastyfikacyjnego wywieranego na EZB przez IDP, specyficznych oddziaływań miedzy zmieszanymi związkami, lub też połączenia obu tych efektów. Jeśli dominującym powodem poprawy fizycznej stabilności EZB byłby efekt antyplastyfikacyjny to otrzymane z eksperymentu wartości T_g dla poszczególnych mieszanin powinny pozostać w zgodzie z przewidzianą przy pomocy wzoru Gordona – Taylora temperaturową zależnością przejścia szklistego od koncentracji stabilizatora. Jak dowiedziono wartości T_g wyznaczone z eksperymentu i modelu Gordona – Taylora są zgodne [A2 Rysunek 2]. Sugeruje to, że molekuły EZB i IDP w badanych mieszaninach nie powinny ze sobą oddziaływać. Aby eksperymentalnie potwierdzić brak specyficznych oddziaływań pomiędzy badanymi substancjami czynnymi leków, układy badano przy pomocy FTIR [A1 Rysunek 3]. Wspomniany eksperyment jednoznacznie potwierdził, że pomiędzy molekułami EZB i IDP w stanie amorficznym nie występują specyficzne oddziaływania.

W kolejnym etapie badań sprawdzano jak dodatek IDP wpływa na dynamikę molekularną EZB. W tym celu EZB, IDP oraz pięć mieszanin zawierających różną koncentrację wymienionych leków badano w obszarze cieczy przechłodzonej przy pomocy BDS. Widma strat dielektrycznych $\varepsilon''(f)$ wszystkich badanych układów charakteryzują się obecnością jednego dobrze widocznego piku odzwierciedlającego relaksację strukturalną [A2 Rysunek 3]. Dzięki analizie wspomnianych widm otrzymano temperaturowe zależności czasów strukturalnej relaksacji wszystkich badanych układów [A2 Rysunek 5]. W obszarze cieczy przechłodzonej zależność $log\tau_\alpha(T)$ zazwyczaj dobrze daje się opisać przy pomocy wzoru Vogela – Fulchera – Tammanna (VFT). Z tego względu, wspomniany wzór użyto do opisania eksperymentalnie wyznaczonej zależności $log\tau_\alpha(T)$. Jak pokazano w A2 na rysunku 5, wzór VFT dobrze opisuje dane z zakresu temperatur pomiędzy T_g a T_{cross}, dlatego został użyty do wyznaczenia wartości kinetycznego przejścia szklistego wszystkich badanych układów [A2 Tabela 3]. Korzystając z parametrów dopasowania równania VFT do eksperymentalnych danych oraz z wyznaczonych wartości T_g, oszacowano parametr

kruchości (m_p) dla wszystkich badanych układów. Na uwagę zasługuje fakt, że wartość wspomnianego parametru maleje wraz ze wzrostem zawartości IDP w mieszaninie. Ponieważ parametr kruchości często używa się do przewidywania tendencji amorficznych farmaceutyków do krystalizacji, możemy podejrzewać, że wraz ze wzrostem zawartości IDP poprawia się fizyczna stabilność mieszaniny EZB i IDP. Wspomniana prawidłowość została eksperymentalnie potwierdzona dzięki izotermicznym pomiarom wykonanym przy pomocy DSC [A2 Rysunek 7].

W kolejnym etapie badań starano się zbadać fizyczną stabilność podwójnie amorficznych mieszanin EZB i IDP przechowywanych w temperaturze pokojowej. W tym celu przeprowadzono długoterminowe pomiary XRD [A1 Rysunek 8]. Z przeprowadzonych pomiarów wynika, że IDP jest świetnym stabilizatorem EZB. Nawet niewielka ilość IDP w mieszaninie (tj. 8.8% wt.) bardzo efektywnie stabilizuje EZB. Nawet po 300 dniach przechowywania w standardowych warunkach, czyli T = 297 K oraz wilgotności = 20% mieszanina EZB z 8.8% wt. IDP jest stabilna*.

Na uwagę zasługuje również fakt, że stworzona podwójnie amorficzna mieszanina dwóch leków: EZB i IDP – poza niesamowitym efektem stabilizującym EZB, powinna przynieść wiele innych dodatkowych zalet, tj. poprawę efektu terapeutycznego (dwie substancje czynne w jednej tabletce), tańszą produkcję (jedno opakowanie, jedna taśma produkcyjna), poprawę komfortu przyjmowania leków przez pacjentów (jedna tabletka zawierająca dwie substancje czynne) oraz lepszą rozpuszczalność (obie substancje w stanie amorficznym).

2.4 Stabilizacja amorficznego ezetimibu przy pomocy porowatych materiałów

Ostatnio porowate materiały są coraz częściej stosowane przy produkcji farmaceutyków w celu kontrolowania ich uwalniania, dostarczania leków dokładnie do leczonego obszaru ciała pacjenta oraz do wytwarzania metastabilnych polimorficznych odmian substancji leczniczej. Powszechna obecność w przemyśle farmaceutycznym materiałów o porowatej naturze motywuje do podjęcia próby stabilizacji ezetimibu przy ich pomocy.

W A3 do stabilizacji łatwo krystalizującej amorficznej formy EZB użyto dwie, nie toksyczne, komercyjnie stosowane nanoporowate substancje: Aeroperl 300 oraz Neusilin US2. Materiały te charakteryzują się taką samą powierzchnią właściwą oraz objętością porów,

* Podany czas fizycznej stabilności podwójnie amorficznych kompozycji ezetimibu i indapamidu odnosi się do czasu podanego w artykule A2. Warto nadmienić, że testy stabilności są cały czas prowadzone i w dalszym ciągu nie zarejestrowano oznak re-krystalizacji.

natomiast różnią się średnią wielkością porów [A3 Rysunek 1]. Podana przez producenta średnia wartość rozmiaru porów w przypadku Aeroperlu 300 wynosi 30 nm, a w przypadku Neusilin US2 – 5 nm.

Po napełnieniu porów Aeroperlu 300 oraz Neusilinu US2 ezetimibem sprawdzano przy pomocy XRD, czy substancja wypełniająca pory jest faktycznie w stanie amorficznym. Przeprowadzone pomiary dyfrakcji rentgenowskiej nie tylko dowiodły amorficzności ezetimibu, ale także potwierdziły obecność leku wewnątrz porów obu testowanych porowatych materiałów [A3 Rysunek 2]. Aby zbadać jak ograniczenie przestrzeni ezetimibu do rozmiarów nano wpłynęło na jego dynamikę molekularną, przygotowane układy badano przy pomocy spektroskopii dielektrycznej. Dokładna analiza otrzymanych widm strat dielektrycznych *ε''(f)* ujawniła obecność dwóch frakcji molekuł charakteryzujących się różną ruchliwości [A3 Rysunek 4]. Do pierwszej, wolniejszej frakcji zaliczono cząsteczki ezetimibu, które sąsiadują ze ściankami porów. Ich spowolniona ruchliwość jest najprawdopodobniej wynikiem oddziaływań zachodzących pomiędzy nimi a ściankami nanoporów. Druga frakcja natomiast składa się ze wszystkich pozostałych molekuły znajdujących się w rdzeniu porów. Ruchliwość tej grupy cząstek znacznie bardziej przypomina ruchliwość molekuł nieograniczonego przestrzennie ezetimibu [A3 Rysunek 6].

Na szczególną uwagę zasługuje fakt, że podczas pomiarów przeprowadzonych w obszarze cieczy przechłodzonej przy pomocy spektroskopii dielektrycznej zauważono, że ezetimib znajdujący się wewnątrz porów Aeroperlu zaczyna krystalizować w T = 361 K, podczas gdy w mniejszych – 5 nm – porach Neusilinu nie zaobserwowano oznak krystalizacji nawet w znacznie wyższej temperaturze równej 407 K [A3 Rysunek 7]. Podkreślić należy, że badane układy przechowywane w temperaturach poniżej przejścia szklistego zachowują się w podobny sposób (tzn. ezetimib wewnątrz porów Aeroperlu szybciej krystalizuje niż wewnątrz porów Neusilinu). Jak pokazano w A3 na rysunku 9 amorficzny ezetimib wypełniający 30 nm pory Aeroperlu zaczyna re-krystalizować po 5 miesiącach przechowywania go w T = 300 K, podczas gdy pozostawiony w tych samych warunkach ezetimib wypełniający 5 nm pory Neusilinu nadal pozostaje w formie amorficznej. Istnieją trzy powody mogące być przyczyną różnej stabilizacji ezetimibu w 5 i 30 nm porach. Po pierwsze, dynamika cząsteczek ezetimibu znajdujących się w rdzeniu mniejszych porów została znacznie bardziej spowolniona od molekuł ezetimib znajdujących się w rdzeniu większych – 30 nm – porów [A3 Rysunek 6]. Po drugie, wewnątrz porów o mniejszej średnicy, o wiele więcej cząsteczek leku jest unieruchomionych przez ścianki porów (większy jest stosunek frakcji wolniejszych, odściankowych molekuł do frakcji szybszych cząsteczek rdzenia). Po trzecie wyliczono, że

krytyczny rozmiar zarodka krystalizacji ezetimibu jest niewiele większy od średnicy porów Neusiliny US2 [A3 Rysunek 10], co oznacza, że badany lek wewnątrz tak małych porów może nie być w stanie wytworzyć kryształu.

3 WYKAZ ARTYKUŁÓW STANOWIĄCYCH PODSTAWĘ ROZPRAWY DOKTORSKIEJ WRAZ Z OŚWIADCZENIAMI WSPÓŁAUTORÓW

3.1 A1 – Knapik J., Wojnarowska Z., Grzybowska K., Hawełek L, Sawicki W., Włodarski K., Markowski J., Paluch M. *Physical Stability of the Amorphous Anticholesterol Agent (Ezetimibe): The Role of Molecular Mobility.* Mol. Pharmaceuticals 2014, 11, 4280–4290.

Impact Factor czasopisma z roku opublikowania pracy: **4.384**.

Liczba punktów ministerialnych MNiSW czasopisma z roku opublikowania pracy: **45 pkt**.

DOI: **10.1021/mp500498e**.

Udział pierwszego autora w poniżej załączonym artykule polegał na wykonaniu części pomiarów dielektrycznych, wykonaniu pomiarów kalorymetrycznych, analizie wszystkich otrzymanych wyników oraz przygotowaniu manuskryptu. Wkład pozostałych współautorów, w formie oświadczeń, zamieszczono na końcu artykułu.

molecular pharmaceutics

Article

pubs.acs.org/molecularpharmaceutics

Physical Stability of the Amorphous Anticholesterol Agent (Ezetimibe): The Role of Molecular Mobility

J. Knapik,*[,†,‡] Z. Wojnarowska,[†,‡] K. Grzybowska,[†,‡] L. Hawelek,[†,‡,§] W. Sawicki,[∥] K. Wlodarski,[∥] J. Markowski,[⊥] and M. Paluch[†,‡]

[†]Institute of Physics, University of Silesia, ul. Uniwersytecka 4, 40-007 Katowice, Poland

[‡]Silesian Center for Education and Interdisciplinary Research, ul. 75 Pułku Piechoty 1a, 41-500 Chorzów, Poland

[§]Institute of Non Ferrous Metals, ul. Sowinskiego 5, 44-100 Gliwice, Poland

[∥]Department of Physical Chemistry, Medical University of Gdansk, 84-416 Gdansk, Poland

[⊥]ENT Department, Silesian Medical University, ul. Francuska 20, Katowice, Poland

ABSTRACT: The purpose of this paper is to examine the role of molecular mobility in the recrystallization process from the amorphous state of the anticholesterol drug ezetimibe. Both the molecular dynamics and crystallization kinetics have been studied using various experimental techniques, such as broadband dielectric spectroscopy (BDS), differential scanning calorimetry (DSC), and X-ray diffraction (XRD). Our investigations have shown that ezetimibe easily recrystallizes from the disordered state, both below and above its glass transition temperature (T_g = 336 K). Moreover, we found that an only slightly elevated pressure (5 MPa) significantly accelerates the recrystallization process at $T > T_g$. We predict that the structural relaxation time of amorphous ezetimibe at 293 K (storage temperature) and ambient pressure is only 22 days. This result corresponds to the characteristic time, determined from XRD measurements, for amorphous ezetimibe to recrystallize during storage at T_{room} = 298 K. It leads to the conclusion that the molecular mobility reflected in structural relaxation of ezetimibe is mainly responsible for devitrification of this drug. Finally, we determined a relatively easy way to improve the physical stability of the drug by preparing a binary amorphous ezetimibe−Soluplus mixture. Ezetimibe in an amorphous mixture with 20 wt % Soluplus has a much better (over six times) solubility than the pure crystalline material.

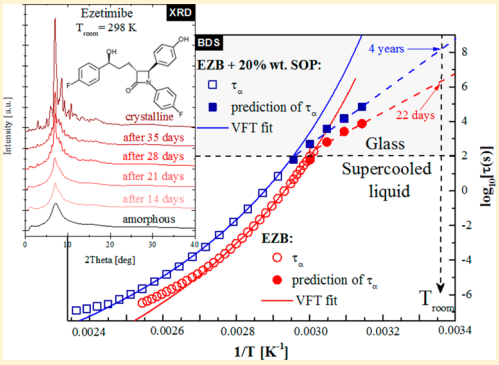

KEYWORDS: *ezetimibe, Soluplus, amorphous drug, molecular dynamics, glass transition, crystallization, physical stability, stability predicting*

INTRODUCTION

Cardiovascular diseases are the most frequent cause of death in developed countries. Numerous studies have shown that cholesterol, which is accumulated within blood vessel walls, is one of the main reasons for these diseases.[1,2] Therefore, an important task of modern pharmacy is to develop improved cholesterol-lowering drugs. A very popular active pharmaceutical ingredients (APIs) used to lower plasma cholesterol levels is ezetimibe (EZB). This drug is collected in the small intestinal brush border membrane, where it selectively inhibits the absorption of cholesterol by binding to Niemman-Pick C1-Like 1 (NPC1L1) proteins.[3,4] As a result, less cholesterol is absorbed into the bloodstream, making EZB extremely useful for the treatment or prevention of hypercholesterolemia. However, the commercial form of this pharmaceutical exhibits low oral bioavailability, attributed to its poor water solubility. For that reason EZB is in the second class of the Biopharmaceutics Classification System (BCS).[5]

There are several methods for increasing the solubility and bioavailability of drugs with poor water solubility.[6] One is based on the preparation of amorphous compounds. In the literature it has been reported that amorphous pharmaceuticals exhibit higher solubility than their crystalline counterparts.[7−9] Consequently, greater bioavailability can be achieved, as well as lowering the drug dose administered to the patient. Although amorphous materials have advantages, they are physically unstable systems and may easily revert to the crystalline form during storage.[10−12]

There are a lot of factors affecting the physical stability of amorphous pharmaceuticals, e.g., the method of amorphization,[13] the water content, chemical purity, existence of isomers,[14−16] the presence of more than one chemical species (e.g., polymer additive), the configurational entropy, the specific surface area, and surface mobility.[17] However, as documented by many authors, the most important factor is the molecular mobility of the material.[18−20] A powerful experimental technique to investigate molecular dynamics is

Received: July 22, 2014
Revised: October 1, 2014
Accepted: October 13, 2014
Published: October 13, 2014

dx.doi.org/10.1021/mp500498e | *Mol. Pharmaceutics* 2014, 11, 4280−4290

broadband dielectric spectroscopy (BDS). This method enables measurements of relaxation processes over a broad range of frequencies (up to 12 decades), temperatures, and even pressures.[21,22] Consequently, it is possible to observe relaxation processes occurring both below and above the glass transition temperature. In the supercooled liquid state (above T_g) the dominant process is structural (α) relaxation, which originates from cooperative motion of many molecules. On the other hand, in the glassy state (below T_g), the α-process becomes very slow, and secondary relaxation processes, which reflect fast local motions having an inter- or intramolecular origin, can be detected. As demonstrated in many papers generally both structural and secondary relaxations are responsible for the physical instability of amorphous drugs. An example of a compound in which secondary processes affect nucleation and crystal growth is celecoxib.[23] Recently, it was shown that mixing polymers with amorphous drugs can enhance their physical stability because the polymer reduces the local molecular motions of API.[24] An additional advantage from dielectric relaxation studies is the possibility of predicting the tendency of pharmaceuticals to recrystallization during storage at room temperature (usually deep in the glassy state). The prediction of physical stability of amorphous drugs is a fundamental problem for the pharmaceutical industry, due to the fact that commercial compounds should be physically stable for long times, i.e., at least 3 years, which is a typical shelf life.[25] For this reason a lot of effort has been dedicated to finding the appropriate method for evaluating the tendency of drugs to crystallize at temperatures below T_g. In the literature a few theoretical and experimental studies have addressed this. In light of recent work, the extended Adam and Gibbs (AG) model seems to be the most suitable for predicting the physical stability of materials in their amorphous state.[26,27]

In this paper we focus on the molecular dynamics of EZB in the supercooled liquid and glassy states. The extended AG model is applied to predict the physical stability at temperatures below the glass transition. The validity of the AG approach will be confirmed by experimental data obtained from long-term studies of the physical stability of EZB. Additionally, we measure the stability of amorphous EZB in a polymer matrix. Finally, the solubility studies of pure EZB as well as its binary mixture are reported.

EXPERIMENTAL METHODS

Materials. Ezetimibe drug of purity greater than 99% and molecular mass M_w = 409.4 g/mol was purchased from Polpharma (Starogard Gdański, Poland) and used as received. This pharmaceutical is described chemically as ((3*R*,4*S*)-1-(4-fluorophenyl)-3-[(3*S*)-3-(4-fluorophenyl)-3-hydroxypropyl]-4-(4-hydroxyphenyl)azetidin-2-one), with its chemical structure presented in Figure 1.

Differential Scanning Calorimetry (DSC). Thermodynamic properties of EZB were examined using a Mettler-Toledo DSC 1 STAR^e System. The measuring device was equipped with liquid nitrogen cooling and a HSS8 ceramic sensor having 120 thermocouples. The instrument was calibrated for temperature and enthalpy using indium and zinc standards. Crystallization and melting points were determined as the onset of the peak, whereas the glass transition temperature was determined as the midpoint of the heat capacity increment. The samples were measured in an aluminum crucible (40 μL). All measurements were carried out in the range from 300.15 to 445.15 K with various (5 K/min or 10 K/min) heating rates. To obtain accurate temperature dependences of the heat capacity for crystalline and amorphous EZB, a stochastic temperature-modulated differential scanning calorimetry (TOPEM) method implemented by Mettler-Toledo TOPEM was employed. These measurements were performed in the temperature range from 300.15 to 365.15 K with a heating rate of 0.5 K/min.

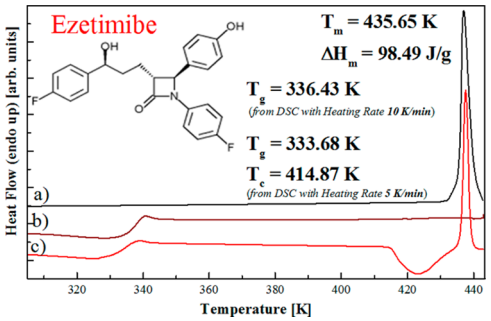

Figure 1. DSC thermograms of (a) the crystalline form of ezetimibe measured with heating rate 10 K/min, (b) the amorphous form of ezetimibe measured with heating rate 10 K/min, and (c) the amorphous form of ezetimibe measured with heating rate 5 K/min.

High-Performance Liquid Chromatography (HPLC). A simple and selective HPLC method was developed and optimized for quantitative evaluation of ezetimibe concentration. The analysis is performed using an HPLC Prominence system, consisting of a UV−vis detector, an automatic injector, a pump, and a column oven (Shimadzu, Japan). For data acquisition and calculations, the LC solution software system was used.

The analysis was carried out using a Nucleodur C-18 column (250 mm × 4.6 mm, 5 μm, 100 Å) operating in reverse phase (RP) with the mobile phase consisting of methanol, acetonitrile, and phosphate buffer adjusted to pH 6.8 (50:10:40 v/v/v) in the isocratic flow with a flow rate of 1 mL/min. The eluent was filtered using 0.2 μm cellulose membrane filters (Olimpeak) and degassed in an ultrasonic bath. The run and retention times of ezetimibe were 5 and 3.15 min, respectively. The analysis was performed at 37 °C with injection of 20 μL and UV detection at a wavelength of 233 nm.

The concentration of ezetimibe was calculated from linear regression for the range of 1−100 μg/mL, R^2 = 0.9991.

X-ray Diffraction (XRD). The X-ray diffraction experiments were performed at ambient temperature on a Rigaku-Denki D/MAX RAPID II-R diffractometer (Rigaku Corporation, Tokyo, Japan) with a rotating anode Ag KR tube (λ = 0.5608 Å), an incident beam (002) graphite monochromator, and an image plate in the Debye−Scherrer geometry. The pixel size was 100 μm × 100 μm. Measurements were performed on sample-filled and empty capillaries, to allow subtraction of the background intensity. The beam width at the sample was 0.1 mm. The two-dimensional diffraction patterns were converted into one-dimensional intensity data.

Broadband Dielectric Spectroscopy (BDS). Isobaric dielectric measurements of EZB at ambient pressure were carried out using a Novo-Control GMBH Alpha dielectric spectrometer, in the frequency range from 3 × 10^{-1} Hz to 10^6 Hz at temperatures from 153.15 to 385.15 K. The temperature was controlled by a Quattro temperature controller with temperature stability better than 0.1 K. Dielectric studies of EZB were performed immediately after its vitrification by fast cooling of the melt in a parallel-plate cell made of stainless steel

dx.doi.org/10.1021/mp500498e | *Mol. Pharmaceutics* 2014, 11, 4280−4290

(diameter 15 mm, for crystallization 20 mm, and a 0.1 mm gap with Teflon spacers). Crystallization kinetics of EZE at ambient pressure was carried out for seven different temperatures, 398.15, 393.15, 388.15, 383.15, 378.15, 373.15, and 368.15 K, and at elevated pressure (5 MPa) at one temperature, 268.15 K.

For the pressure dependent dielectric measurements, we used a capacitor (with diameter 15 mm) filled with the EZB, compressed using silicone fluid via a piston in contact with a hydraulic press. The sample was in contact only with stainless steel and Teflon. Pressure was measured by a Nova Swiss tensometric pressure meter with a resolution of 0.1 MPa. The temperature was controlled within 0.1 K by means of liquid flow from a thermostatic bath.

Water Solubility Study. In order to determine the solubility of ezetimibe in water, saturated solutions were prepared of both a crystalline form and its solid dispersion with Soluplus. For this purpose, an excess of powder was suspended in 30 mL of purified water in a 50 mL conical flask and shaken (150 rpm) for 24 h in a water bath at 37 ± 0.5 °C. The resulting solutions were filtered through polyester syringe filters with a pore size 0.45 μm (Chromafil PET-45/25), previously heated to 37 °C, and then analyzed using high-performance liquid chromatography (HPLC). Each measurement was repeated twice by triple injection and calculation of the average.

Density Function Theory (DFT) Simulation Details. All calculations of the ezetimibe molecule were performed using the density functional theory in the ORCA package.[28] In the first step optimizations of a dozen random ezetimibe structures were carried out with the use of the hybrid B3LYP functional and 6-31G* basis set. Transition states and minima were confirmed by performing vibrational analysis. Frequencies were calculated numerically at the same level of theory. Molecules were visualized using the Avogadro package.[29]

RESULTS AND DISCUSSION

Preparation and Chemical Stability Studies. Amorphous EZB was prepared by the most common method: vitrification by rapid cooling of molten sample below T_g. Note that this method of amorphization cannot be employed when the sample undergoes thermal degradation near the melting point. DSC was used to determine the melting temperature with the curve of the crystalline form taken at a heating rate of 10 K/min, presented in Figure 1a.

The sharp endothermic peak near 436 K corresponds to the melting point of EZB. This value is in agreement with that reported in the literature (436.15−439.15 K). The purity of the vitrified sample, determined by HPLC, was found to be ≥99.5%. This indicates that EZB does not undergo chemical decomposition when heated to its melting point. Consequently, the vitrification method is an appropriate method for preparation of amorphous EZB drug. As can be seen in the DSC thermogram in Figure 1b, amorphous EZB, prepared by quench-cooling of the melt, has a glass transition T_g = 336 K, when measured with heating rate of 10 K/min. At this heating rate the sample does not recrystallize above T_g. To test the tendency of EZB to recrystallization we performed an additional DSC experiment at lower heating rate, 5 K/min. The DSC curve, obtained from that measurement, shows an exothermic peak corresponding to the crystallization (see Figure 1c). Based on that, we conclude that the material, in the supercooled liquid state, is unstable and recrystallizes relatively easily.

To ensure that the vitrified samples are completely amorphous, X-ray diffraction (XRD) measurements were performed. As seen in Figure 2, the XRD pattern measured

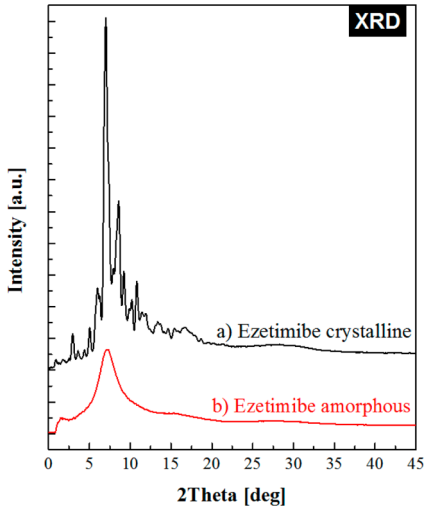

Figure 2. X-ray diffraction patterns for (a) crystalline form of EZB and (b) amorphous EZB measured immediately after quench-cooling of the melt.

immediately after quenching is characterized by a broad amorphous halo, in contrast to that for the crystalline sample, for which numerous sharp Bragg peaks can be observed. This confirms that EZB prepared by the vitrification method is indeed amorphous.

Dielectric Relaxation Studies of Ezetimibe in the Supercooled Liquid State. Representative dielectric loss spectra of EZB above its glass transition temperature are presented in Figure 3a. There is one well-resolved loss peak, which is connected to the structural relaxation process of EZB. This mode moves toward higher frequency during heating of the sample, which indicates increased molecular mobility. At T > 385 K the dielectric strength of the α-relaxation ($\Delta\varepsilon_\alpha$) begins to rapidly decrease with temperature.

$\Delta\varepsilon_\alpha$ is proportional to the amount of units participating in the structural relaxation process, so that such a sudden drop in the dielectric strength is attributed to the sample crystallization. This result is in agreement with our DSC measurements, which show that EZB undergoes crystallization at T > 385 K.

From analysis of dielectric loss spectra, we determined the relaxation map for EZB presented in Figure 3b. The structural relaxation time τ_α was calculated from the frequency at the maximum dielectric loss of the α-relaxation ($\tau_\alpha = 1/2\pi f_{max}$). In the supercooled liquid state, the temperature dependence of the α-relaxation times shows the usual non-Arrhenius behavior described by the Vogel−Fulcher−Tammann (VFT) equation:[30−32]

$$\tau_\alpha(T) = \tau_\infty \exp\left(\frac{B}{T - T_0}\right) \quad (1)$$

where τ_∞, T_0, and B are fitting parameters. However, we noticed that the temperature evolution of the relaxation time τ_α for EZB does not conform over the entire experimental temperature range to a single VFT equation. This situation is quite common, encountered previously, for example, in the $\tau_\alpha(T)$ dependences of telmisartan, ibuprofen, salol, and

dx.doi.org/10.1021/mp500498e | Mol. Pharmaceutics 2014, 11, 4280−4290

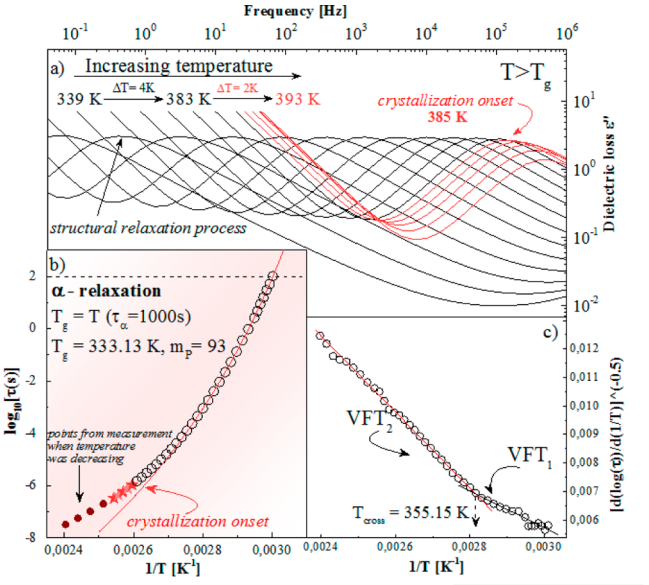

Figure 3. (a) Dielectric loss spectra for EZB collected above T_g. (b) The relaxation map of EZB. The $\tau_\alpha(T)$ dependence, in the selected range, was described by the VFT equation (solid red line). Star symbols show $\tau_\alpha(T)$ in the crystallization range. Crimson points were obtained from measurements performed during cooling of the sample from its melting temperature. (c) The results of the derivative analysis focused on the validity of VFT parametrization. The intersection of the two VFT lines denotes the crossover temperature T_{cross} = 355.15 K.

glycerol.[33−35] For a detailed analysis of the temperature dependence τ_α, we applied the derivative method proposed by Stickel.[36] According to this method, a plot of the values of the derivative operator $[\mathrm{d}\log(\tau_\alpha)/\mathrm{d}(1/T)]^{(-1/2)}$ versus inverse of temperature should be linear for a single VFT function (eq 1). As can be seen in Figure 3c, two distinct linear regions are observed, thus, for EZB two sets of VFT fitting parameters are required to describe the data over the entire temperature range. The first VFT_1 equation, with fitting parameters equal to $\log_{10}(\tau_\infty/\mathrm{s}) = -18.53 \pm 0.55$, $T_0 = 259.46 \pm 2.43$ K, and $B = 3482.99 \pm 209.78$ K, describes the temperature dependence of τ_α below 355.15 K. The $\tau_\alpha(T)$ at temperatures higher than 355.15 K follow VFT_2 with $\log_{10}(\tau_\infty/\mathrm{s}) = -11.81 \pm 0.03$, $T_0 = 301.12 \pm 0.33$ K, and $B = 1129.96 \pm 11.07$ K. The intersection of these two VFT lines, seen in Figure 3c, gives a crossover temperature equal to 355.15 K. In the literature this crossover has been attributed to a strong increase in intermolecular cooperatively.[37] It is of interest that the dynamic crossover between two VFT fits is usually observed around 10^{-6}−10^{-7} s, while in the case of EZB, it is four decades longer (about 10^{-2} s). Similar behavior is found in phenolphthalein dimethyl ether (PDE),[38] which underlines common mechanistic origins of this transformation.

From the VFT_1 parameters we estimated the glass transition temperature of EZB as T_g = 333 K, which is defined as the temperature at which τ_α = 100 s. This value is in good agreement with the glass transition temperature obtained using the DSC technique (T_g = 334 K − see Figure 1c). Additionally, based on the VFT_1 fitting parameters, the fragility m_p (called also steepness index) was calculated using

$$m_p \equiv \left.\frac{\mathrm{d}\log\tau_\alpha}{\mathrm{d}(T_g/T)}\right|_{T=T_g} \quad (2)$$

The typical values of fragility for various materials are in the range from 16 to 200. According to the Angell approach, m_p can be used to classify supercooled liquids into three classes: "strong", "intermediate", and "fragile". The steepness index is of interest for pharmaceutical research dealing with amorphous drugs because it is commonly believed that this parameter may characterize the physical stability of amorphous materials. It is also supported by a theoretical model, the two order parameter (TOP) model proposed by Tanaka.[39] The TOP model assumes that, in any liquid, two competing orderings exist: long-range density ordering connected with the crystallization and short-range bond ordering associated with formation of local favored structures, which have no crystallographic symmetry. The latter comes from hydrogen bonding, covalent bonding, van der Waals interactions, or electrostatic interactions in the substance. According to the TOP model the competition between these long and short orderings leads to energetic frustration of the system, and consequently it affects the behavior of $\tau_\alpha(T)$. Therefore, "strong" liquids are expected to be more physically stable than fragile, because their frustration against crystallization is stronger.

Since the fragility index may play a crucial role in predicting the physical stability of amorphous drugs, much effort has been put into defining this parameter only from thermodynamic variables. The most commonly known empirical relation between the steepness index and thermodynamic properties was proposed by Wang and Angell,[40] and is given by an equation that involves the enthalpy of fusion ΔH_m and the jump in the heat capacity ΔC_p at T_g:

$$m \equiv 56\frac{T_g\Delta C_p}{\Delta H_m} \quad (3)$$

Another, similar correlation has been proposed by Lubchenco and Wolynes:[41]

$$m \equiv 34.7\frac{T_m\Delta C_p}{\Delta H_m} \quad (4)$$

where T_m is the melting temperature. The values of the fragility calculated using both equations are in Table 1.

Table 1. Comparison of the Values of the Fragility Parameter Obtained by Three Different Equations

type of fragility param	eq no.	value of fragility param
steepness index	2	93
by Wang and Angell[39]	3	97
by Lubchenko and Wolynes[40]	4	78

As can be seen, the steepness index calculated from the Wang and Angell method is in good agreement with that from dielectric relaxation. Additionally, the large value of fragility obtained for EZB corresponds with its tendency to recrystallize.

Based on data for various groups of glass-forming materials, Böhmer et al. observed that there is a linear correlation between the fragility parameter and the stretch exponent β_{KWW} of the Kohlrausch−Williams−Watts (KWW) function ($m_{p(corr)}$ = 250(±30) − 320β_{KWW}).[42] According to this rule, the "fragile" material having a large value of m_p should be characterized by a broad α-relaxation peak near T_g, i.e., a small value of β_{KWW}. Thus, from the exponent β_{KWW} one can estimate the steepness index and, consequently, characterize the physical stability of an amorphous drug. This postulate corresponds to the hypothesis

dx.doi.org/10.1021/mp500498e | Mol. Pharmaceutics 2014, 11, 4280−4290

of Shamblin et al. that the distribution of molecular motions described by the β_{KWW} parameter plays a key role in the physical stability of amorphous drugs.[43] It is often considered that faster modes of molecular motions within the distribution of relaxation times can be responsible for nucleation in the glassy state.[44] In order to determine the value of β_{KWW} for EZB, as well as to check whether temperature affects the shape of the α-process, we constructed a master plot (see Figure 4a) by horizontal shifting of spectra (taken at different temperatures from 341 to 357 K) to superimpose on the reference spectrum at 337 K.

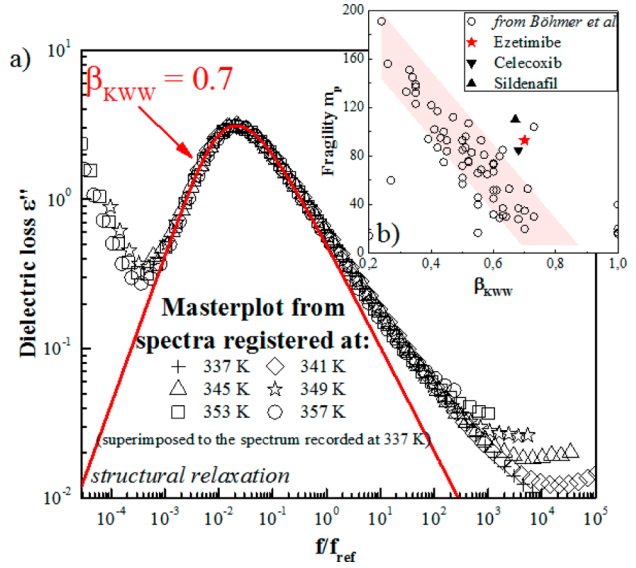

Figure 4. (a) The master plot of EZB formed by horizontally shifting of spectra to overlap that at 337.15 K. The red line represents the KWW fit to the α-peak at 337.15 K with β_{KWW} = 0.7. (b) Comparison of the values of m_p and β_{KWW} for EZB (red star), sildenafil (black triangle), celecoxib (black inverted triangle), and various other compounds (open circles, from Böhmer et al.[42]).

As can be seen, temperature does not influence the shape of the structural loss peak; β_{KWW} equals 0.7 for all spectra. According to the Böhmer correlation, EZB with $m_p = 93 \pm 5$ should have a value of β_{KWW} close to 0.5. However, the actual value is much larger (β_{KWW} = 0.7). Note that similar behavior has been previously observed for other compounds, i.e., sildenafil,[27] celecoxib,[24] and ROY[45] (see Figure 4b).

Crystallization Kinetics Study of Ezetimibe in Supercooled Liquid. As shown above, amorphous EZB is physically unstable and easily undergoes crystallization above T_g. To describe the crystallization kinetics of EZB and determine a value for the crystallization activation energy, we studied the isothermal crystallization process by broadband dielectric spectroscopy. The kinetics of crystallization was measured at several isothermal conditions above T_g: 398.15, 393.15, 388.15, 383.15, 378.15, 373.15, and 368.15 K. For each measurement a new amorphous sample was prepared by the vitrification method. As can be seen in Figures 5a and 5b, the crystallization process can be followed directly in both the real (ε') and imaginary (ε'') parts of the complex dielectric permittivity, reflected by a decrease of the static permittivity and increase in the intensity of the loss peak with time, respectively.

After isothermal recrystallization were completed, the degree of crystallinity was measured by DSC. This confirmed that,

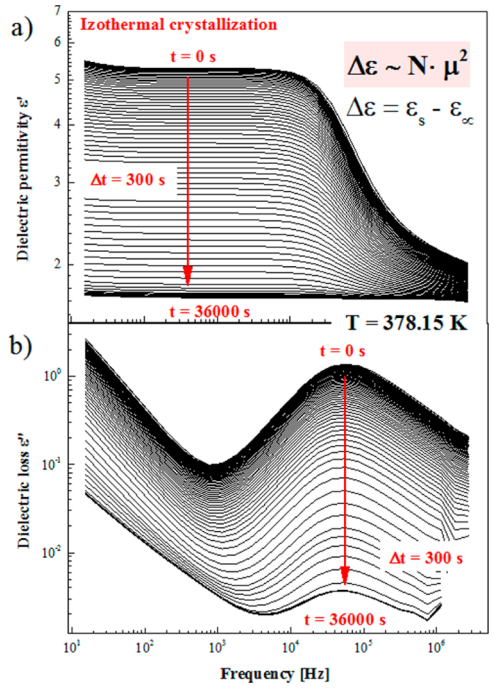

Figure 5. Dielectric spectra of the real (upper panel) and imaginary (lower panel) parts of the complex dielectric permittivity during an isothermal crystallization at 378.15 K.

after each isothermal recrystallization measurement, the degree of crystallization of EZB reached 100%.

Usually the progress of crystallization is analyzed in terms of the normalized real permittivity ε'_N defined as follows:

$$\varepsilon'_N(t) = \frac{\varepsilon'(0) - \varepsilon'(t)}{\varepsilon'(0) - \varepsilon'(\infty)} \quad (5)$$

where $\varepsilon'(0)$ is the initial static dielectric permittivity, $\varepsilon'(\infty)$ is the long-time limiting value, and $\varepsilon'(t)$ is the value at time t. The data, normalized in this way and plotted versus time, are shown in Figure 6a. As can be seen, the entire crystallization process at the highest temperatures (398.15 and 393.15 K) takes no more than 30 min. Since the measurement of a single dielectric spectrum takes ~5 min, we could register only a few spectra during the entire recrystallization. For this reason the dielectric experiments at 398.15 and 393.15 K were performed only at one frequency. On the other hand, the crystallization process at 373.15 and 368.15 K is sufficiently long that during a 20 h BDS experiment we observed no crystallization. Therefore, to investigate the kinetics of crystallization at these temperatures, the samples were first heated to 383.15 K to initialize nucleation.

In addition, the isothermal crystallization kinetics were measured at elevated pressure. This experiment was carried out at 368.15 K. The kinetic curves obtained at this temperature (368.15 K) but different pressures (0.1 and 5 MPa) are compared in Figure 6b. As can be seen, the recrystallization process at 5 MPa starts rapidly without the higher temperature induction, and additionally it occurs much faster when compared to crystallization at 0.1 MPa. Consequently, one can conclude that even low pressure can change drastically the kinetics of crystallization. This finding is of a great importance for future application of amorphous EZB, since compression in the range from 50 to 250 MPa is usually used during the tableting process.

dx.doi.org/10.1021/mp500498e | Mol. Pharmaceutics 2014, 11, 4280−4290

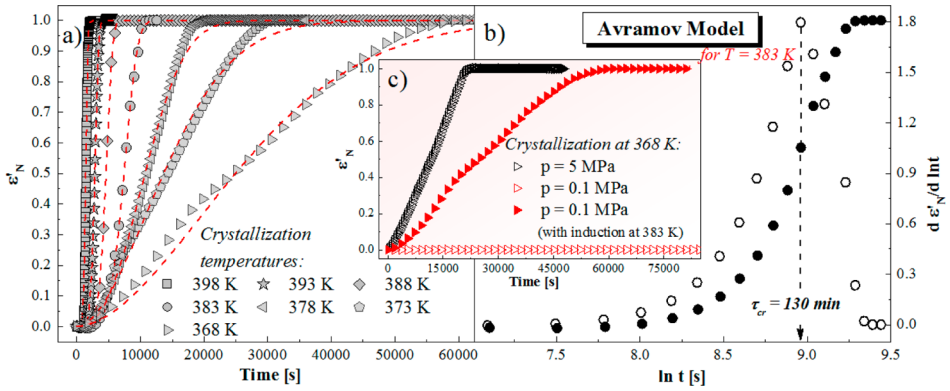

Figure 6. (a) Normalized dielectric constants ε'_N as a function of time from crystallization processes occurring at 398.15, 393.15, 388, 383.15, 378.15, 373.15, and 368.15 K. (b) Time evolution of ε'_N (closed circles) and its first derivative versus the natural logarithm of time (open circles). (c) Comparison of crystallization at the same temperature (368.15 K) but different pressures: 0.1 MPa (closed red triangles) and 5 MPa (black triangles).

The Avrami model is usually applied to describe the crystallization kinetics under isothermal conditions.[46,47] However, in the case of EZB this model is not able to parametrize all the experimental data satisfactorily. For this reason we employed the so-called Avramov model[48] to analyze the time evolution of the normalized real permittivity for EZB. In this approach the dependence of ε'_N together with its first derivative is plotted versus ln t on the same axis (see Figure 6b). The value of τ_{cr}, the characteristic time of the crystallization process, can be determined from the $d(\varepsilon'_N)'/[d(\ln t)]$ peak maximum (this maximum has been found as the highest row data point). Based on the Avramov model we also calculate another parameter that describes the crystallization. This factor, denoted as n, is directly related to the nucleation dimensionality, and its value usually falls in the range of 2−3. In order to calculate n, the following equation was used:

$$n = \frac{(\varepsilon_N')'_{max}}{0.368} \quad (6)$$

where $(\varepsilon_N')'_{max}$ is the maximum of $d(\varepsilon'_N)'/[d(\ln t)]$ dependence. The values of parameters τ_{cr} and n obtained from Avramov analysis are collected in Table 2.

Table 2. Comparison of the values of the Parameters τ_{cr} and n Obtained from the Avramov Model for Different Temperatures of Crystallization

	Avramov model	
temp [K]	n	τ_{cr} [min]
398.15	7.54 ± 0.01	25 ± 1
393.15	7.31 ± 0.05	49 ± 1
388.15	5.86 ± 0.01	80 ± 1
383.15	4.89 ± 0.01	130 ± 1
378.15	3.07 ± 0.01	246 ± 2
373.15	2.31 ± 0.01	372 ± 2
368.15	2.03 ± 0.01	602 ± 2

It can be seen that the value of n becomes higher with increase of crystallization temperature. Moreover, it is significantly larger than usually observed for glass-forming liquids. This suggests that crystallization of EZB is very complicated; other compounds have been characterized by similar values of n, e.g., β-pentaacetylglucose.[49]

To estimate the activation energy barrier for EZB crystallization (E_a), the logarithm of τ_{cr} was plotted versus reciprocal temperature. As seen in Figure 7, the dependence of

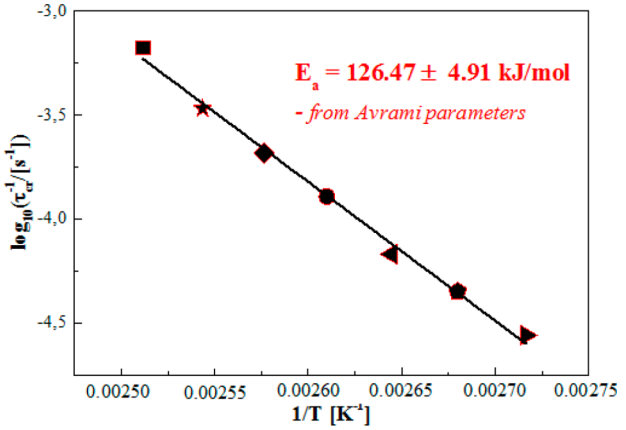

Figure 7. Temperature dependence of the logarithm of τ_{cr}^{-1}. The solid line denotes the linear fit of eq 7.

$\log \tau_{cr}^{-1}$ vs $1000/T$ is linear. Thus, to find the activation energy of EZB crystallization the Arrhenius law can be applied:

$$\log \tau_{cr}^{-1} = \log \tau_{cr0}^{-1} - \frac{E_a}{RT}\log e \quad (7)$$

where τ_{cr0} and E_a are fitting parameters and R is the gas constant. The obtained activation energy E_a = 127.88 ± 4.29 kJ/mol.

Predicting of the Temperature Behavior of Structural Relaxation of EZB in the Glassy State. In the previous sections we investigated the molecular dynamics of EZB in the supercooled liquid state. However, knowledge about the dependence of $\log \tau_\alpha(T)$ measured above the glass transition temperature can be used also to predict the physical stability of amorphous pharmaceuticals below T_g. One of the simplest methods to determine the time scale of structural relaxation in the glassy state is to construct master plots, obtained by horizontal shift of the α-loss peak from the region above T_g to below T_g, where only the right side of the α-peak is detected directly. This procedure is valid only if the shape of the α-mode is almost temperature independent. The structural relaxation

dx.doi.org/10.1021/mp500498e | Mol. Pharmaceutics 2014, 11, 4280−4290

times in the glassy state determined in this way are presented in Figure 8a.

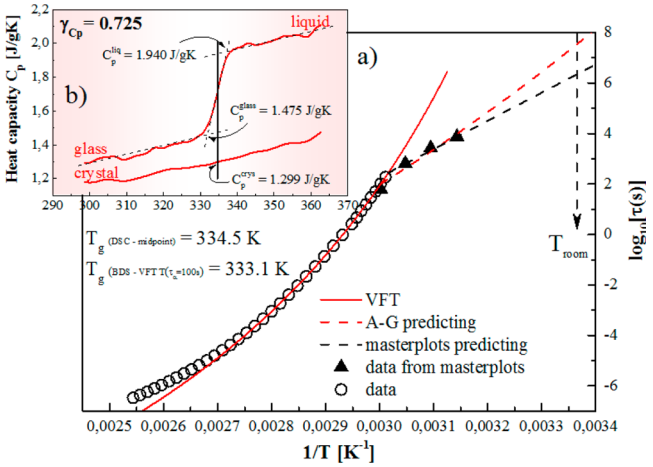

Figure 8. (a) The relaxation map of EZB. Data obtained from BDS measurements (open circles) and from master plots (closed triangles). The solid line presents the VFT fit, while the dashed lines represent the predictions from the AG model (red) and from master plots (black). (b) Temperature dependence of the heat capacity for crystalline and amorphous EZB from TOPEM measurements near T_g.

Another approach to predict the $\tau_\alpha(T)$ dependence below T_g for EZB is based on the modified Adam and Gibbs (AG) equation proposed by Hodge:[50]

$$\tau_\alpha(T, T_f) = \tau_\infty \exp\left(\frac{B}{T(1 - T_0/T_f)}\right) \quad (8)$$

where τ_∞, B, and T_0 are fitting parameters from the VFT equation (eq 1) for the liquid state, and T_f is the so-called fictive temperature defined as

$$\frac{1}{T_f} = \frac{\gamma_{C_p}}{T_g} + \frac{1 - \gamma_{C_p}}{T} \quad (9)$$

where γ_{C_p} is a thermodynamic parameter given as follows:

$$\gamma_{C_p} = \left.\frac{C_p^{liq} - C_p^{glass}}{C_p^{liq} - C_p^{cryst}}\right|_{T=T_g} \quad (10)$$

The values of the heat capacity C_p in the above equation for crystalline (C_p^{cryst}), liquid (C_p^{liq}), and amorphous (C_p^{glass}) EZB were determined at T_g from temperature modulated DSC measurements. As seen in the DSC thermograms (Figure 8b): C_p^{liq} = 1.94 J/(g K), C_p^{glass} = 1.48 J/(g K), and C_p^{cryst} = 1.30 J/(g K) at the glass transition temperature. Based on eq 8 we obtained the $\tau_\alpha(T)$ dependence in the glassy state by using the fitting parameters from the VFT_1 equation and these values of the heat capacity. The τ_α predicted from the AG model are shown in Figure 8a as a red dashed line. As can be seen, the AG model inadequately describes the behavior of EZB below T_g when compared to the data from the master plot. The master plot predicts $\tau_\alpha \approx 10^{6.3}$ s (22 days) at 298.15 K, whereas the time of structural relaxation from the AG approach is $10^{7.38}$ s, which corresponds to 278 days. Based on these predictions we conclude that amorphous EZB will not satisfy the requirement of 3 years stability at room temperature. To verify this result we performed a series of XRD measurements of freshly vitrified, amorphous EZB during its storage at room tempeartature (which is 38 K lower than T_g). XRD measurements after specified periods of time revealed that recrystallization of EZB begins after 14 days. This confirms that the drug is unstable during storage under normal conditions. This motivated us to improve the stability of amorphous EZB as described below.

Dielectric Relaxation Studies of Ezetimibe in the Glassy State. In the glassy state, where the α-relaxation becomes too slow to be experimentally observed, it is possible to monitor faster secondary relaxation processes associated with the local (inter- or intramolecular) motions. It has been shown for many pharmaceuticals, e.g., celecoxib[24] and sildenafil,[27] that this kind of motion is correlated with the physical stability. In order to check whether or not EZB has secondary motions we measured the dielectric spectra below T_g at frequencies from 10^{-1} to 10^6 Hz and at temperatures from 153.15 to 335.15 K. Representative spectra are shown in Figure 9a.

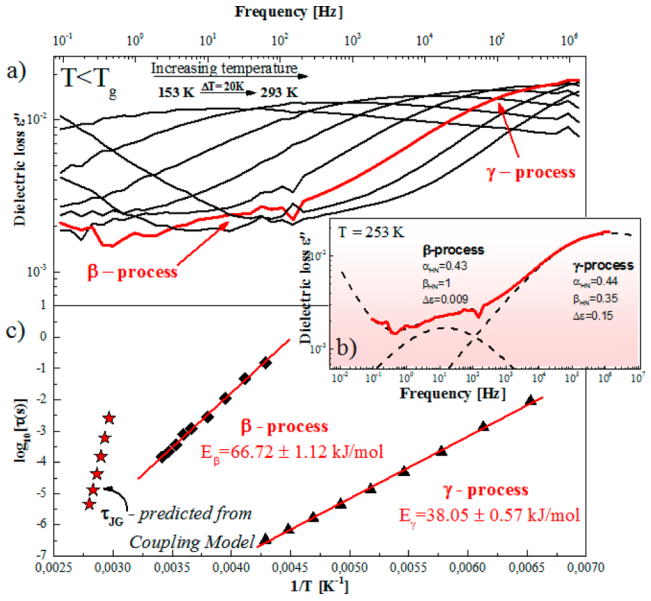

Figure 9. (a) The dielectric loss spectra of EZB at temperatures below T_g. (b) Selected spectra of two visible secondary relaxation processes: β and γ. (c) The temperature dependences of τ_β (black diamonds), τ_γ (black triangles), and found from CM, τ_{JG} (red stars).

It is seen that EZB has two secondary relaxations (β and γ). Both modes move toward lower frequencies on cooling, which indicates decrease in molecular mobility. To determine the values of τ_β and τ_γ, two functions: Cole−Cole (for the β-process) and Havrilak−Nagami (for the γ-process) were fit to the spectra (see Figure 9b). From the fits the temperature dependences of the relaxation times were determined (see Figure 9c). From the Arrhenius dependences of τ_β and τ_γ we determine the value of the activation energies: 66.72 ± 1.12 kJ/mol and 38.05 ± 0.57 kJ/mol for the β-process and γ-process, respectively.

It should be noted that secondary relaxations can be divided into two groups: processes originating from specific motion which involves only a subset of the entire molecule (intramoleular secondary relaxations) and those due to local motion of the entire the molecule (Johari−Goldstein (JG) or intermolecular secondary relaxations). The JG process is believed to be the precursor of structural relaxation.[51]

dx.doi.org/10.1021/mp500498e | Mol. Pharmaceutics 2014, 11, 4280−4290

In order to determine if the secondary relaxations in EZB are the JG type, we applied the coupling model (CM) criteria of Ngai and Paluch.[52] According to this model, the primitive relaxation time τ_0 at several temperatures above T_g is given by

$$\tau_0 = (t_c)^{1-\beta_{KWW}}(\tau_\alpha)^{\beta_{KWW}} \quad (11)$$

where τ_α are taken from the VFT fit, t_c is equal to 2 ps (for small molecules and polymeric glass formers), and β_{KWW} is equal to 0.7 (a previous section). As seen in Figure 9c, the dependence of $\tau_0(T)$, denoted by the stars, agrees with the dependence of neither $\tau_\beta(T)$ nor $\tau_\gamma(T)$, thus neither secondary relaxation in EZB is a JG process. These relaxations have an intramolecular origin. On the other hand, the closer inspection of the primitive relaxation frequency ($f_0 = 1/2\pi\tau_0$) determined at 337.15 K indicates that the maximum of JG-relaxation should lie within the range of frequencies where the departure from the power law of the α-relaxation is observed (see Figure 10).

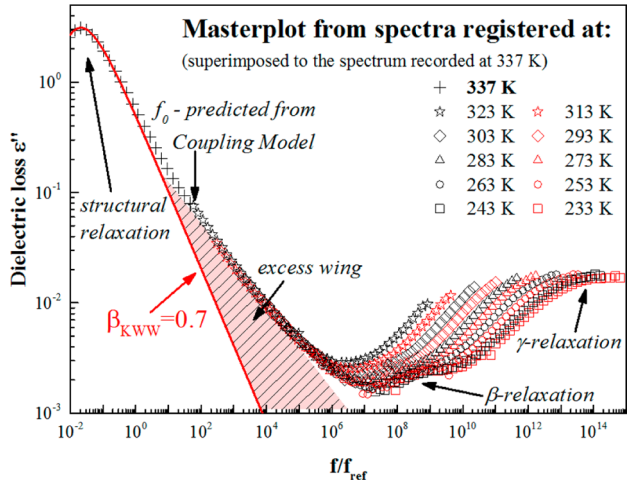

Figure 10. Master plot of EZB formed by horizontally shifting several spectra to overlap the spectrum at 337.15 K. The red line represents the KWW fit to the α-peak at 337.15 K with β_{KWW} = 0.7. The second from the left black arrow denotes the position of the primitive frequency f_0 calculated at 337.15 K using the coupling model.

Since the close proximity of the JG process to the α-relaxation is common,[53] we can assume that the JG process may be hidden under the high frequency flank of the α-relaxation peak and it is manifested by the excess wing.

To shed further light on the secondary relaxations in EZB, we performed DFT calculations. As seen in Figure 11a, the activation energy for motion of the $C_2H_4CHOHC_6H_4F$ group, calculated at the B3LYP/6-31++G(2d,2p) level, is equal to 40 kJ/mol. This value is in good agreement with the activation energy for the γ-process determined from the dielectric measurements. Therefore, we assume that the origin of the γ-relaxation is indeed intramolecular and reflects movements of the $C_2H_4CHOHC_6H_4F$ group.

Effect of Soluplus Polymer on the Physical Stability of Ezetimibe. To enhance the physical stability of amorphous EZB, we used the solid dispersion method to prepare binary mixture containing ezetimibe and 20 wt % Soluplus (EZB–SOP). This commercially available polymer was designed to increase the solubility of amorphous drugs. The sample was dried at 433 K for 1 min; the obtained thermogram of anhydrous SOP is presented in Figure 12.

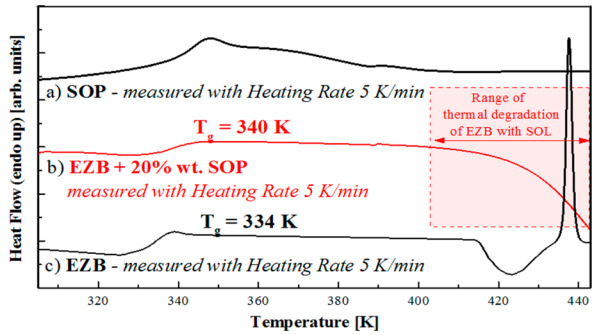

Figure 12. DSC thermograms of (heating rate 5 K/min): (a) pure Soluplus polymer, (b) binary amorphous ezetimibe–20 wt % Soluplus mixture, and (c) pure ezetimibe.

DSC measurements were also obtained of the anhydrous EZB–SOP mixture over temperatures from 300 to 445 K at a

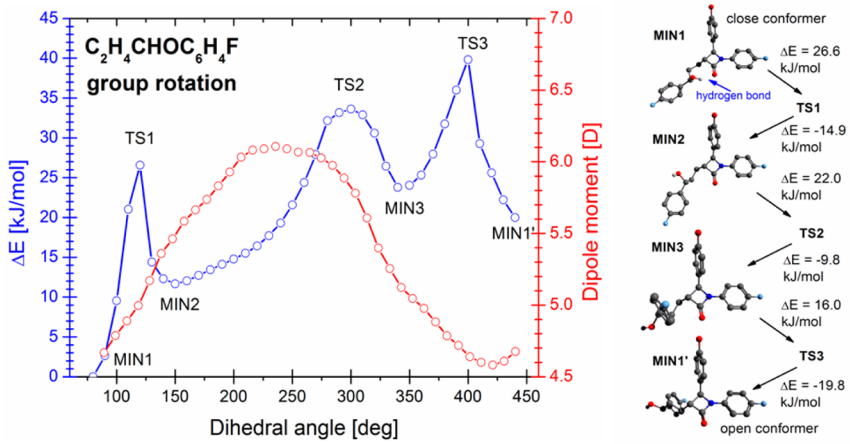

Figure 11. (a) The diagram that represent changes of the energy and magnitude of the dipole moment during rotation of the $C_2H_4CHOHC_6H_4F$ group. The electronic energy surface of these molecules was explored within density functional theory on the B3LYP/6-31G* level. MIN, minimum; TS, transition state. (b) Conformational interconversion during the $C_2H_4CHOHC_6H_4F$ group rotation. All hydrogens (besides the hydrogen bond) are masked for clarity. The energy barriers were calculated using DFT on the B3LYP/6-31++G(2d,2p) level. The minus sign represents the inverse energy change direction.

dx.doi.org/10.1021/mp500498e | Mol. Pharmaceutics 2014, 11, 4280–4290

heating rate of 5 K/min (Figure 12b). From the thermogram, the glass transition temperature of the EZB−SOP mixture equals 340 K. Moreover, we found that this binary system does not recrystallize during heating at 5 K/min, in contrast to pure amorphous EZB. This suggests that SOP stabilizes the EZB drug.

Additionally, we measured dielectric spectra of the EZB−SOP mixture (Figure 13).

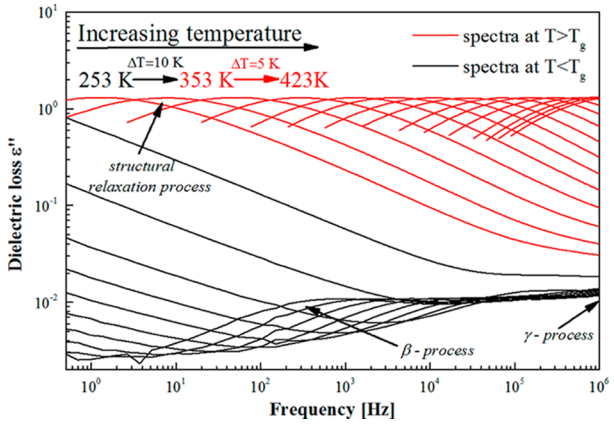

Figure 13. Dielectric loss spectra of EZB with 20 wt % SOP. Red lines are spectra measured above T_g, while black lines are spectra measured below T_g.

As can be seen, no decrease in $\Delta\varepsilon_\alpha$ is obtained, which indicates an absence of crystallization. SOP enhances the stability of amorphous EZB. From analysis of the dielectric spectra we also determined the temperature dependence of the structural relaxation times for the EZB−SOP mixture (Figure 14). We found that the molecular mobility related to the

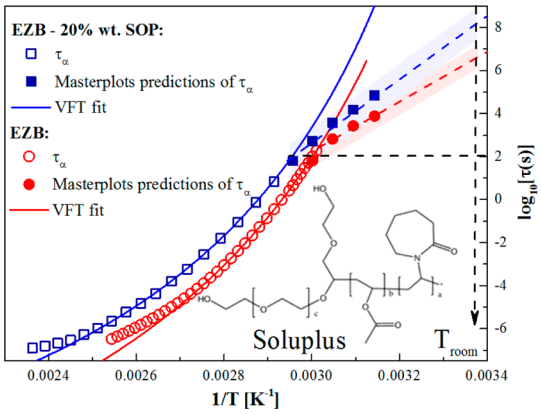

Figure 14. Temperature dependences of the α-relaxation times for pure EZB and EZB−SOP mixture. Solid lines (blue for EZB−SOP and red for pure EZB) are the VFT fits (region above T_g), while the dashed lines (blue for EZB−SOP and red for pure EZB) represent predictions from the master plots (the shadow areas indicate the prediction uncertainties).

structural relaxations of the mixture EZB with 20 wt % SOP is slower than that for pure EZB (T_g of the mixture is greater than T_g of pure EZB). This slower molecular mobility can result in a better physical stability of the mixture.

From fitting the VFT to the $\tau_\alpha(T)$, just like for pure EZB, we are not able to describe the data by a single VFT equation. For this reason we limited the range of temperatures to 393.15 K. The fitting parameters are $\log(\tau_0/s) = -15.8 \pm 0.5$, $A = 2950 \pm 200$, and $T_0 = 266 \pm 3$ K. We estimate the glass transition temperature to equal 338.5 K and the fragility parameter to equal 84. This value is lower than m_p for pure EZB (93), consistent with the assumption that more stable materials have lower values of fragility. In order to predict the structural relaxation times in the glassy state of the binary system, we applied the master curve procedure as in the case of pure EZB. The time estimated from the α-relaxation at room temperatures is $10^{8.1}$ s $\approx$ 4 years. This shows that the physical stability of amorphous EZB improves by mixing with SOP.

Finally, we measured the water solubility of the materials. The amorphous binary mixture of EZB with 20 wt % of SOP has a solubility over 6 times higher than pure crystalline EZB (Table 3). Thus, we conclude that the binary system containing

Table 3. Values of Solubility of Pure Crystalline EZB and EZB−20 Wt % SOP Mixture

	crystalline EZB	EZB−20 wt % SOP
solubility (μg/mL)	6.32	43.15

ezetimibe and SOP, due to its high water solubility and satisfactory stability in the glassy state, is very promising from a therapeutic point of view.

CONCLUSIONS

In this paper, we investigated the relationship between the physical stability and molecular mobility of the amorphous drug ezetimibe. The molecular dynamics were studied by dielectric spectroscopy in both the liquid and glassy states. Based on the analysis of the spectra above the glass transition temperature (T_g = 336 K), we determined the parameters, m_p and β_{KWW}, which characterize the structural α-relaxation process. Both parameters are measures of the physical stability of amorphous systems. Large value of m_p and broad α-peaks (i.e., small values of β_{KWW}) correspond to low stability. Our studies show that the relatively large value of m_p = 93 obtained for EZB corresponds well to its tendency to recrystallize. On the other hand, there is no correlation between the narrow distribution of α-relaxation times of supercooled EZB and its physical stability. In this context, the tested API behaves similarly to sildenafil and celecoxib. Moreover, we investigated the influence of elevated pressure on the recrystallization process of EZB above T_g. We find that pressures as low as 5 MPa significantly accelerate this process. This finding is important because drugs are subjected to elevated pressure during the tableting process.

The physical stability of amorphous pharmaceuticals during their storage at standard conditions (i.e., room temperature and an ambient pressure) is of great interest from an application point of view; we predicted the physical stability of amorphous ezetimibe during its storage at T_{room} = 298 K (which is about 40 K below its T_g). By construction of a master plot for structural relaxation in the glassy state, we determined that the time scale of the α-relaxation is about 14 days at T_{room} = 298 K. This result corresponds well with the storage time of amorphous ezetimibe (determined from long-term isothermal XRD measurements). At longer times glassy EZB begins to recrystallize at room temperature. The suggestion is that structural relaxation can be responsible for the devitrification.

Although the time scale of the α-relaxation correlates with the time for amorphous ezetimibe to recrystallize, we cannot exclude a role of the faster secondary relaxation processes. In

dx.doi.org/10.1021/mp500498e | Mol. Pharmaceutics 2014, 11, 4280−4290

particular the JG process may be responsible for crystal nucleation in the glass. However, glassy EZB is characterized by two secondary relaxations, which have an intramolecular origin (i.e., are not JG processes).

In order to enhance the stability of amorphous EZB, the binary amorphous mixture containing 20 wt % Soluplus (SOP) was prepared. We found that SOP inhibits recrystallization of ezetimibe. By construction of a master plot for structural relaxation of the binary mixture, we predicted that the stability of amorphous EZB in the SOP matrix exceeds 4 years at room temperature. Moreover, we found that 20 wt % SOP not only improves the physical stability of EZB but also significantly increases (>6 times) the solubility of the drug in comparison with EZB in the crystalline form. Thus, the binary amorphous mixture of EZB−20 wt % SOP has potential in the pharmaceutical industry.

■ AUTHOR INFORMATION

Corresponding Author

*E-mail: jknapik@us.edu.pl.

Notes

The authors declare no competing financial interest.

■ ACKNOWLEDGMENTS

The authors Z.W., K.G., M.P., K.W., and W.S. are grateful for the financial support of the National Science Centre within the Opus3 project (Grant No. DEC-2012/05/B/NZ7/03233). Z.W. acknowledges financial assistance from FNP START (2014). The authors wishes to express their thanks for the critical reading of the manuscript by C. M. Roland, Naval Research Laboratory Washington.

■ REFERENCES

(1) Hokanson, J. E.; Austin, M. A. Plasma Triglyceride Level is a Risk Factor for Cardiovascular Disease Independent of High-Density Lipoprotein Cholesterol Level: A Metaanalysis of Population-Based Prospective Studies. *J. Cardiovasc. Risk* **1996**, *3*, 213−219.

(2) Gordon, D. J.; Probstfield, J. L.; Garrison, R. J.; Neaton, J. D.; Castelli, W. P.; Knoke, J. D.; Jacobs, D. R., Jr; Bangdiwala, S.; Tyroler, H. A. High-density lipoprotein cholesterol and cardiovascular disease. Four prospective American studies. *Circulation* **1989**, *79*, 8−15.

(3) Garcia-Calvoa, M.; Lisnocka, J. M.; Bulla, H. G.; Hawesc, B. E.; Burnettc, D. A.; Braunc, M. P.; Cronac, J. H.; Davis, H. R.; Deanc, D. C.; Detmersc, P. A.; Grazianoc, M. P.; Hughesa, M.; MacIntyrec, D. E.; Ogawac, A.; O'Neillc, K. O.; Iyerc, S. P. N.; Shevellc, D. E.; Smithc, M. M.; Tangc, Y. S.; Makarewiczc, A. M.; Ujjainwallac, F.; Altmannc, S. W.; Chapmanc, K. T.; Thornberrya, N. A. The target of ezetimibe is Niemann−Pick C1-Like 1 (NPC1L1). *Proc. Natl. Acad. Sci. U.S.A.* **2004**, *102*, 8132−8137.

(4) Taylor, A. J.; Villines, T. C.; Stanek, E. J.; Devine, P. J.; Griffen, L.; Miller, M.; Weissman, N. J.; Turco, M. Extended-release niacin or ezetimibe and carotid intima-media thickness. *N. Engl J. Med.* **2009**, *361* (22), 2113−2122.

(5) Williams, H. D.; Trevaskis, N. L.; Charman, S. A.; Shanker, R. M.; Charman, W. N.; Pouton, C. W.; Porter, C. J. H. Strategies to Address Low Drug Solubility in Discovery and Development. *Pharm. Rev.* **2013**, *65*, 315−499.

(6) Kaminski, K.; Adrjanowicz, K.; Wojnarowska, Z.; Grzybowska, K.; Hawelek, L.; Paluch, M.; Zakowiecki, D.; Mazgalski, J. Molecular dynamics of the cryomilled base and hydrochloride ziprasidones by means of dielectric spectroscopy. *J. Pharm. Sci.* **2011**, *10*, 22479.

(7) Hancock, B. C.; Parks, M. What is the true solubility advantage for amorphous pharmaceuticals? *Pharm. Res.* **2000**, *17*, 397.

(8) Craig, D. Q. M.; Royall, P. G.; Kett, V.; Hopton, M. The relevance of the amorphous state to pharmaceutical dosage forms: glassy drugs and freeze dried systems. *Int. J. Pharm.* **1999**, *179*, 179−207.

(9) Adrjanowicz, K.; Kaminski, K.; Paluch, M.; Wlodarczyk, P.; Grzybowska, K.; Wojnarowska, Z.; Hawelek, L.; Sawicki, W.; Lepek, P.; Lunio, R. Dielectric relaxation studies and dissolution behavior of amorphous verapamil hydrochloride. *J. Pharm. Sci.* **2010**, *99*, 828−839.

(10) Yoshioka, M.; Hancock, B. C.; Zografi, G. Crystallization of indomethacin from the amorphous state below and above its glass transition temperature. *J. Pharm. Sci.* **1994**, *83*, 1700.

(11) Saleki-Gerhardt, A.; Zografi, G. Nonisothermal and Isothermal Crystallization of Sucrose from the Amorphous State. *Pharm. Res.* **1994**, *11*, 1166.

(12) Zhou, D.; Geoff, G.; Zhang, Z.; Law, D.; Grant, D.; Schmitt, E. A. Thermodynamics, molecular mobility and crystallization kinetics of amorphous griseofulvin. *Mol. Pharmaceutics* **2008**, *5*, 927.

(13) Bhugra, C.; Pikal, M. J. Role of thermodynamic, molecular, and kinetic factors in crystallization from the amorphous state. *J. Pharm. Sci.* **2008**, *97*, 1329−1349.

(14) Wojnarowska, Z.; Grzybowska, K.; Adrjanowicz, K.; Kaminski, K.; Paluch, M.; Hawelek, L.; Wrzalik, R.; Dulski, M.; Sawicki, W.; Mazgalski, J.; Tukalska, A.; Bieg, T. Study of the Amorphous Glibenclamide Drug: Analysis of the Molecular Dynamics of Quenched and Cryomilled Material. *Mol. Pharmaceutics* **2010**, *7*, 1692−1707.

(15) Wojnarowska, Z.; Paluch, M.; Pionteck, J. The tautomerization phenomenon of glibenclamide drug monitored by means of volumetric measurements. *J. Chem. Phys.* **2011**, *135*, 214506.

(16) Wojnarowska, Z.; Wlodarczyk, P.; Kaminski, K.; Grzybowska, K.; Hawelek, L.; Paluch, M. On the Kinetics of Tautomerism in Drugs—New Application of Broadband Dielectric Spectroscopy. *J. Chem. Phys.* **2010**, *133*, 094507.

(17) Crowley, K.; Zografi, G. Cryogenic grinding of indomethacin polymorphs and solvates: assessment of amorphous phase formation and amorphous phase physical stability. *J. Pharm. Sci.* **2002**, *91*, 492.

(18) Hancock, B. C.; Shamblin, S. L.; Zografi, G. Molecular mobility of amorphous pharmaceutical solids below their glass transition temperatures. *Pharm. Res.* **1995**, *12*, 799.

(19) Yoshioka, S.; Aso, Y. Correlations between molecular mobility and chemical stability during storage of amorphous pharmaceuticals. *J. Pharm. Sci.* **1007**, *96*, 960.

(20) Shamblin, S. L.; Tang, X.; Chang, L.; Hancock, B. C.; Pikal, M. J. Characterization of the time scales of molecular motion in pharmaceutically important glasses. *J. Phys. Chem. B* **1999**, *103*, 4113−4121.

(21) Adrjanowicz, K.; Wojnarowska, Z.; Grzybowska, K.; Hawelek, L.; Kaminski, K.; Paluch, M.; Kasprzycka, A.; Walczak, K. Molecular dynamics and crystallization phenomenon of supercooled and glassy DNA and RNA nucleosides: β-adenosine, β-thymidine, and β-uridine. *Phys. Rev. E* **2011**, *84*, 051507.

(22) *Broadband Dielectric Spectroscopy*; Kremer, F., Schönhals, A., Eds.; Springer-Verlag: New York, 2003; pp 37−48.

(23) Grzybowska, K.; Paluch, M.; Grzybowski, A.; Wojnarowska, Z.; Hawelek, L.; Kolodziejczyk, K.; Ngai, K. L. Molecular dynamics and physical stability of amorphous anti-inflammatory drug: celecoxib. *J. Phys. Chem. B* **2010**, *114*, 12792−12801.

(24) Grzybowska, K.; Paluch, M.; Wlodarczyk, P.; Grzybowski, A.; Kaminski, K.; Hawelek, L.; Zakowiecki, D.; Kasprzycka, A.; Jankowska - Sumara, I. Enhancement of amorphous celecoxib stability by mixing it with octaacetylmaltose: the molecular dynamics study. *Mol. Pharmaceutics* **2012**, *9* (4), 894−904.

(25) Adrjanowicz, K.; Kaminski, K.; Wojnarowska, Z.; Dulski, M.; Hawelek, L.; Pawlus, S.; Paluch, M. Dielectric Relaxation and Crystallization Kinetics of Ibuprofen at Ambient and Elevated Pressure. *J. Phys. Chem. B* **2010**, *114* (19), 6579−6593.

(26) Adrjanowicz, K.; Grzybowska, K.; Kaminski, K.; Hawelek, L.; Paluch, M.; Zakowiecki, D. Comprehensive studies on physical and chemical stability in liquid and glassy states of telmisartan (TEL): solubility advantages given by cryomilled and quenched material. *Philos. Mag.* **2011**, *91*, 1926−1948.

(27) Kolodziejczyk, K.; Paluch, M.; Grzybowska, K.; Grzybowski, A.; Wojnarowska, Z.; Hawelek, L.; Ziolo, J. D. Relaxation Dynamics and Crystallization Study of Sildenafil in the Liquid and Glassy States. *Mol. Pharmaceutics* **2013**, *10* (6), 2270−2282.
(28) Neese, F. *ORCA—an ab initio density functional and semi-empirical program package, Version 2.8*; University of Bonn: 2006.
(29) *Avogadro: an open-source molecular builder and visualization tool. Version 1.0.3*. http://avogadro.openmolecules.net/.
(30) Vogel, H. Das Temperaturabhangigkeitgesetz der Viskosität von Flüssigkeiten. *J. Phys. Z.* **1921**, *22*, 645−646.
(31) Fulcher, G. S. Analysis of Recent Measurements of the Viscosity of Glasses. *J. Am. Ceram. Soc.* **1925**, *8*, 339−355.
(32) Tammann, G.; Hesse, W. Die Abhängigkeit der Viscosität von der Temperatur bie unterkühlten Flüssigkeiten. *Z. Anorg. Allg. Chem.* **1926**, *156*, 245−257.
(33) Bras, A. R.; Noronha, J. P.; Antunes, A. M. M.; Cardoso, M. M.; Schonhals, A.; Affouard, F.; Dionisio, M.; Correia, N. T. Molecular Motions in Amorphous Ibuprofen As Studied by Broadband Dielectric Spectroscopy. *J. Phys. Chem. B* **2008**, *112*, 11087−11099.
(34) Adrjanowicz, K.; Wojnarowska, Z.; Wlodarczyk, P.; Kaminski, K.; Paluch, M.; Mazgalski, J. Molecular mobility in liquid and glassy states of Telmisartan (TEL) studied by Broadband Dielectric Spectroscopy. *Eur. J. Pharm. Sci.* **2009**, *38*, 395.
(35) *Broadband Dielectric Spectroscopy*; Kremer, F.; Schönhals, A., Eds.; Springer-Verlag: New York, 2003; pp 109−115.
(36) Stickel, F.; Fischer, E. W.; Richert, R. Dynamics of glass-forming liquids. I. Temperature-derivative analysis of dielectric relaxation data. *J. Chem. Phys.* **1995**, *102*, 6251.
(37) Casalini, R.; Ngai, K. L.; Roland, C. M. Connection between the high-frequency crossover of the temperature dependence of the relaxation time and the change of intermolecular coupling in glass-forming liquids. *Phys. Rev. B* **2003**, *68*, 014201.
(38) Paluch, M.; Casalini, R.; Roland, C. M. Cohen-Grest model for the dynamics of supercooled liquids. *Phys. Rev. E* **2003**, *67*, 021508.
(39) Tanaka, H. Relationship among glass-forming ability, fragility, and short-range bond ordering of liquids. *J. Non-Cryst. Solids* **2005**, *351*, 678−690.
(40) Wang, L.-M.; Angell, C. A. Response to "Comment on 'Direct determination of the fragility indexes of glassforming liquids by differential scanning calorimetry. Kinetic vs thermodynamic fragilities'". *J. Chem. Phys.* **2003**, *118*, 10353−10355.
(41) Lubchenko, V.; Wolynes, P. G. J. *Chem. Phys.* **2003**, *119*, 9088−9105.
(42) Böhmer, R.; Ngai, K. L.; Angell, C. A.; Plazek, D. J. Nonexponential relaxations in strong and fragile glass formers. *J. Chem. Phys.* **1993**, *99*, 4201.
(43) Shamblin, S. L.; Tang, X.; Chang, L.; Hancock, B. C.; Pikal, M. J. Characterization of the time scales of molecular motion in pharmaceutically important glasses. *J. Phys. Chem. B* **1999**, *103*, 4113−4121.
(44) Tombari, E.; Ferrari, C.; Johari, G. P.; Shanker, R. M. *J. Phys. Chem. B* **2008**, *112*, 10806−10814.
(45) Sun, Y.; Xi, H.; Ediger, M. D.; Richert, R.; Yu, L. Diffusion-controlled and "diffusionless" crystal growth near the glass transition temperature: Relation between liquid dynamics and growth kinetics of seven ROY polymorphs. *J. Chem. Phys.* **2009**, *131*, 074506.
(46) Avrami, M. Kinetics of Phase Change. I General Theory. *J. Chem. Phys.* **1939**, *7*, 1103.
(47) *Broadband Dielectric Spectroscopy*; Kremer, F., Schönhals, A., Eds.; Springer-Verlag: New York, 2003; pp 338−343.
(48) Avramov, I.; Avramova, K.; Russel, C. New Method to Analyze Data on Overall Crystallization Kinetics. *J. Cryst. Growth* **2005**, *285*, 394−399.
(49) Kaminski, K.; Adrjanowicz, K.; Wojnarowska, Z.; Paluch, M.; Kaminska, E.; Kasprzycka, A. Do intermolecular interactions control crystallization abilities of glass forming liquids? *J. Phys. Chem. B* **2011**, *115* (40), 11537−11547.
(50) Hodge, I. M. Effects of annealing and prior history on enthalpy relaxation in glassy polymers. 6. Adam−Gibbs formulation of nonlinearity. *Macromolecules* **1987**, *20*, 2897.
(51) Johari, G. P.; Kim, S.; Shanker, R. M. Dielectric study of equimolar acetaminophen-aspirin, acetaminophen-quinidine, and benzoic acid-progesterone molecular alloys in the glass and ultra-viscous states and their relevance to solubility and stability. *J. Pharm. Sci.* **2010**, *99*, 1358−1374.
(52) Ngai, K. L.; Paluch, M. Classification of secondary relaxation in glass-formers based on dynamic properties. *J. Chem. Phys.* **2004**, *120*, 857−873.
(53) *Broadband Dielectric Spectroscopy*; Kremer, F., Schönhals, A., Eds.; Springer-Verlag: New York, 2003; p 124.

Dr Żaneta Wojnarowska
Instytut Fizyki
Uniwersytet Śląski
Zakład Biofizyki i Fizyki Molekularnej
ul. 75 Pułku Piechoty 1A, 41-500 Chorzów

Chorzów, 02.05.2016r.

OŚWIADCZENIE

Oświadczam, że w pracy:

Knapik J., Wojnarowska Z., Grzybowska K., Hawełek L, Sawicki W., Włodarski K., Markowski J., Paluch M. *Physical Stability of the Amorphous Anticholesterol Agent (Ezetimibe): The Role of Molecular Mobility.* Mol. Pharmaceuticals 2014, 11, 4280–4290

mój udział polegał na wykonaniu części badań dielektrycznych.

Z. Wojnarowska
.....

Podpis

Dr Katarzyna Grzybowska
Instytut Fizyki
Uniwersytet Śląski
Zakład Biofizyki i Fizyki Molekularnej
ul. 75 Pułku Piechoty 1A, 41-500 Chorzów

Chorzów, 02.05.2016r.

OŚWIADCZENIE

Oświadczam, że w pracy:

Knapik J., Wojnarowska Z., Grzybowska K., Hawełek L, Sawicki W., Włodarski K., Markowski J., Paluch M. *Physical Stability of the Amorphous Anticholesterol Agent (Ezetimibe): The Role of Molecular Mobility.* Mol. Pharmaceuticals 2014, 11, 4280–4290

mój udział polegał na nadzorowaniu przeprowadzonych analiz, dyskusji otrzymanych wyników oraz korekcji tekstu manuskryptu

Katarzyna Grzybowska
.....

Podpis

Dr Łukasz Hawełek

Instytut Metali Nieżelaznych

ul. Sowińskiego 5

44-100 Gliwice

Gliwice, 02.05.2016r.

OŚWIADCZENIE

Oświadczam, że w pracy:

Knapik J., Wojnarowska Z., Grzybowska K., Hawełek L, Sawicki W., Włodarski K., Markowski J., Paluch M. *Physical Stability of the Amorphous Anticholesterol Agent (Ezetimibe): The Role of Molecular Mobility.* Mol. Pharmaceuticals 2014, 11, 4280–4290

mój udział polegał na wykonaniu pomiarów i analizie wyników dyfrakcji rentgenowskiej.

.....

Podpis

Prof. zw. dr hab. Marian Paluch
Instytut Fizyki
Uniwersytet Śląski
Zakład Biofizyki i Fizyki Molekularnej
ul. 75 Pułku Piechoty 1A, 41-500 Chorzów

Chorzów, 02.05.2016r.

OŚWIADCZENIE

Oświadczam, że w pracy:

Knapik J., Wojnarowska Z., Grzybowska K., Hawełek L, Sawicki W., Włodarski K., Markowski J., Paluch M. *Physical Stability of the Amorphous Anticholesterol Agent (Ezetimibe): The Role of Molecular Mobility.* Mol. Pharmaceuticals 2014, 11, 4280–4290

mój udział polegał na uczestnictwie w dyskusji wyników oraz korekcji manuskryptu.

.....

Podpis

3.2 A2 – Knapik J., Wojnarowska Z., Grzybowska K., Jurkiewicz K., Tajber L., Paluch M. *Molecular Dynamics and Physical Stability of Coamorphous Ezetimib and Indapamide Mixtures.* Mol. Pharmaceuticals 2015, 12, 3610–3619.

Impact Factor czasopisma z roku opublikowania pracy: **4.384**.

Liczba punktów ministerialnych MNiSW czasopisma z roku opublikowania pracy: **45 pkt**.

DOI: **10.1021/acs.molpharmaceut.5b00334**.

Udział pierwszego autora w poniżej załączonym artykule polegał koordynowaniu oraz zaplanowaniu eksperymentu, wykonaniu pomiarów dielektrycznych oraz kalorymetrycznych, analizie wszystkich otrzymanych wyników (za wyjątkiem FTIR) oraz przygotowaniu manuskryptu. Wkład pozostałych współautorów, w formie oświadczeń, zamieszczono na końcu artykułu.

molecular pharmaceutics

Article

pubs.acs.org/molecularpharmaceutics

Molecular Dynamics and Physical Stability of Coamorphous Ezetimib and Indapamide Mixtures

J. Knapik,[*,†,‡] Z. Wojnarowska,[†,‡] K. Grzybowska,[†,‡] K. Jurkiewicz,[†,‡] L. Tajber,[§] and M. Paluch[†,‡]

[†]Institute of Physics, University of Silesia, ul. Uniwersytecka 4, 40-007 Katowice, Poland

[‡]SMCEBI, ul. 75 Pułku Piechoty 1a, 41-500 Chorzów, Poland

[§]School of Pharmacy and Pharmaceutical Sciences, Trinity College Dublin, College Green, Dublin 2, Ireland

ABSTRACT: Low physical stability is the main reason limiting the widespread use of amorphous pharmaceuticals. One approach to overcome this problem is to mix these drugs with various excipients. In this study coamorphous drug−drug compositions of different molar ratios of ezetimib and indapamid (i.e., EZB 10:1 IDP, EZB 5:1 IDP, EZB 2:1 IDP, EZB 1:1 IDP and EZB 1:2 IDP) were prepared and investigated using differential scanning calorimetry (DSC), broadband dielectric spectroscopy (BDS), and X-ray diffraction (XRD). Our studies have shown that the easily recrystallizing ezetimib drug can be significantly stabilized in its amorphous form by using even a small amount of indapamid (8.8 wt %). DSC experiments indicate that the glass transition temperature (T_g) of the tested mixtures changes with the drug concentration in accordance with the Gordon−Taylor equation. We also investigated the effect of indapamid on the molecular dynamics of the ezetimib. As a result it was found that, with increasing indapamid content, the molecular mobility of the binary drug−drug system is slowed down. Finally, using the XRD technique we examined the long-term physical stability of the investigated binary systems stored at room temperature. These measurements prove that low-molecular-weight compounds are able to significantly improve the physical stability of amorphous APIs.

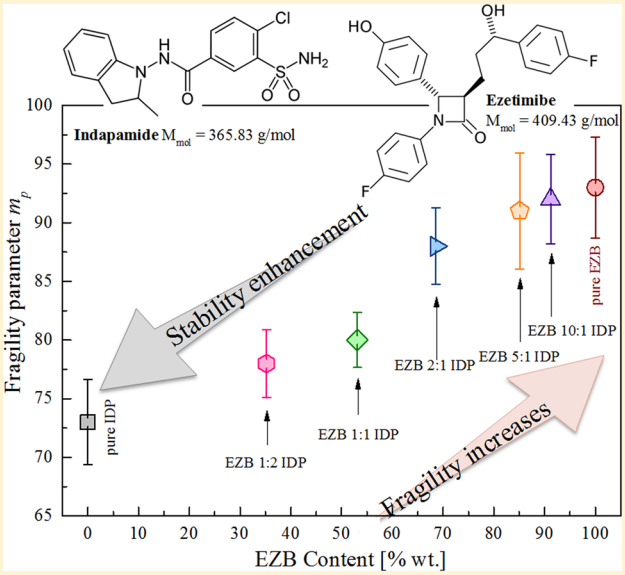

KEYWORDS: *ezetimibe, indapamide, coamorphous mixture, drug−drug mixture, molecular dynamics, glass transition, physical stability*

INTRODUCTION

In recent years, amorphous drugs have become the subject of considerable interest due to their favorable properties such as higher apparent solubility, faster dissolution rate, and potentially better bioavailability when compared to their crystalline counterparts.[1−4] Although the benefits of amorphous pharmaceuticals are unquestionable, it should be pointed out that these materials are thermodynamically unstable. Consequently, during manufacturing or storage they may revert to the crystalline form and lose their superior properties.[5−7] Thus, to fully exploit the advantages given by drugs in the disordered state it is necessary to stabilize them in the amorphous form.[8]

Currently, the most effective strategy to suppress devitrification of amorphous active pharmaceutical ingredients (APIs) is to mix them with various excipients.[9−11] The mechanisms responsible for the stabilization of drugs in binary systems remain still unclear, however it is generally believed that the antiplasticizing effect exerted by an additive as well as the specific molecular interactions between drug and excipient may play crucial roles.[12,13]

Until recently, polymers with high glass transition temperature (T_g) were the most frequently recommended crystallization inhibitors.[14] However, due to the limited solubility of some drugs in polymeric matrix as well as other drawbacks of drug−polymer systems (e.g., difficulties in pulverization or poor compressibility), researchers are trying to find new, more effective stabilizers.[15,16] Currently, binary amorphous mixtures comprising low-molecular-weight compounds instead of polymers have become the subject of significant interest.[17−19] Numerous experimental studies have consistently shown that small molecules such as saccharides or other APIs can improve the physical stability of easily recrystalling amorphous pharmaceuticals more effectively than polymers.[20−22] Allesø et al. and Löbmann et al. reported that even very unstable drugs such as naproxen can be significantly stabilized by using another

Received: April 29, 2015
Revised: August 21, 2015
Accepted: August 24, 2015
Published: August 24, 2015

DOI: 10.1021/acs.molpharmaceut.5b00334
Mol. Pharmaceutics 2015, 12, 3610−3619

amorphous pharmaceutical: cimetidine or indomethacin.[23,24] It should be pointed out that appropriate coamorphous combinations of two drugs can give a lot of benefits. Beyond improving water solubility and physical stability, the second API may improve the therapeutic effect and consequently bring economic advantages: cheaper production associated with smaller quantities of drugs and excipients, one production line, and one packing.

The present study deals with the coamorphous combination of two drugs, i.e., the cholesterol-lowering ezetimibe (EZB) and indapamid (IDP), that is commonly used for the treatment of hypertension. The binary amorphous EZB−IDP mixture is interesting for multiple reasons. First, such composition may provide a therapeutic advantage in the treatment of combined hypertension and hypercholesterolemia, as medical studies indicate that abnormal lipids and high blood pressure frequently coexist and both are the main risk factors for cardiovascular disease.[25−27] Second, both EZB and IDP belong to class II drugs according to the Biopharmaceutics Classification System (BCS), which means that their bioavailability is limited due to their low water solubility.[28,29] Consequently, transformation of these APIs into their amorphous, more soluble forms is expected to enhance their bioavailability. Third, the dosing intervals are very similar for EZB and IDP, i.e., both drugs should be administered once daily, which justifies a need for preparing such binary mixtures.[30,31] Ultimately, it is anticipated that a suitable stoichiometric combination of EZB with IDP will lead to a high physical stability, which will be beneficial from a manufacturing and storage perspective.

In the present study, binary amorphous mixtures of ezetimib and indapamid in various molar ratios were prepared by quench cooling from the melt. The physicochemical properties of the EZB−IDP compositions were studied by X-ray diffraction (XRD), differential scanning calorimetry (DSC), and FTIR (Fourier transform infrared spectroscopy). Furthermore, the molecular mobility that is generally considered as the main factor governing the physical stability of amorphous materials[32−34] was investigated for mentioned coamorphous drug−drug systems by means of broadband dielectric spectroscopy (BDS). From these results, one can answer the question: how does the IDP content affect the crystallization tendency of binary EZB−IDP mixture? Additionally, the long-term physical stability of EZB−IDP systems was studied by XRD.

EXPERIMENTAL METHODS

Materials. Ezetimibe (M_w = 409.4 g/mol) and indapamide (M_w = 365.8 g/mol) drugs of purity greater than 99% were purchased from Polpharma (Starogard Gdański, Poland) and used as received. These pharmaceuticals are described chemically as (3*R*,4*S*)-1-(4-fluorophenyl)-3-[(3*S*)-3-(4-fluorophenyl)-3-hydroxypropyl]-4-(4-hydroxyphenyl)azetidin-2-one and 4-chloro-*N*-[(2*RS*)-2-methyl-2,3-dihydro-1*H*-indol-1-yl)-3-sulfamoylbenzamide, respectively. Their chemical structures are presented in the inset of Figure 2.

Preparation of Binary Systems. The coamorphous mixtures of EZB and IDP drugs with various molar ratios EZB 10:1 IDP (8.8 wt % of IDP), EZB 5:1 IDP (19.9 wt % of IDP), EZB 2:1 IDP (31.4 wt % of IDP), EZB 1:1 IDP (46.9 wt % of IDP), and EZB 1:2 IDP (64.8 wt % of IDP) were prepared by the quench cooling technique. In order to obtain the homogeneous binary systems prior to the quenching, we have prepared the physical mixtures of these compounds by gentle mixing in a mortar for 5 min. After that we dried these mixtures for 10 min at 373 K to remove the water. This is because the IDP drug that was used in our experiment was hemihydrates. When the samples were dried, the crystalline mixtures were melted in aluminum dishes on a hot plate (CAT M. Zipperer GmbH H 17.5D) at T = 440 K. Time of the sample melting was no longer than 2 min. When the mixtures were fully melted, we vitrified them by fast transfer of the dish from the hot plate to a cold copper plate. The coamorphous binary mixtures of EZB and IDP obtained in the presented way were analyzed immediately after preparation to protect them from moisture.

Differential Scanning Calorimetry (DSC). Thermodynamic properties of pure EZB, pure IDP, EZB 10:1 IDP, EZB 5:1 IDP, EZB 2:1 IDP, EZB 1:1 IDP, and EZB 1:2 IDP were examined using a Mettler-Toledo DSC 1 STAR^e System. The measuring device was calibrated for temperature and enthalpy using zinc and indium standards. The instrument was equipped with an HSS8 ceramic sensor having 120 thermocouples and liquid nitrogen cooling station. Crystallization as well as melting points were determined as the onset of the peak, whereas the glass transition temperature was determined as the midpoint of the heat capacity increment. The samples were measured in an aluminum crucible (40 μL). All measurements were carried out in the range from 298 to 450 K with a variety—5 K/min or 10 K/min—of heating rates.

To obtain accurate temperature dependences of the heat capacity for pure amorphous EZB, IDP, and their binary mixtures, a stochastic temperature-modulated differential scanning calorimetry (TOPEM) method implemented by Mettler-Toledo TOPEM was employed. These measurements were performed in the temperature range from 300 to 390 K with a heating rate of 0.5 K/min.

Attenuated Total Reflection Fourier Transform Infrared Spectroscopy (ATR-FTIR). Infrared spectra were recorded on a PerkinElmer Spectrum One FT-IR spectrometer and evaluated using Spectrum v5.0.1 software. Each spectrum was scanned in the range of 650−4000 cm^{-1} with a resolution of 4 cm^{-1}, and a minimum of four scans were collected and averaged in order to obtain good quality spectra. The spectra were normalized and background corrected.

Broadband Dielectric Spectroscopy (BDS). Dielectric measurements of pure EZB, pure IDP, EZB 10:1 IDP, EZB 5:1 IDP, EZB, EZB 1:1 IDP, and EZB 1:2 IDP were carried out using Novo-Control GMBH Alpha dielectric spectrometer, in the frequency range from 10^{-2} Hz to 10^6 Hz at temperatures from 339 to 423 K with step of 2 K. The temperature was controlled by a Quattro temperature controller with temperature stability better than 0.1 K. Dielectric studies of all samples were performed immediately after fast cooling of the melt in a parallel-plate cell made of stainless steel (diameter 15 mm and a 0.1 mm gap with Teflon spacers).

X-ray Diffraction (XRD). The X-ray diffraction measurements were performed using a Rigaku-Denki D/MAX RAPID II-R diffractometer equipped with a rotating Ag anode ($\lambda_{K\alpha}$ = 0.5608 Å), an incident beam (002) graphite monochromator, and an image plate in the Debye−Scherrer geometry as a detector. The X-ray beam width at the sample was 0.3 mm. The investigated samples were placed inside glass capillaries with a diameter of 1.5 mm and wall thickness of 0.01 mm. The measurements were carried out for the capillaries filled with samples and empty. The diffraction intensity for the empty capillary was then subtracted. The obtained two-dimensional diffraction patterns were converted into one-dimensional

DOI: 10.1021/acs.molpharmaceut.5b00334
Mol. Pharmaceutics 2015, 12, 3610−3619

functions of intensity versus the scattering angle using suitable software.

THERMAL PROPERTIES OF AMORPHOUS MIXTURES OF EZETIMIB AND INDAPAMID DRUGS

The quench-cooled amorphous EZB has a glass transition temperature of 333.5 K, when measured by using DSC with heating rate of 5 K/min. The DSC thermogram, obtained at this heating rate, exhibits an exothermic peak at 415 K corresponding to the sample cold crystallization (see Figure 1). This indicate

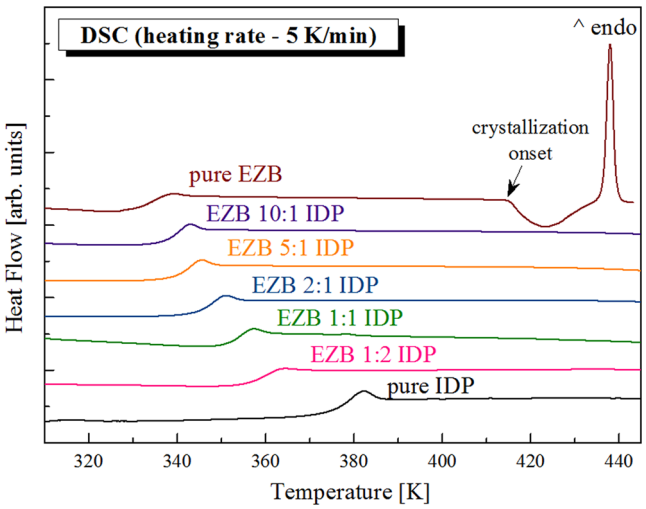

Figure 1. DSC thermograms of (heating rate 5 K/min): pure amorphous EZB drug, red line; binary amorphous EZB 10:1 IDP mixture, purple line; binary amorphous EZB 5:1 IDP mixture, orange line; binary amorphous EZB 2:1 IDP mixture, blue line; binary amorphous EZB 1:1 IDP mixture, green line; binary amorphous EZB 1:2 IDP mixture, pink line; and pure amorphous IDP drug, black line.

that pure amorphous EZB reveals quite strong crystallization tendency above T_g. The opposite behavior occurs for the pure amorphous IDP drug, that has T_g almost 40 K higher than that for EZB. In this case, recrystallization processes were not be observed both below and above the glass transition temperature even with a heating rate as slow as 1 K/min.

In order to find out how the thermal properties of the mentioned drugs will vary when the drugs are mixed together, five coamorphous mixtures containing various molar ratios of EZB and IDP (EZB−IDP: 10:1, 5:1, 2:1, 1:1, 1:2), have been measured using the DSC technique. All these measurements were carried out over the same temperature range, from 298 to 450 K, and at two different heating rates: 5 K/min and 10 K/min. As can be seen in Figure 1, the mixtures containing EZB and IDP are characterized by a single glass transition event which moves toward higher temperatures with IDP content.

These was no evidence of phase separation as there was only a single glass transition event for the binary mixtures. If components are not or are only partially miscible, the DSC curve of an amorphous composition should reveal two separate T_g: one for first component and one for the second component.[35] The values of T_g obtained using the DSC technique are collected in the Table 1.

In Figure 1 we can also observed that all coamorphous compositions do not recrystallize when heated with a rate of 5 K/min. This indicates that even a small content of IDP may significantly suppress the crystallization tendency of EZB. There

Table 1. Comparison of the T_g and ΔC_p Values of Pure EZB and IDP Drugs and Their Binary Amorphous Mixtures at Molar Ratios 10:1, 5:1, 2:1, 1:1, 1:2

		T_g [K]				T_g [K]
EZB−IDP [molar ratio]	wt fraction of IDP [%]	DSC 10 K/min	DSC 5 K/min	TMDSC 0.5 K/min	ΔC_p [J/gK]	predicted-GT
1:0	0	336.4	333.5	334.8	0.47	
10:1	8.8	340.6	338.8	337.9	0.47	337.9
5:1	19.9	343.6	341.3	340.3	0.46	340.3
2:1	31.4	348.1	345.9	345.5	0.46	346.5
1:1	46.9	353.8	353.1	351.4	0.46	352.7
1:2	64.8	360.4	358.8	359.2	0.42	360.0
0:1	100	276.2	375.1	375.4	0.49	

are two possible reasons for such behavior: an antiplasticizing effect exerted by the second drug or specific interactions between compounds, or eventually a combination of both these effects.[36] If the antiplastization effect is dominant, the changes of the glass transition temperatures with compound concentration should correlate with the theoretical dependence that was for the first time proposed by Gordon and Taylor:[37,38]

$$T_g = \frac{w_1 T_{g1} + K w_2 T_{g2}}{w_1 + K w_2} \quad (1)$$

where w_1 and w_2 are the weight fractions of each component, and T_{g1} and T_{g2} correspond to the glass transition temperature of each component. T_g is the glass transition temperature of the mixture, while K is a measure of the interaction between the components, and it can be defined as follows:[39]

$$K \approx \frac{\Delta C_{p2}}{\Delta C_{p1}} \quad (2)$$

ΔC_p in eq 2 denotes the change in heat capacity at T_g.

In order to check whether or not the antiplastization effect is the dominant mechanism responsible for better stability of EZB−IDP systems, the theoretical values of glass transition temperature for mixtures of various IDP content have been calculated by using eq 1. The predicted values of T_g were subsequently compared with the experimentally determined data (see Figure 2). The values of ΔC_p, that are required in eq 2, as well as the values of the experimentally derived T_g were taken from stochastic temperature-modulated differential scanning calorimetry (TMDSC) measurements, where the heating rate was equal to 0.5 K/min.

It can be clearly seen that T_g values grow continuously with increasing IDP content. At 8.8 wt % and 14.9 wt % of IDP the experimentally determined T_g values are in perfect agreement with those calculated theoretically. In the case of higher IDP content (~30 to ~65 wt % of IDP) a slight negative deviation from the predicted glass transition temperatures can be observed. This deviation lies within the range 1−1.5 K. Because the difference between theoretically and experimentally determined T_g values is very small, one can expect that there are no significant molecular interactions between EZB and IDP. Thus, the enhancement of the physical stability of EZB drug is mainly due to the antiplasticizing effect. It is worth noting that small molecules like IDP are able to exert comparable or even better antiplasticizing effects than polymers, due to their high T_g values.

In order to confirm the absence of the specific chemical interactions between both mixed drugs we performed a series of

DOI: 10.1021/acs.molpharmaceut.5b00334
Mol. Pharmaceutics 2015, 12, 3610−3619

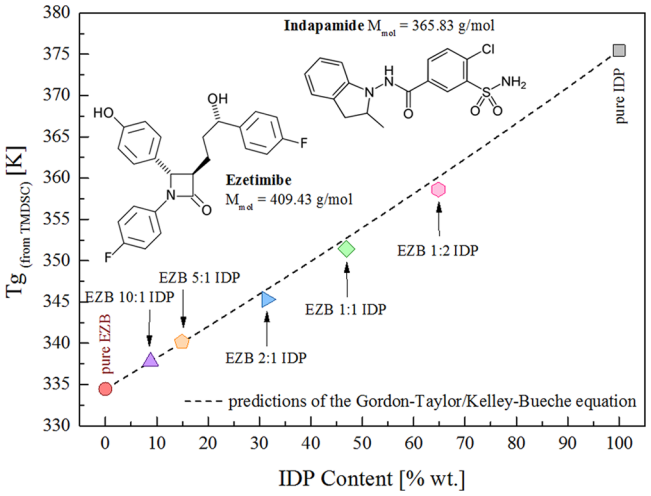

Figure 2. Glass transition temperatures of coamorphous EZB−IDP mixtures. The symbols correspond to the experimentally determined T_g values (heating rate 0.5 K/min), whereas the dashed line represents the prediction of the Gordon−Taylor/Kelley−Bueche equation calculated from the T_g values of the single EZB and IDP drugs. In the inset we present the chemical structures of EZB and IDP.

FTIR experiments. As it can be seen in Figure 3 and Table 2, no considerable shifts of absorption bands associated with H-bonds

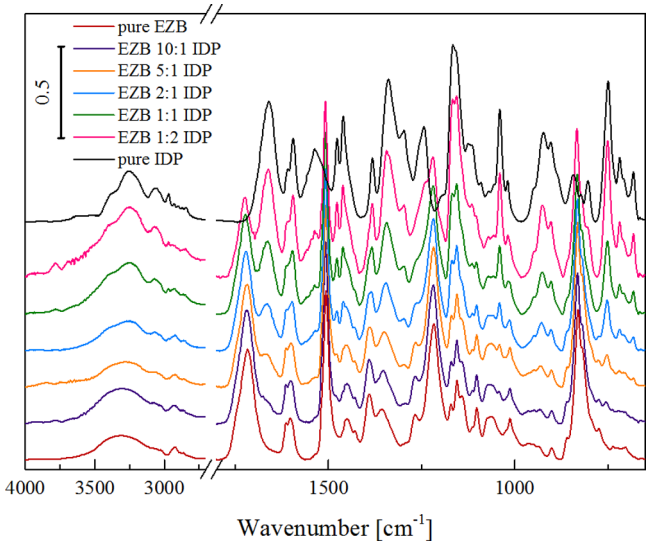

Figure 3. FTIR spectra of binary amorphous mixtures: EZB 10:1 IDP, purple line; EZB 5:1 IDP, orange line; EZB 2:1 IDP, blue line; EZB 1:1 IDP, green line; EZB 1:2 IDP, pink line; and pure EZB and IDP (wine and black lines).

(−C═O and −S═O) and $\pi-\pi$ interactions (−C═C− of aromatic groups) are shown. This result indicates that EZB and IDP did not interact in the amorphous phase.

MOLECULAR DYNAMICS OF AMORPHOUS MIXTURES OF EZETIMIB AND INDAPAMID DRUGS ABOVE THE GLASS TRANSITION

In this section the effects of IDP drug on the molecular dynamics of EZB in their binary amorphous mixture are presented. To experimentally establish how the molecular mobility of coamorphous EZB−IDP composition changes with IDP content, the dielectric loss spectra of five mixtures containing various molar ratios of EZB and IDP were measured by means of broadband dielectric spectroscopy (BDS). In all these measurements, the temperature was increased from 339 to 423 K in step of 2 K. The representative spectra of binary EZB−IDP mixtures containing 46.9, 31.4, and 8.8 wt % of IDP drug are shown in Figures 4a−4c, respectively.

Table 2. Comparison of Absorption Band Positions [cm^{-1}] of Examined Systems: Data from FTIR[a]

assignment	pure EZB	EZB 10:1 IDP	EZB 5:1 IDP	EZB 2:1 IDP	EZB 1:1 IDP	EZB 1:2 IDP	pure IDP
−C═O EZB	1717	1718	1717	1721	1723	1723	N/A
−C═O IDP	N/A	N/A	N/A	1664	1663	1662	1661
−C═C arom EZB	1507	1508	1507	1508	1508	1508	N/A
−C−O EZB	1217	1219	1218	1219	1219	1220	N/A
−S═O sym IDP	N/A	1156	1155	1156	1156	1156	1156

[a]N/A: not analyzed.

The dielectric loss spectra of all examined systems exhibit the same main features: one well-resolved loss peak corresponding to the structural (α) relaxation process as well as dc conductivity. As can be seen, the α-relaxation mode moves toward higher frequencies with heating as well as with increasing of IDP content. Additionally, during heating of the examined samples we do not observe any drop in the intensity of structural relaxation peak that indicates an absence of mixture cold crystallization. According to the literature reports, pure amorphous EZB drug measured in similar conditions begins to recrystallize at a temperature at which the maximum of the α-relaxation is located at frequency equal to 10^5 Hz (what corresponds to $\tau_\alpha = 1.6\ \mu s$).[40] In view of the fact that the mixtures do not begin to crystallize at $\tau_\alpha \sim 1.6\ \mu s$, one can conclude that the enhancement of the EZB physical stability in binary EZB−IDP mixture is governed not only by a kinetic factor (i.e., molecular mobility) but also by a thermodynamical factor (i.e., configurational entropy, enthalpy, or Gibbs free energy).

From analysis of dielectric loss spectra the temperature dependences of α-relaxation times for all examined coamorphous systems were obtained (see Figure 5a). To determine the values of τ_α as well as dc conductivity at various temperatures, the experimental data have been fitted using the Havrilak−Negami (HN) function with the dc conductivity term:[41]

$$\varepsilon^*(\omega) = \varepsilon_\infty + \frac{\Delta\varepsilon}{[1 + (i\,\omega\tau_{HN})^a]^b} + \frac{\sigma_{dc}}{\varepsilon_0\, i\,\omega} \quad (3)$$

where ε_∞ is high frequency limit permittivity, ε_0 denotes the permittivity of vacuum, $\Delta\varepsilon$ is dielectric strength, ω is equal to $2\pi f$, τ_{HN} is the HN relaxation time, and a and b represent symmetric and asymmetric broadening of the relaxation peak. On the basis of fit parameters determined above, the values of τ_α were calculated as[42−44]

$$\tau_\alpha = \tau_{max} = \tau_{HN}\left[\sin\left(\frac{\pi a}{2 + 2b}\right)\right]^{-1/a}\left[\sin\left(\frac{\pi ab}{2 + 2b}\right)\right]^{1/a} \quad (4)$$

DOI: 10.1021/acs.molpharmaceut.5b00334
Mol. Pharmaceutics 2015, 12, 3610−3619

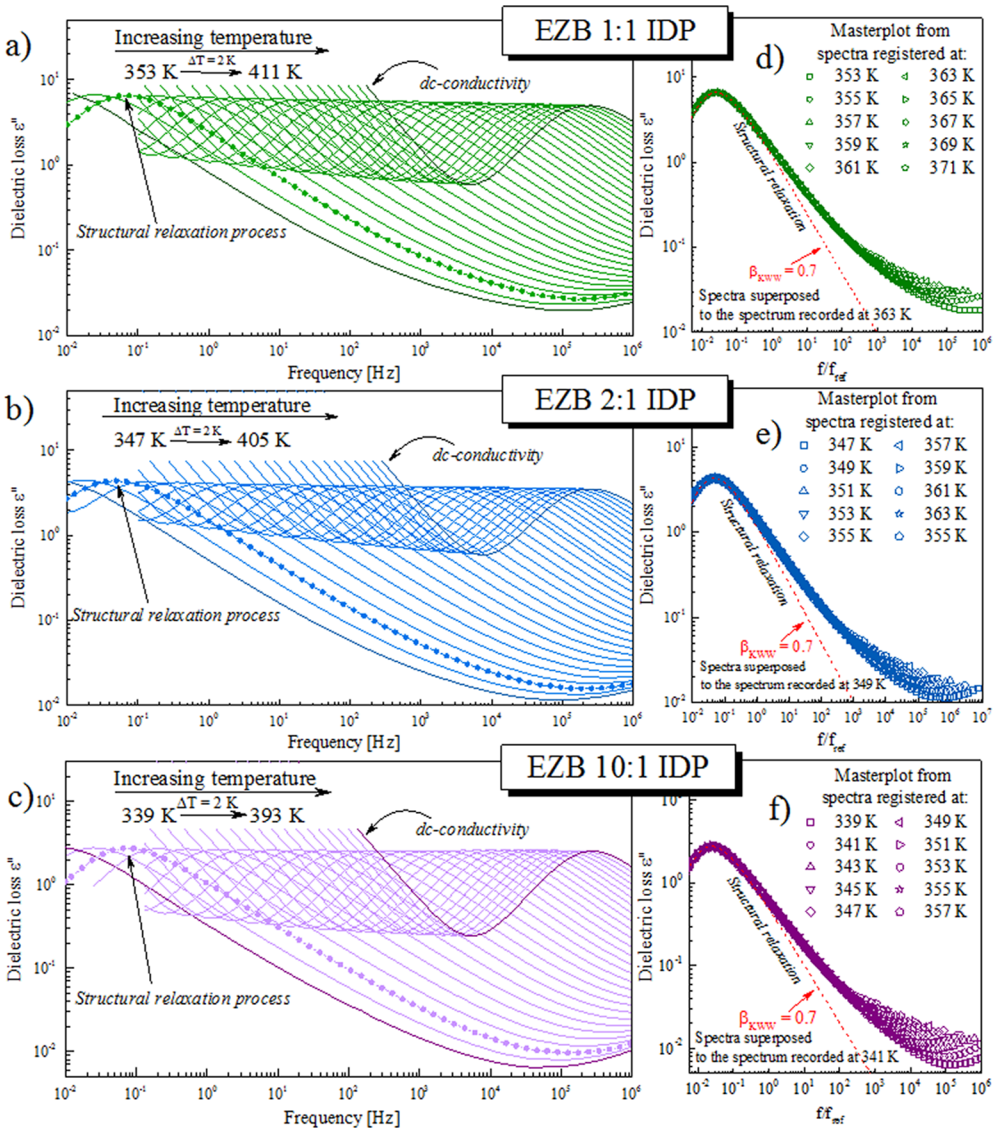

Figure 4. (a–c) Dielectric loss spectra collected above the glass transition temperature of coamorphous EZB–IDP mixtures with molar rations 10:1, 2:1, and 1:1. (d–f) Masterplots for the binary mixtures, EZB 10:1 IDP, EZB 2:1 IDP, EZB 1:1 IDP, that were formed by horizontal shift of arbitrarily chosen spectra to superpose all together with the unshifted spectra at 341 K (for molar ratio 10:1), 349 K (for molar ratio 2:1), and 355 K (for molar ratio 1:1).

In the supercooled liquid region, the $\tau_\alpha(T)$ dependence usually shows non-Arrhenius behavior and follows the Vogel–Fulcher–Tammann (VFT) equation:

$$\tau_\alpha(T) = \tau_\infty \exp\left(\frac{B}{T - T_0}\right) \quad (5)$$

where τ_∞, T_0, and B are fitting parameters.[45−47] Moreover, we found that in the case of pure amorphous samples as well as their mixtures the temperature dependence of structural relaxation time, measured over 8 decades, cannot be described properly by means of a single VFT fit. Thus, to parametrize these data over the entire temperature range, two VFT equations are required. Such behavior is often observed in organic glass-forming materials.[48,49] Good examples of pharmaceuticals that require employing of two VFT equations to describe the τ_α data over wide temperature range are ibuprofen and telmisartan.[50,51]

First we analyzed the relaxation data by applying the derivative method proposed by Stickel.[52] Using this method it is possible to identify the temperature range of validity of both VFT equations. The Stickel method requires the use of the operator $[d(\log(\tau_\alpha))/dT]^{-1/2} = (T - T_0)B^{-1/2}$, which linearized the Vogel–Fulcher–Tammann equation. The results of the derivative analysis are presented in Figure 5b. As can be seen, two distinct linear regions may be observed for all measured samples, confirming the necessity for use of two sets of VFT parameters to describe properly the $\tau_\alpha(T)$ dependences of studied mixtures. The temperature at which the VFT_1 and VFT_2 intersect (T_{cross}) as well as all the fitting parameters are collected in Table 3. Additionally, the VFT_1 fits are shown in Figure 5a as solid lines.

Since the VFT_1 equation describes well the data in the region below the crossover temperature, it was used to estimate the kinetic glass transition temperature of each coamorphous mixture. The T_g values, calculated from commonly known definition $T_g = T(\tau_\alpha = 100\ s)$, are equal to 336.5 K, 339.2 K, 344.9 K, 349.0 K, and 357.8 K for mixtures containing 8.8, 14.9, 31.4, 46.9, and 64.8 wt % of IDP, respectively. These values are slightly smaller than the T_g obtained by using TMDSC (see inset of Figure 6). This little discrepancy between the kinetic and the

DOI: 10.1021/acs.molpharmaceut.5b00334
Mol. Pharmaceutics 2015, 12, 3610–3619

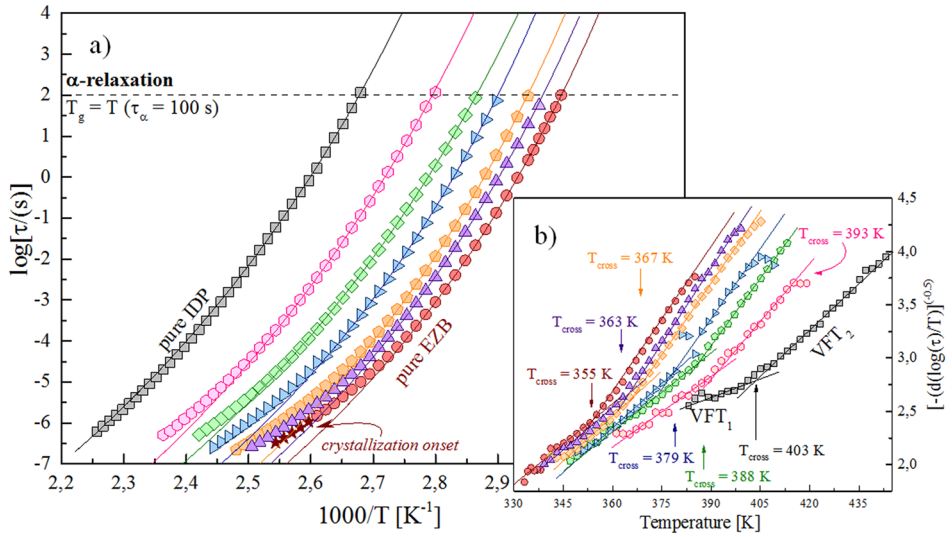

Figure 5. (a) Temperature dependence of the structural relaxation times determined by using the BDS technique for pure amorphous EZB drug (red circles), pure IDP drug (black squares), and their binary mixtures that contain various molar ratios of EZB and IDP: EZB 1:2 IDP (pink hexagons), EZB 1:1 IDP (green diamonds), EZB 2:1 IDP (blue inverted triangles), EZB 5:1 IDP (orange pentagons), and EZB 10:1 IDP (purple triangles). Solid lines (black for pure IDP, pink for EZB 1:2 IDP, green for EZB 1:1 IDP, blue for EZB 1:2 IDP, orange for EZB 5:1 IDP, purple for EZB 10:1 IDP, and red for pure EZB) are the VFT_1 fits. (b) Results of the derivative analysis that was focused on the validity of VFT parameters. The intersection of the two VFT lines in the case of each sample denotes the crossover temperature.

Table 3. Comparison of the Values of T_g Obtained from TMDSC, T_{cross}, and T_g Obtained from BDS, Fragility Parameters, and Fitting Parameters from the VFT_1 and VFT_2 for Pure EZB and IDP Drugs, and Their Binary Amorphous Mixtures at Molar Ratios 10:1, 5:1, 2:1, 1:1, 1:2

			VFT_1 and VFT_2 params			T_g [K]		
EZB–IDP [molar ratio]	wt fraction of IDP [%]	T_{cross} [K]	log τ_0	$B = DT_0$	T_0 [K]	BDS	TMDSC	fragility param m_p
1:0	0	355	−18.5 ± 0.6	3483.0 ± 209.8	259.5 ± 2.4	333.1	334.8	93.0 ± 4.3
			−11.8 ± 0.1	1130.0 ± 11.1	301.1 ± 0.3			
10:1	8.8	363	−19.1 ± 0.5	3767.6 ± 197.9	258.7 ± 2.4	336.5	337.9	92.0 ± 3.8
			−11.7 ± 0.1	1095.7 ± 10.4	305.9 ± 0.3			
5:1	19.9	367	−19.4 ± 0.6	3913.5 ± 273.6	259.7 ± 3.2	339.2	340.3	91.0 ± 4.9
			−11.9 ± 0.1	1171.5 ± 7.1	306.7 ± 0.2			
2:1	31.4	379	−18.5 ± 0.4	3747.3 ± 181.1	265.4 ± 2.2	344.9	345.5	88.0 ± 3.2
			−12.9 ± 0.4	1581.7 ± 157.5	301.3 ± 4.4			
1:1	46.9	388	−19.2 ± 0.3	4553.3 ± 160.3	255.8 ± 1.9	349.0	351.4	80.0 ± 2.3
			−12.3 ± 0.1	1403.2 ± 24.3	312.6 ± 0.7			
1:2	64.8	393	−20.4 ± 0.5	5258.5 ± 266.0	255.8 ± 3.0	357.8	359.2	78.0 ± 2.9
			−13.7 ± 0.3	1958.6 ± 114.7	307.6 ± 2.8			
0:1	100	403	−18.8 ± 0.7	5072.3 ± 352.2	267.4 ± 4.0	373.5	375.4	73.0 ± 3.6
			−15.3 ± 0.2	2906.5 ± 87.1	304.1 ± 1.7			

calorimetric values of T_g is due to different heating rate used in these two different experiments.

Based on the VFT_1 fitting parameters as well as on the values of T_g, determined previously from dielectric relaxation data, we have estimated the fragility parameter m_p (called also steepness index) for all measured systems:[53]

$$m_p = \left.\frac{\mathrm{d}\log\tau_\alpha}{\mathrm{d}(T_g/T)}\right|_{T=T_g} = D\frac{T_0}{T_g}\left(1-\frac{T_0}{T_g}\right)^{-2}\log_{10}\mathrm{e} \quad (6)$$

It should be noted that this parameter is of particular interest for the pharmaceutical industry, because it is often used to predict the tendency of disordered materials toward recrystallization.[54] In the literature the fragility parameter is reported to vary from 16 to 200. But, in the case of APIs, the typical m_p values range between 60 and 120. The compounds characterized by a low value of steepness index are classified as strong materials, whereas a large value of m_p corresponds to fragile systems. According to the two order parameter (TOP) model proposed by Tanaka, strong materials are expected to be more physically stable than fragile materials.[55] This is because they have stronger frustration against crystallization. This frustration of the system results from the competition between long and short ordering existing in any liquids. Long-range ordering is responsible for nucleation and crystal growth, while short-range ordering is associated with formation of the local favored structures that have no crystallographic symmetry. As illustrated in Figure 6, the fragility parameter decreases continuously with increasing IDP content. This result suggests that the physical stability of the examined mixtures should improve with increasing IDP concentration. Since our measurements do not reveal crystallization of coamorphous compositions containing EZB and IDP, the

DOI: 10.1021/acs.molpharmaceut.5b00334
Mol. Pharmaceutics 2015, 12, 3610−3619

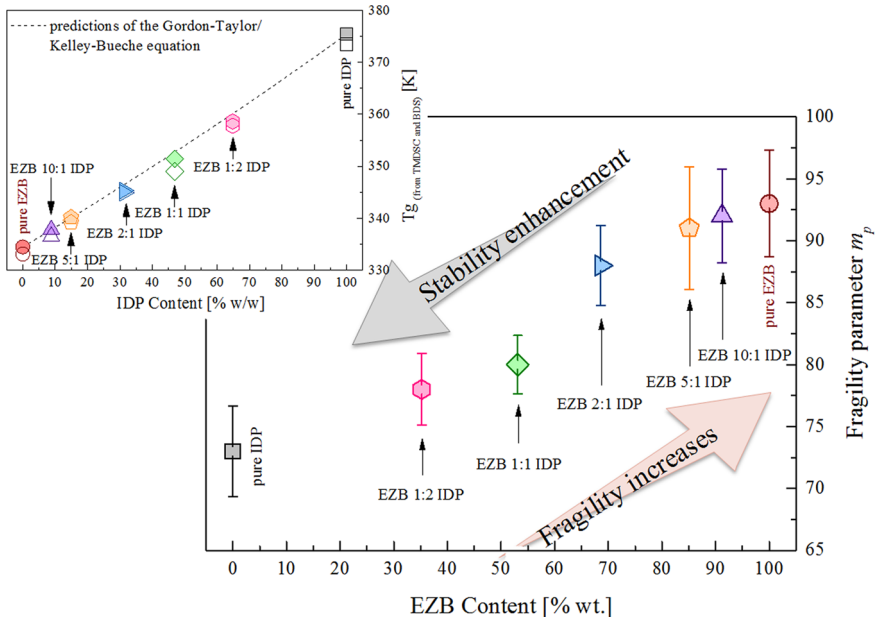

Figure 6. Isobaric fragility parameter estimated from eq 6 plotted versus EZB content. In the inset we compare the glass transition temperatures of coamorphous EZB–IDP mixtures determined by using DSC (filled symbols) and BDS (open symbols) techniques. The dashed line represents the prediction of the Gordon–Taylor/Kelley–Bueche equation.

trend of stability has been checked at elevated temperature (T = 398 K) by means of DSC (see Figure 7). These experiments

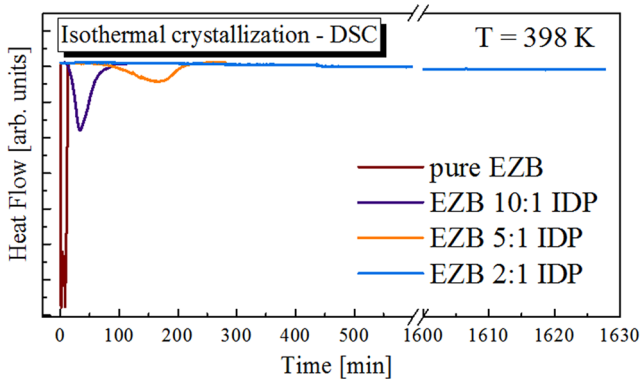

Figure 7. Isothermal crystallization of pure EZB (wine line), EZB 10:1 IDP (purple line), EZB 5:1 IDP (orange line), and EZB 2:1 IDP (blue line) at 398 K.

show that the mixture crystallization slows down with increasing IDP content (exothermic peak is shifted to higher times), which proves that the fragility parameter indeed reflects the physical stability of the examined systems.

An alternative measure of the physical stability of amorphous materials is the β_{KWW} parameter, which describes the distribution of relaxation times.[56] Shamblin et al. have suggested that, when β_{KWW} parameter decreases (i.e., the distribution of relaxation times becomes broader), the tendency of a pharmaceutical to recrystallization should increase. For many drugs this parameter was shown to correctly predict their physical stability. The best examples may be aspirin, ibuprofen, and quinidine.[57]

In order to determine the values of β_{KWW} for the measured binary amorphous EZB–IDP mixtures as well as to check whether or not the temperature affects the shape of the α-relaxation process, the master curves of individual EZB–IDP mixtures were prepared (see Figure 4d–f). They were constructed by horizontal shift of arbitrarily chosen spectra to superpose all together with the reference spectrum recorded at 363 K, 355 K, 349 K, 345 K, and 341 K for mixtures containing 64.8, 46.9, 31.4, 19.9, and 8.8 wt % of IDP, respectively. As can be seen, the shapes of structural relaxation peaks of each EZB–IDP composition do not change with temperature and IDP content. All investigated mixtures have the same value of β_{KWW} parameter equal to 0.7. This value is identical with that for pure amorphous EZB drug. This invariability of the β_{KWW} suggests that the mentioned parameter does not correlate with the physical stability of the herein studied coamorphous mixtures.

LONG-TERM PHYSICAL STABILITY STUDIES OF EZB–IDP COAMORPHOUS MIXTURES

As it was indicated by both BDS and DSC data, the coamorphous mixtures containing EZB and IDP drugs are characterized by greater physical stability than the pure EZB. Naturally, the questions arise: *what is the minimal amount of IDP guaranteeing appropriate physical stability of the amorphous EZB?* and consequently, *how long we can safely store these compositions at room temperature?* In order to answer these questions we have performed time dependent isothermal XRD studies for all investigated binary mixtures. During this experiment samples were kept at constant temperature equal to 297 K and under quasi-constant humidity conditions RH = 25%. On the basis of the obtained X-ray diffraction patterns we determined the relative degree of crystallization D_c for all measured samples. The values of D_c for each sample were determined as a ratio: A_p/A_c, where A_p and A_c are areas under the sharp XRD peaks of the partly crystalline sample and the crystalline reference sample, respectively. The values of D_c plotted versus time of storage as well as the representative XRD patterns are presented in the Figure 8.

As can be seen, the X-ray diffraction patterns for the initially amorphous compounds are characterized by broad amorphous halos which confirm that in the investigated samples there were no three-dimensional long-range ordered structures. This finding

DOI: 10.1021/acs.molpharmaceut.5b00334
Mol. Pharmaceutics 2015, 12, 3610–3619

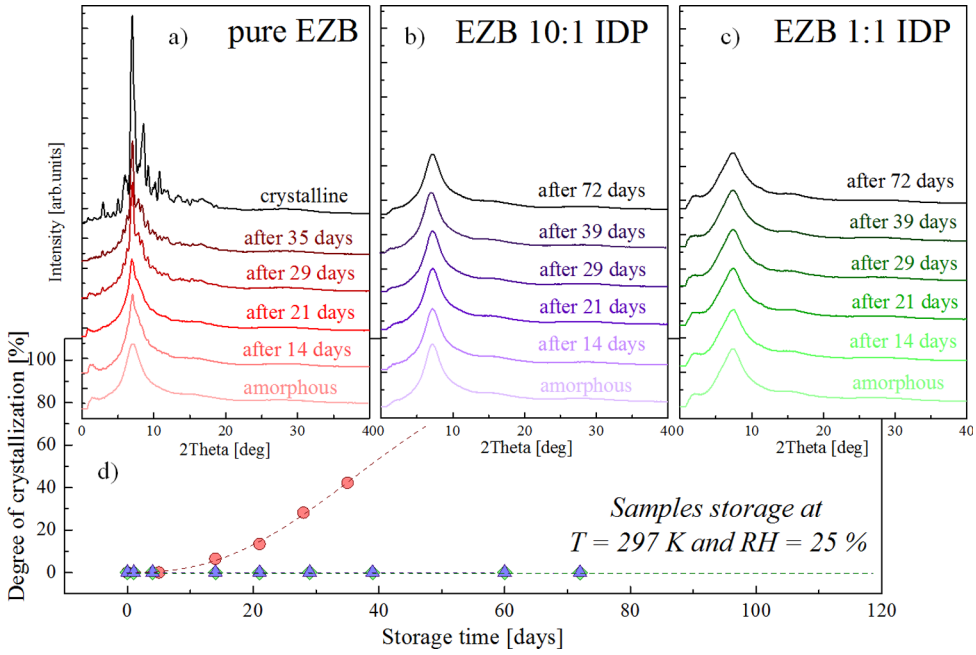

Figure 8. (a–c) The representative X-ray diffraction patterns for pure EZB, EZB 10:1 IDP, and EZB 1:1 IDP measured after specified time period. (d) The relative degree of crystallization D_c of amorphous EZB, EZB 10:1 IDP, and EZB 1:1 IDP as a function of storage time at T = 297 K and RH = 25%. Data for pure EZB were taken from ref 40.

indicates that the tested systems just after preparation were fully amorphous. After 21 days of storage small and sharp crystalline peaks might be observed only on the EZB XRD pattern, proving that a small portion of amorphous EZB recrystallized (D_c = 15%). Others systems, after the same period of time, remained unchanged, and their degree of crystallization was equal to zero. Interestingly, even after 72 days, all investigated EZB–IDP mixtures were still physically stable, i.e., we did not observe any Bragg peaks in XRD patterns.

The XRD studies show that mixtures containing EZB and IDP are characterized by high physical stability. Even a small amount of IDP drug (8.8 wt %) is able to suppress the EZB's recrystallization for at least 72 days, when the mixture is stored at 297 K. It should be noted that, from a medical point of view, the best seems to be EZB–IDP mixture containing 11.1 to 33.3 wt % of IDP. Since these values are higher than 8.8 wt % of IDP, it is obvious that such binary compositions will be very stable.

CONCLUSIONS

In this article the coamorphous binary mixture of ezetimib and indapamide was investigated by using differential scanning calorimetry, broadband dielectric spectroscopy, and X-ray diffraction. We found that the simple quench cooling method can be applied for the production of homogeneous composition of these two pharmaceuticals. Thermal analysis of mixtures characterized by various molar ratios of EZB and IDP indicated that the glass transition temperature (T_g) rises with increasing IDP content in accordance with the Gordon–Taylor equation. This result suggests that improvement of the physical stability of highly unstable amorphous EZB drug in binary mixture is mainly caused by an antiplasticizing effect exerted by IDP.

The effect of IDP on the molecular dynamics of amorphous EZB in their coamorphous compositions was investigated over a broad temperature and frequency range by using dielectric spectroscopy. These experiments have shown that, besides an antiplasticizing effect, an additional factor is also responsible for the physical stability improvement of the measured mixtures. Based on dielectric data we determined the m_p and β_{KWW} parameters that characterize the structural relaxation process. These parameters are generally considered as a measure of the physical stability of systems in disordered state. A low value of fragility parameter and a narrow α-relaxation peak (i.e., high value of β_{KWW}) correspond to high stability. Our studies have shown that the m_p parameter indeed reflects the tendency to recrystallization of coamorphous binary EZB–IDP mixtures. However, such a correlation was not observed in the case of β_{KWW}. The shape of the structural relaxation loss peak is fixed for mixtures with different concentrations of EZB–IDP drugs. The value of β_{KWW} parameter for all tested binary systems as well as for pure amorphous EZB is equal to 0.7. Using XRD techniques we also examined the long-term physical stability of binary mixtures that contain EZB and IDP drugs. These measurements have proven that even a small amount of IDP drug (8.8 wt %) may significantly suppress the devitrification of amorphous EZB drug: after 60 days the tested mixture was fully amorphous. As a consequence the coamorphous binary ezetimib–indapamid system is a very promising candidate for new formulations intended for combined therapy. Apart from the medical and economic benefits of using these drugs together in amorphous forms, such a binary composition provides high physical stability that is essential for further commercial application.

AUTHOR INFORMATION

Corresponding Author

*E-mail: jknapik@us.edu.pl.

Notes

The authors declare no competing financial interest.

ACKNOWLEDGMENTS

The authors Z.W., K.G., and M.P. are grateful for the financial support of the National Science Centre within the Opus3 project (Grant No. DEC-2012/05/B/NZ7/03233). The authors wishes

DOI: 10.1021/acs.molpharmaceut.5b00334
Mol. Pharmaceutics 2015, 12, 3610–3619

to express their thanks for the critical reading of the manuscript by E. Mc Court, Queen's University of Belfast. L.T. is funded by Science Foundation Ireland under grant No. 12/RC/2275 (Synthesis and Solid State Pharmaceuticals Centre).

REFERENCES

(1) Rasenack, N.; Müller, B. W. Poorly water-soluble drugs for oral delivery: a challenge for pharmaceutical development. Part I: Physicochemical and biopharmaceutical background/strategies in pharmaceutical development. *Pharm. Ind.* **2005**, *67* (3), 323−326.
(2) Lipinski, C. Poor aqueous solubility − an industry wide problem in drug delivery. *Am. Pharm. Rev.* **2002**, *5*, 82−85.
(3) Bhardwaj, S. P.; Suryanarayanan, R. Molecular mobility as an effective predictor of the physical stability of amorphous trehalose. *Mol. Pharmaceutics* **2012**, *9* (11), 3209−3217.
(4) Wojnarowska, Z.; Grzybowska, K.; Hawelek, L.; Dulski, M.; Wrzalik, R.; Gruszka, I.; Paluch, M.; Pienkowska, K.; Sawicki, W.; Bujak, P.; Paluch, K. J.; Tajber, L.; Markowski, J. Molecular Dynamics, Physical Stability and Solubility Advantage from Amorphous Indapamide Drug. *Mol. Pharmaceutics* **2013**, *10* (10), 3612−3627.
(5) Bhugra, C.; Pikal, M. Role of thermodynamic, molecular, and kinetic factor in crystallization from amorphous state. *J. Pharm. Sci.* **2008**, *97*, 1329−1349.
(6) Yoshioka, M.; Hancock, B. C.; Zografi, G. Crystallization of indomethacin from the amorphous state below and above its glass transition temperature. *J. Pharm. Sci.* **1994**, *83*, 1700.
(7) Kothari, K.; Ragoonanan, V.; Suryanarayanan, R. Influence of Molecular Mobility on the Physical Stability of Amorphous Pharmaceuticals in the Supercooled and Glassy States. *Mol. Pharmaceutics* **2014**, *11*, 3048−3055.
(8) Priemel, P. A.; Laitinen, R.; Barthold, S.; Grohganz, H.; Lehto, V.-P.; Rades, T.; Strachan, C. J. Inhibition of surface crystallisation of amorphous indomethacin particles in physical drug−polymer mixtures. *Int. J. Pharm.* **2013**, *456*, 301−306.
(9) Van Eerdenbrugh, B.; Taylor, L. S. Small Scale Screening To Determine the Ability of Different Polymers To Inhibit Drug Crystallization upon Rapid Solvent Evaporation. *Mol. Pharmaceutics* **2010**, *7* (4), 1328−1337.
(10) Taylor, T. S.; Zografi, G. *Pharm. Res.* **1997**, *14* (12), 1691−1698.
(11) Miyazaki, T.; Yoshioka, S.; Aso, Y. Physical Stability of Amorphous Acetanilide Derivatives Improved by Polymer Excipients. *Chem. Pharm. Bull.* **2006**, *54* (8), 1207−1210.
(12) Matsumoto, T.; Zografi, G. Physical Properties of Solid Molecular Dispersions of Indomethacin with Poly(Vinylpyrrolidone) and Poly-(Vinylpyrrolidone-Co-Vinyl-Acetate) in Relation to Indomethacin Crystallization. *Pharm. Res.* **1999**, *16* (11), 1722−1728.
(13) Kothari, K.; Ragoonanan, V.; Suryanarayanan, R. The Role of Drug−Polymer Hydrogen Bonding Interactions on the Molecular Mobility and Physical Stability of Nifedipine Solid Dispersions. *Mol. Pharmaceutics* **2015**, *12*, 162−170.
(14) Gupta, P.; Thilagavathi, R.; Chakraborti, A. K.; Bansal, A. K. Role of Molecular Interaction in Stability of Celecoxib-PVP Amorphous Systems. *Mol. Pharmaceutics* **2005**, *2* (5), 384−391.
(15) Laitinen, R.; Lobmann, K.; Strachan, C. J.; Grohganz, H.; Rades, T. Emerging trends in the stabilization of amorphous drugs. *Int. J. Pharm.* **2013**, *453*, 65−79.
(16) Serajuddin, A. T. Solid dispersion of poorly water-soluble drugs: early promises, subsequent problems, and recent breakthroughs. *J. Pharm. Sci.* **1999**, *88* (10), 1058−66.
(17) Shrivastava, A. R.; Ursekar, B.; Kapadia, C. J. Design, optimization, preparation and evaluation of dispersion granules of valsartan and formulation into tablets. *Curr. Drug Delivery* **2009**, *6* (1), 28−37.
(18) Löbmann, K.; Strachan, C.; Grohganz, H.; Rades, T.; Korhonen, O.; Laitinen, R. Co-amorphous simvastatin and glipizide combinations show improved physical stability without evidence of intermolecular interactions. *Eur. J. Pharm. Biopharm.* **2012**, *81* (1), 159−69.
(19) Chieng, N.; Aaltonen, J.; Saville, D.; Rades, T. Physical characterization and stability of amorphous indomethacin and ranitidine hydrochloride binary systems prepared by mechanical activation. *Eur. J. Pharm. Biopharm.* **2009**, *71* (1), 47−54.
(20) Grzybowska, K.; Paluch, M.; Wlodarczyk, P.; Grzybowski, A.; Kaminski, K.; Hawelek, L.; Zakowiecki, D.; Kasprzycka, A.; Jankowska-Sumara, I. Enhancement of amorphous celecoxib stability by mixing it with octaacetylmaltose: the molecular dynamics study. *Mol. Pharmaceutics* **2012**, *9* (4), 894−904.
(21) Kaminska, E.; Adrjanowicz, K.; Tarnacka, M.; Kolodziejczyk, K.; Dulski, M.; Mapesa, E. U.; Zakowiecki, D.; Hawelek, L.; Kaczmarczyk-Sedlak, I.; Kaminski, K. Impact of inter- and intramolecular interactions on the physical stability of indomethacin dispersed in acetylated saccharides. *Mol. Pharmaceutics* **2014**, *11* (8), 2935−2947.
(22) Yamamura, S.; Gotoh, H.; Sakamoto, Y.; Momose, Y. Physicochemical properties of amorphous salt of cimetidine and diflunisal system. *Int. J. Pharm.* **2002**, *241* (2), 213−21.
(23) Allesø, M.; Chieng, M.; Rehder, S.; Rantanen, J.; Rades, T.; Aaltonen, J. Enhanced dissolution rate and synchronized release of drugs in binary systems through formulation: Amorphous naproxen−cimetidine mixtures prepared by mechanical activation. *J. Controlled Release* **2009**, *136*, 45−53.
(24) Löbmann, K.; Laitinen, R.; Grohganz, H.; Gordon, C.; Strachan, C.; Rades, T. Coamorphous Drug Systems: Enhanced Physical Stability and Dissolution Rate of Indomethacin and Naproxen. *Mol. Pharmaceutics* **2011**, *8*, 1919−1928.
(25) Wong, N. D.; Lopez, V.; Tang, S.; Williams, G. R. Prevalence, treatment, and control of combined hypertension and hypercholesterolemia in the United States. *Am. J. Cardiol.* **2006**, *98* (2), 204−208.
(26) Eaton, C. B.; Feldman, H. A.; Assaf, A. R.; McPhillips, J. B.; Hume, A. L.; Lasater, T. M.; Levinson, P.; Carleton, P. A. Prevalence of hypertension, dyslipidemia, and dyslipidemic hypertension. *J. Fam. Pract.* **1994**, *38*, 17−23.
(27) Johnson, M. L.; Pietz, K.; Battleman, D. S.; Beyth, R. J. Prevalence of comorbid hypertension and dyslipidemia and associated cardiovascular disease. *Am. J. Managed Care* **2004**, *10*, 926−932.
(28) Yaro, P.; He, X.; Liu, W.; Xun, M.; Ma, Y.; Li, Z.; Shi, X. In vitro−in vivo correlations for three different commercial immediate-release indapamide tablets. *Drug Dev. Ind. Pharm.* **2014**, *40* (12), 1670−1676.
(29) Bali, V.; Ali, M.; Ali, J. Study of surfactant combinations and development of a novel nanoemulsion for minimising variations in bioavailability of ezetimibe. *Colloids Surf., B* **2010**, *76* (2), 410−420.
(30) Knopp, R. H.; Gitter, H.; Truitt, T.; Bays, H.; Manion, C. V.; Lipka, L. J.; LeBeaut, A. P.; Suresh, R.; Yang, B.; Veltri, E. P. Effects of ezetimibe, a new cholesterol absorption inhibitor, on plasma lipids in patients with primary hypercholesterolemia. *Eur. Heart J.* **2003**, *24* (8), 729−741.
(31) Leonetti, G. Clinical Positioning of Indapamide Sustained Release 1.5mg in Management Protocols for Hypertension. *Drugs* **2000**, *59* (2), 27−38.
(32) Adrjanowicz, K.; Wojnarowska, Z.; Grzybowska, K.; Hawelek, L.; Kaminski, K.; Paluch, M.; Kasprzycka, A.; Walczak, K. Molecular dynamics and crystallization phenomenon of supercooled and glassy DNA and RNA nucleosides: β-adenosine, β-thymidine, and β-uridine. *Phys. Rev. E* **2011**, *84*, 051507.
(33) Kolodziejczyk, K.; Paluch, M.; Grzybowska, K.; Grzybowski, A.; Wojnarowska, Z.; Hawelek, L.; Ziolo, J. D. Relaxation Dynamics and Crystallization Study of Sildenafil in the Liquid and Glassy States. *Mol. Pharmaceutics* **2013**, *10* (6), 2270−2282.
(34) Bhardwaj, S. P.; Arora, K. K.; Kwong, E.; Templeton, A.; Clas, S.-D.; Suryanarayanan, R. Correlation between Molecular Mobility and Physical Stability of Amorphous Itraconazole. *Mol. Pharmaceutics* **2013**, *10*, 694−700.
(35) Baird, J. A.; Taylor, L. S. Evaluation of amorphous solid dispersion properties using thermal analysis techniques. *Adv. Drug Delivery Rev.* **2012**, *64* (5), 396−421.
(36) Van den Mooter, G.; Wuyts, M.; Blaton, N.; Busson, R.; Grobet, P.; Augustijns, P.; Kinget, R. Physical stabilisation of amorphous ketoconazole in solid dispersions with polyvinylpyrrolidone K25. *Eur. J. Pharm. Sci.* **2001**, *12* (3), 261−269.

DOI: 10.1021/acs.molpharmaceut.5b00334
Mol. Pharmaceutics 2015, 12, 3610−3619

(37) Gordon, M.; Taylor, J. S. Ideal copolymers and the 2nd-order transitions of synthetic rubbers 1. Non-crystalline copolymers. *J. Appl. Chem.* **1952**, *2*, 493−500.
(38) Kelley, F. N.; Bueche, F. Viscosity and glass temperature relations for polymer diluent systems. *J. Polym. Sci.* **1961**, *50*, 549−556.
(39) Couchman, P. R.; Karasz, F. E. A classical thermodynamic discussion on the effect of composition on glass-transition temperatures. *Macromolecules* **1978**, *11*, 117−119.
(40) Knapik, J.; Wojnarowska, Z.; Grzybowska, K.; Hawelek, L.; Sawicki, W.; Wlodarski, K.; Markowski, J.; Paluch, M. Physical Stability of the Amorphous Anticholesterol Agent (Ezetimibe): The Role of Molecular Mobility. *Mol. Pharmaceutics* **2014**, *11*, 4280−4290.
(41) Kremer, F., Schönhals, A., Eds. *Broadband Dielectric Spectroscopy*; Springer: Berlin, 2003.
(42) Wojnarowska, Z.; Grzybowska, K.; Adrjanowicz, K.; Kaminski, K.; Paluch, M.; Hawelek, L.; Wrzalik, R.; Dulski, M.; Sawicki, W.; Mazgalski, J.; Tukalska, A.; Bieg, T. Study of the Amorphous Glibenclamide Drug: Analysis of the Molecular Dynamics of Quenched and Cryomilled Material. *Mol. Pharmaceutics* **2010**, *7*, 1692−1707.
(43) Wojnarowska, Z.; Wlodarczyk, P.; Kaminski, K.; Grzybowska, K.; Hawelek, L.; Paluch, M. On the Kinetics of Tautomerism in Drugs - New Application of Broadband Dielectric Spectroscopy. *J. Chem. Phys.* **2010**, *133*, 094507.
(44) Floudas, G.; Paluch, M.; Grzybowski, A.; Ngai, K. *Molecular Dynamics of Glass-Forming Systems: Effects of Pressure*; Springer-Verlag: Berlin Heidelberg, 2011.
(45) Tammann, G.; Hesse, W. Die Abhängigkeit der Viscosität von der Temperatur bie unterkühlten Flüssigkeiten. *Z. Anorg. Allg. Chem.* **1926**, *156*, 245−257.
(46) Fulcher, G. S. Analysis of Recent Measurements of the Viscosity of Glasses. *J. Am. Ceram. Soc.* **1925**, *8*, 339−355.
(47) Vogel, H. Das Temperaturabhangigkeitgesetz der Viskosität von Flüssigkeiten. *J. Phys. Z.* **1921**, *22*, 645−646.
(48) Casalini, R.; Paluch, M.; Roland, C. M. The dynamics crossover region in phenol- and cresol-phthalein-dimethylethers under different conditions of pressure and temperature. *J. Phys.: Condens. Matter* **2003**, *15*, S859−S867.
(49) Casalini, R.; Paluch, M.; Roland, C. M. Dynamic crossover in supercooled liquids induced by high pressure. *J. Chem. Phys.* **2003**, *118* (13), 5701−5703.
(50) Bras, A. R.; Noronha, J. P.; Antunes, A. M. M.; Cardoso, M. M.; Schonhals, A.; Affouard, F.; Dionisio, M.; Correia, N. T. Molecular Motions in Amorphous Ibuprofen As Studied by Broadband Dielectric Spectroscopy. *J. Phys. Chem. B* **2008**, *112*, 11087−11099.
(51) Adrjanowicz, K.; Wojnarowska, Z.; Wlodarczyk, P.; Kaminski, K.; Paluch, M.; Mazgalski, J. Molecular mobility in liquid and glassy states of Telmisartan (TEL) studied by Broadband Dielectric Spectroscopy. *Eur. J. Pharm. Sci.* **2009**, *38*, 395.
(52) Stickel, F.; Fischer, E. W.; Richert, R. Dynamics of glass-forming liquids. I. Temperature-derivative analysis of dielectric relaxation data. *J. Chem. Phys.* **1995**, *102*, 6251.
(53) Bohmer, R.; Ngai, K. L.; Angell, C. A.; Plazek, D. J. Nonexponential relaxations in strong and fragile glass formers. *J. Chem. Phys.* **1993**, *99*, 4201.
(54) Grzybowska, K.; Paluch, M.; Grzybowski, A.; Wojnarowska, Z.; Hawelek, L.; Kolodziejczyk, K.; Ngai, K. L. Molecular dynamics and physical stability of amorphous anti-inflammatory drug: celecoxib. *J. Phys. Chem. B* **2010**, *114*, 12792−12801.
(55) Tanaka, H. Relationship among glass-forming ability, fragility, and short-range bond ordering of liquids. *J. Non-Cryst. Solids* **2005**, *351*, 678−690.
(56) Shamblin, S. L.; Tang, X.; Chang, L.; Hancock, B. C.; Pikal, M. J. Characterization of the time scales of molecular motion in pharmaceutically important glasses. *J. Phys. Chem. B* **1999**, *103*, 4113−4121.
(57) Goodwin, A. A.; Mercer, F. W.; McKenzie, M. T. Thermal Behavior of Fluorinated Aromatic Polyethers and Poly(ether ketone)s. *Macromolecules* **1997**, *30*, 2767−2774.

DOI: 10.1021/acs.molpharmaceut.5b00334
Mol. Pharmaceutics 2015, 12, 3610−3619

Dr Żaneta Wojnarowska
Instytut Fizyki
Uniwersytet Śląski
Zakład Biofizyki i Fizyki Molekularnej
ul. 75 Pułku Piechoty 1A, 41-500 Chorzów

Chorzów, 02.05.2016r.

OŚWIADCZENIE

Oświadczam, że w pracy:

Knapik J., Wojnarowska Z., Grzybowska K., Jurkiewicz K., Tajber L., Paluch M. *Molecular Dynamics and Physical Stability of Coamorphous Ezetimib and Indapamide Mixtures.* Mol. Pharmaceuticals 2015, 12, 3610–3619

mój udział polegał na udziale w dyskusji otrzymanych wyników.

Ż. Wojnarowska
.....

Podpis

mgr Karolina Jurkiewicz
Instytut Fizyki
Uniwersytet Śląski
Zakład Biofizyki i Fizyki Molekularnej
ul. 75 Pułku Piechoty 1A, 41-500 Chorzów

Chorzów, 02.05.2016r.

OŚWIADCZENIE

Oświadczam, że w pracy:

Knapik J., Wojnarowska Z., Grzybowska K., Jurkiewicz K., Tajber L., Paluch M. *Molecular Dynamics and Physical Stability of Coamorphous Ezetimib and Indapamide Mixtures.* Mol. Pharmaceuticals 2015, 12, 3610–3619

mój udział polegał na wykonaniu pomiarów XRD.

Karolina Jurkiewicz

Podpis

Dr Lidia Tajber

School of Pharmacy and Pharmaceutical Sciences,
Trinity College Dublin,
College Green, Dublin 2, Ireland

Dublin, 1.04.2016

OŚWIADCZENIE

Oświadczam, że w pracy:

Knapik J., Wojnarowska Z., Grzybowska K., Jurkiewicz K., Tajber L., Paluch M. *Molecular Dynamics and Physical Stability of Coamorphous Ezetimib and Indapamide Mixtures.* Mol. Pharmaceutics 2015, 12, 3610−3619

mój udział polegał na wykonaniu pomiarów FTIR badanych układów, ich przeanalizowaniu oraz opisaniu otrzymanych wyników.

.....

Podpis

Prof. zw. dr hab. Marian Paluch
Instytut Fizyki
Uniwersytet Śląski
Zakład Biofizyki i Fizyki Molekularnej
ul. 75 Pułku Piechoty 1A, 41-500 Chorzów

Chorzów, 02.05.2016r.

OŚWIADCZENIE

Oświadczam, że w pracy:

Knapik J., Wojnarowska Z., Grzybowska K., Jurkiewicz K., Tajber L., Paluch M. *Molecular Dynamics and Physical Stability of Coamorphous Ezetimib and Indapamide Mixtures.* Mol. Pharmaceuticals 2015, 12, 3610–3619

mój udział polegał na uczestnictwie w dyskusji wyników oraz korekcji manuskryptu.

.....

Podpis

3.3 A3 – Knapik J., Wojnarowska Z., Grzybowska K., Jurkiewicz K., Stankiewicz A., Paluch M. *Stabilization of the Amorphous Ezetimib Drug by Confining Its Dimension.* Mol. Pharmaceuticals 2016, 13, 1308–1316.

Impact Factor czasopisma z roku opublikowania pracy: **4.384**.

Liczba punktów ministerialnych MNiSW czasopisma z roku opublikowania pracy: **40 pkt**.

DOI: **10.1021/acs.molpharmaceut.5b00903**.

Udział pierwszego autora w poniżej załączonym artykule polegał koordynowaniu oraz zaplanowaniu eksperymentu, wykonaniu pomiarów dielektrycznych oraz kalorymetrycznych, analizie wszystkich otrzymanych wyników oraz przygotowaniu manuskryptu. Wkład pozostałych współautorów, w formie oświadczeń, zamieszczono na końcu artykułu.

molecular pharmaceutics

Article

pubs.acs.org/molecularpharmaceutics

Stabilization of the Amorphous Ezetimibe Drug by Confining Its Dimension

J. Knapik,*[,†,‡] Z. Wojnarowska,[†,‡] K. Grzybowska,[†,‡] K. Jurkiewicz,[†,‡] A. Stankiewicz,[§] and M. Paluch[†,‡]

[†]Institute of Physics, University of Silesia, ul. Uniwersytecka 4, 40-007 Katowice, Poland

[‡]SMCEBI, ul. 75 Pułku Piechoty 1a, 41-500 Chorzów, Poland

[§]F1 Pharma sp. z o.o., ul. Bobrzyńskiego 14, 30-348 Kraków, Poland

ABSTRACT: The purpose of this paper is to investigate the influence of nanoconfinement on the molecular mobility, as well as on the physical stability, of amorphous ezetimibe drug. Two guest/host systems, ezetimibe−Aeroperl 300 and ezetimibe−Neusilin US2, were prepared and studied using various experimental techniques, such as X-ray diffraction (XRD), differential scanning calorimetry (DSC), and broadband dielectric spectroscopy (BDS). Our investigation has shown that the molecular mobility of the examined anticholesterol agent incorporated into nanopore matrices strongly depends on the pore size of the host system. Moreover, it was found that the amorphous ezetimibe confined in 30 nm pores of Aeroperl 300 has a tendency to recrystallize, while the drug incorporated into the smaller—5 nm—pores of Neusilin US2 is not able to crystallize. It has been shown that this significant stabilization of ezetimibe drug can be achieved by an interplay of three factors: changes in molecular dynamics of the confined amorphous drug, the immobilization effect of pore walls on a part of ezetimibe molecules, and the use of host materials with pores that are smaller than the critical size of the drug crystal nuclei.

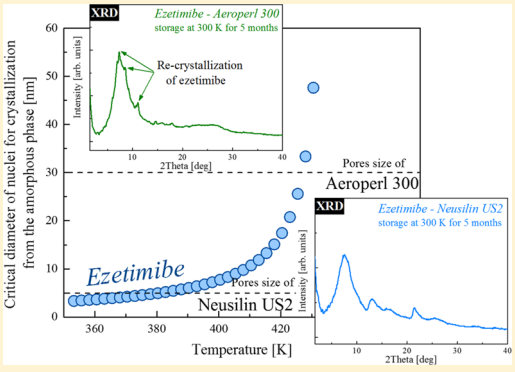

KEYWORDS: *ezetimibe, Neusilin US2, Aeroperl 300, physical stability, confinement, molecular dynamics, glass transition, host/guest system, nanopores*

INTRODUCTION

In recent years, significant attention has been focused on nanoscience and nanotechnology.[1,2] Nanostructured materials such as silica-based systems or metal−organic frameworks are indispensable in almost all fields of science.[3,4] From 2001, when the mesoporous material MCM-41 was first proposed as a drug carrier, nanoporous systems have become widely used in the pharmaceutical industry.[5] Currently, in this field, silica host systems are applied for controlling drug release, delivering active pharmaceutical ingredient (API) to a treated body area, as well as for producing metastable polymorphs of pharmaceuticals.[6−11]

In spite of the widespread use of nanoporous materials in the drug industry, one important feature of these substances is still unexploited. Namely, these materials may be able to significantly suppress devitrification of compounds which easily crystallize.[12,13] According to the classical theory of homogeneous nucleation, a crystal can only be formed and grow when a critical nucleation size is reached.[14] Thus, if a cluster of molecules are confined to suitable small pores, their nucleation and crystal growth should be prevented. Consequently, the host/guest systems should permanently exist in an intrinsically disordered state.[15,16]

By exploiting this interesting feature of nanoporous materials in the drug industry, it becomes possible to produce physically stable amorphous APIs. It should be highlighted that drugs in a disordered state are an interesting class of substances for pharmaceutical applications.[17−20] They exhibit higher apparent solubility and consequently better bioavailability when compared to conventional crystalline drugs.[21] Taking into account that nearly 40% of existing APIs are characterized by low aqueous solubility, production and stabilization of their amorphous, more soluble forms has attracted great interest in the past decade.[22−24]

In this paper we investigate the efficacy of two commercially used porous materials (Aeroperl 300 and Neusilin US2) in inhibiting devitrification of the amorphous ezetimibe drug. As we have shown in a previous paper, this anticholesterol agent reveals a strong tendency toward recrystallization, therefore many efforts have been made to develop the best way to stabilize it.[25,26] It should be noted that the selected host systems have pore diameters an order of magnitude different. The predominant pore size of Aeroperl 300 is equal to 30 nm, while Neusilin's pores have a diameter of 5 nm.[27,28] Consequently, we are able to find out how the pore size affects the physical stability of the examined drug. In this context, it is worth noting that the pore's size should also

Received: December 2, 2015
Revised: February 19, 2016
Accepted: March 16, 2016
Published: March 16, 2016

DOI: 10.1021/acs.molpharmaceut.5b00903
Mol. Pharmaceutics 2016, 13, 1308−1316

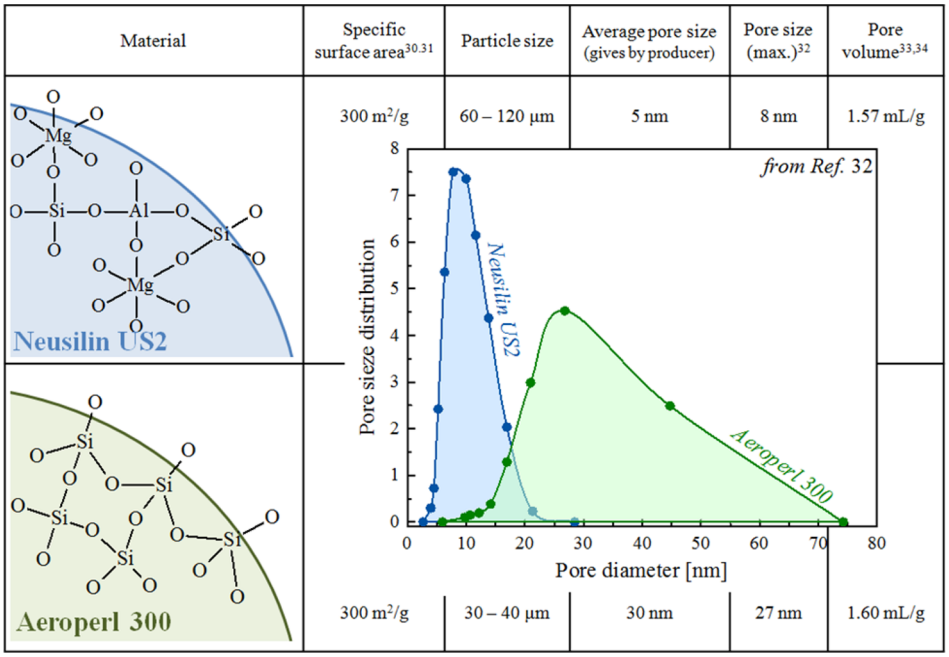

Figure 1. Surface chemistry characterization of Aeroperl 300 and Neusilin US2.[30−34]

change the dynamics of the guest molecules.[29] In order to investigate how the confinement changes the molecular mobility of the loaded drug, we used broadband dielectric spectroscopy (BDS). The examined host/guest systems were additionally investigated by X-ray diffraction (XRD) as well as differential scanning calorimetry (DSC) techniques. As in this paper we clearly show which factors play the crucial role in the stabilization of amorphous ezetimibe, we believe that our research can be used as a guide in the selection of appropriate porous materials for suppressing devitrification of disordered pharmaceuticals.

MATERIALS AND METHODS

Materials. Ezetimibe drug (M_w = 409.4 g/mol) of purity greater than 99% was purchased from Polpharma (Starogard Gdański, Poland) and used as received. This pharmaceutical is described chemically as ((3*R*,4*S*)-1-(4-fluorophenyl)-3-[(3*S*)-3-(4-fluorophenyl)-3-hydroxypropyl]-4-(4-hydroxyphenyl)-azetidin-2-one).

Aeroperl 300 (fumed silica granulate) was purchased from Evonic and Neusilin US2 (magnesium aluminometasilicate) from Fuji Chemicals Industry Co. Ltd. More detailed information about Aeroperl 300 and Neusilin US2 is presented in Figure 1.[30−34]

Preparation of Binary Systems. Ezetimibe (1.50 g) was placed in a 250 mL pear shape evaporating flask and dissolved in 50 mL of anhydrous ethanol. An equal quantity (1.50 g) of appropriate carrier was added in one portion. The flask was installed on a rotavapor (Heidolph Hei-Vap Value rotavapor equipped with vacuum system KNF SC 920) and rotated with the speed of 150 rpm. The temperature of the water bath was set at 40 °C to avoid possible thermal decomposition of ingredients during the evaporation process. The initial pressure was set at 300 mbar and quickly lowered to 90 mbar when the evaporation process began. When evaporation of the majority of the solvent volume resulted in a wet white slurry, the walls of the flask were washed with an additional 10 mL of ethanol to dissolve residual unabsorbed ezetimibe. The process of evaporation was continued until the pressure reached 30 mbar to produce white dry powder of carrier/ezetimibe binary system. Powder was removed from the flask and dried in air at room temperature.

X-ray Diffraction (XRD). The X-ray diffraction measurements were performed using a Rigaku-Denki D/MAX RAPID II-R diffractometer equipped with a rotating Ag anode ($\lambda_{K\alpha}$ = 0.5608 Å), an incident beam (002) graphite monochromator, and an image plate in the Debye−Scherrer geometry as a detector. The X-ray beam width at the sample was 0.3 mm. The investigated samples were placed inside glass capillaries with a diameter of 1.5 mm and wall thickness of 0.01 mm. The measurements were carried out for sample filled capillaries and empty. The diffraction intensity for the empty capillary was then subtracted. The obtained two-dimensional diffraction patterns were converted into one-dimensional functions of intensity versus the scattering angle using suitable software.

Differential Scanning Calorimetry (DSC). Thermodynamic properties of pure ezetimibe as well as guest/host systems ezetimibe−Neusilin US2 and ezetimibe−Aeroperl 300 were examined using a Mettler−Toledo DSC 1 STAR^e System. The measuring device was calibrated for temperature and enthalpy using zinc and indium standards. The instrument was equipped with an HSS8 ceramic sensor having 120 thermocouples and a liquid nitrogen cooling station. The glass transition temperature was determined as the midpoint of the heat capacity increment. The samples were measured in an aluminum crucible (40 μL). All measurements were carried out in the range from 298 to 450 K with heating rate equal to 10 K/min.

Broadband Dielectric Spectroscopy (BDS). Dielectric measurements of ezetimibe−Neusilin US2 as well as ezetimibe−Aeroperl 300 systems were carried out using Novo-Control GMBH Alpha dielectric spectrometer, in the frequency range from 10^{-1} Hz to 10^6 Hz at temperatures from 133 to 413 K with step of 2 K. The temperature was controlled by a Quattro temperature controller with temperature stability better than 0.1 K. Dielectric studies of all samples were

DOI: 10.1021/acs.molpharmaceut.5b00903
Mol. Pharmaceutics 2016, 13, 1308−1316

performed in a parallel-plate cell made of stainless steel (diameter 20 mm and a 0.1 mm gap with Teflon spacers).

RESULTS AND DISCUSSION

Physicochemical Properties of Examined Host/Guest Systems. To verify that the ezetimibe drug inside the nanopores of Aeroperl 300 and Neusilin US2 was completely amorphous, X-ray diffraction (XRD) was applied as a technique. Diffraction patterns for pure components (ezetimibe, Aeroperl 300, and Neusilin US2), and for the guest/host systems (ezetimibe–Aeroperl 300 and ezetimibe–Neusilin US2) are presented in Figures 2a–e. A broad amorphous

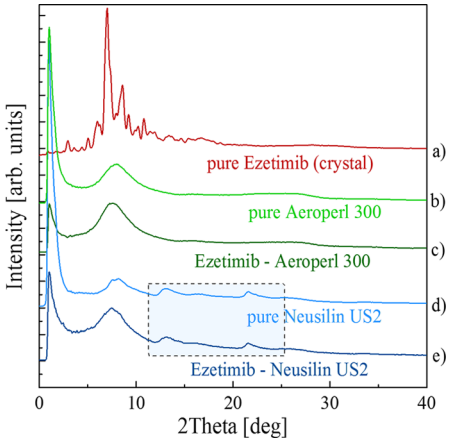

Figure 2. X-ray diffraction patterns for (a) pure crystalline EZB, (b) pure Aeroperl 300, (c) ezetimibe–Aeroperl 300 host/guest system, (d) pure Neusilin US2 and (e) ezetimibe–Neusilin US2 host/guset system.

halo observed in the case of ezetimibe in Aeroperl 300 (see Figure 2c) suggests that in this system there is no long-range three-dimensional molecular order. This result indicates that the ezetimibe drug in this porous material was indeed in the amorphous state. The XRD pattern of the second system, in which ezetimibe fills Neusilin US2's pores, has sharp Bragg peaks in addition to the amorphous halo. As can be seen in Figures 2d,e, these peaks originate from Neusilin US2. Lack of detectable ezetimibe diffraction peaks in the XRD pattern of ezetimibe–Neusilin US2 indicates the existence of only the amorphous form of the drug inside the Neusilin's pores.

The diffraction patterns presented in Figure 2b–e reveal also a sharp peak at low angle scattering. Such a peak is characteristic for porous materials.[35,36] It can be clearly seen that, due to pore filling by ezetimibe, the intensity of this diffraction peak substantially decreases. Such a decrease in the low angle diffraction peak intensity indicates that ezetimibe was incorporated in the Aeroperl 300's and Neusilin US2's pores.

The value of glass transition temperature of the studied systems was determined using differential scanning calorimetry (DSC). The DSC curves that were obtained during heating of the measured samples are shown in Figure 3. The heating rate applied in this experiment was equal to 10 K/min. As can be seen, the bulk ezetimibe and ezetimibe in Aeroperl 300 are characterized by one T_g, while two glass transition temperatures can be observed in the guest/host system of ezetimibe–Neusilin US2. The existence of the second T_g in the ezetimibe–Neusilin US2 system may be caused by the interaction between layer of the pore surface and the layer of the confined drug's

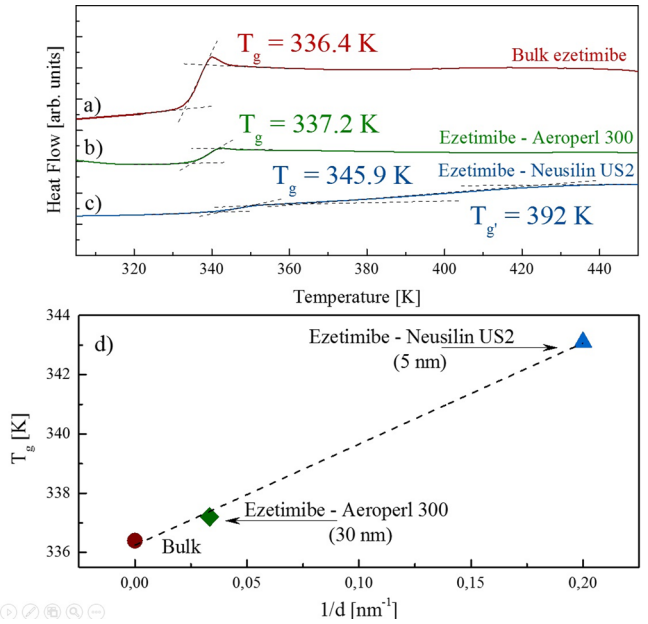

Figure 3. (a–c) DSC thermograms of (heating rate 10 K/min) pure amorphous EZB drug, system of ezetimibe–Aeroperl 300, and system of ezetimibe–Neusilin US2. (d) A plot showing growth of T_g with decreasing pore diameter (increasing 1/d) for ezetimibe in commercially used in pharmaceutical industry porous materials.

molecules. The T_g values, interpreted as the midpoint of the transition region of the DSC curves, are given in Table 1. Our

Table 1. Comparison of the Values of T_g Obtained from Standard DSC (Heating Rate: 10 K/min)

system	av pore size [nm]	T_g [K]	$T_{g'}$ [K]
ezetimibe–Neusilin US2	5	343.1	392.0
ezetimibe–Aeroperl 300	30	337.2	
ezetimibe, bulk		336.4	

results show that the glass transition temperature is shifted to higher temperatures when the system size is reduced by confining the ezetimibe to small pores. A similar pattern of behavior was observed, for example, in glycerol after incorporation in MCM-41.[37] In this case the increase in T_g was rationalized by an entropy model as well as the free volume concept. Further research of Jackson and McKenna has shown that as the pore size decreases, the glass transition temperature of the confined system can also decrease or even remain unaffected.[38,39] Because there is no clear explanation why certain compounds behave differently than predicted by the free volume models, a generally accepted picture of T_g behavior in confined matter is still lacking.

Molecular Dynamic Studies of Ezetimibe Confined in the Pores. To investigate the molecular dynamics of ezetimibe confined in pores with various pore diameters (5 and 30 nm), we have performed dielectric measurements in a wide frequency range: from $f = 10^{-1}$ Hz to $f = 10^{6}$ Hz. During the experiments the temperature was increased from 133 to 413 K with step of 2 K. In Figure 4a,b the dielectric response of examined host/guest systems above their glass transition temperature is presented. As can be seen in both drug–matrix combinations, one well-resolved loss peak connected to the structural (α) relaxation process can be observed. This mode shifts toward higher frequencies with increasing temperature,

DOI: 10.1021/acs.molpharmaceut.5b00903
Mol. Pharmaceutics 2016, 13, 1308–1316

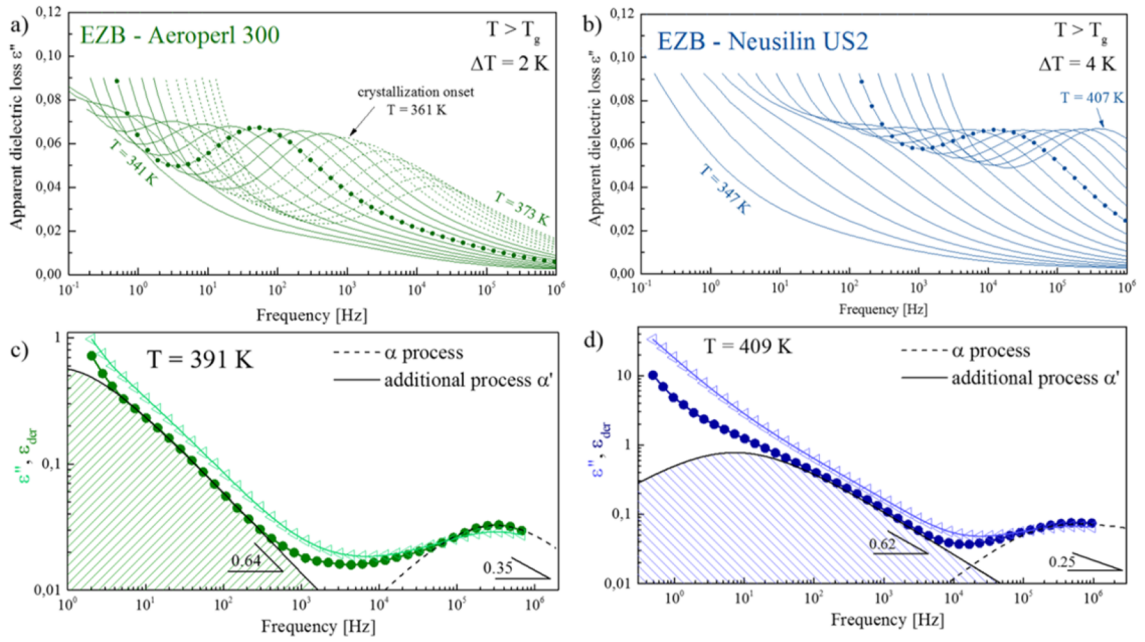

Figure 4. (a, b) Apparent dielectric loss spectra collected above the glass transition temperature of host/guest systems of ezetimibe−Aeroperl 300 and ezetimibe−Neusilin US2. (c, d) The model spectra that were obtained after elimination of the conductivity (green and blue filled circles).

indicating that the structural relaxation of the systems becomes faster. The dielectric spectra show also the presence of dc conductivity. For the system of ezetimibe−Neusilin US2 the dc contribution is especially pronounced, causing the α-relaxation peak to be hardly visible at temperatures lower than 371 K. Therefore, in order to correctly estimate the values of structural relaxation times, the derivative formalism, which eliminates the conductivity from loss spectra, was used:[40,41]

$$\varepsilon_{der} = -\frac{\pi}{2}\frac{d\varepsilon'(f)}{d\ln f} \quad (1)$$

The model spectra that were obtained based by the presented method are displayed in Figure 4c,d. As can be seen, this procedure, apart from better visualizing the structural relaxation, also revealed a slower, additional α'-process. It should be pointed out that the liquid molecules inside the pores can be distinguished into two groups: inner pore volume (core) molecules and surface layer molecules. The latter may interact with the pore walls, which consequently can slow down their molecular mobility.[42,43] Therefore, a typical feature of host/guest systems is the appearance of extra relaxation processes positioned within the conductivity wing at frequencies even several decades below the structural α-relaxation process. It is worth noting that the effect associated with the immobilization of molecules in the surface layer by pore walls is most relevant in the ezetimibe−Neusilin US2 system. This is because the mentioned system has a smaller pore size, which means that the fraction of interfacial material is bigger and, consequently, a greater part of the surface layer of ezetimibe is immobilized.

To analyze the dielectric data of ezetimibe confined in 30 and 5 nm pores, we employed the model function, which was proposed by Havriliak and Negami (HN).[44] Because multiple peaks are observed in the available frequency window, the experimental data have been fitted using a sum of HN functions:

$$\varepsilon^*(\omega) = \varepsilon_\infty + \sum_j \left(\frac{\Delta\varepsilon_j}{[1 + (i\omega\tau_{HNj})^{a_j}]^{b_j}} \right) \quad (2)$$

where j is the index over which the relaxation processes are summed, ε_∞ is high frequency limit permittivity, $\Delta\varepsilon$ is dielectric strength, ω is equal to $2\pi f$, τ_{HN} is the HN relaxation time, and a and b represent symmetric and asymmetric broadening of the relaxation peak. The fitting examples are shown in Figure 4c,d. It should be highlighted that confinements have an impact also on the distribution of α-relaxation times of ezetimibe. The shapes of structural relaxation of bulk and confined ezetimibe are compared in Figure 5. As can be seen with decreasing the pore size, the α-relaxation of the drug becomes broader. A similar behavior has been previously observed by McKenne,

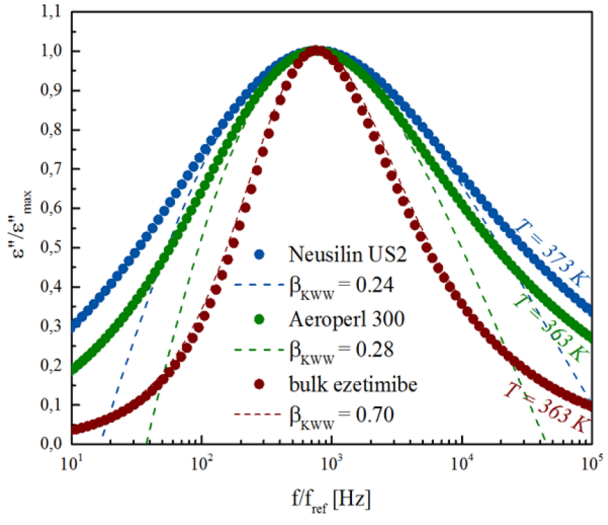

Figure 5. Normalized α-relaxation process for ezetimibe bulk (red points) and confined to Aeroperl 300 (green points) and Neusilin US2 (blue points).

DOI: 10.1021/acs.molpharmaceut.5b00903
Mol. Pharmaceutics 2016, 13, 1308−1316

Floudas, and Kremer in many spatially confined materials such as glycerol, ice, PEO-1070, PCL-770, and ethylene glycol.[38,45−47]

On the basis of the fitting parameters determined by the sum of HN functions, the values of τ_α and $\tau_{\alpha'}$ were calculated as follows:

$$\tau_{\alpha \text{ or } \alpha'} = \tau_{\max} = \tau_{\mathrm{HN}}\left[\sin\left(\frac{\pi a}{2+2b}\right)\right]^{-1/a}\left[\sin\left(\frac{\pi ab}{2+2b}\right)\right]^{1/a} \quad (3)$$

Variations in the log τ_α and log $\tau_{\alpha'}$ with temperature are presented in Figure 6.

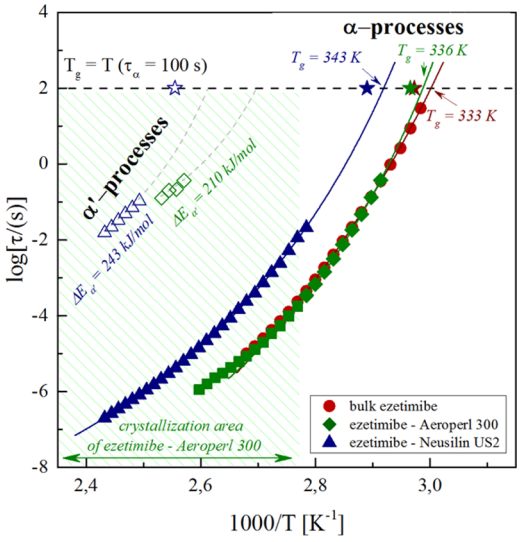

Figure 6. Temperature dependence of the α (filled symbols) and α' (open symbols) relaxation times determined by using BDS technique for bulk ezetimibe (red circles), ezetimibe−Aeroperl 300 system (green diamonds) and ezetimibe−Neusilin US2 (blue triangles). Star symbols represent the T_g obtained by the DSC technique. A slight divergence from values of T_g determined by DSC and BDS is due to the varying rate of heating used in mentioned experiments (DSC heating rate, 10 K/min; BDS heating rate, slower than 0.5 K/min).

As can be seen, the confinement effect on molecular dynamics of ezetimibe, apart from the appearance of an additional slower α'-process and the broadening of the main α-relaxation, is revealed also in the shifting of the structural relaxation process to lower frequencies (i.e., the α-relaxation becomes slower due to confinement). To describe the temperature evolution of α-relaxation time, the Vogel−Fulcher−Tamman (VFT) equation was used:[48−50]

$$\tau_\alpha(T) = \tau_\infty \exp\left(\frac{B}{T - T_0}\right) \quad (4)$$

where τ_∞, T_0, and B are fitting parameters. The corresponding parameters from eq 4 are collected in Table 2. From the VFT fitting parameters we estimated the glass transition temperature for the core dynamics (defined as τ_α = 100 s) of both drug−matrix combinations. The values of T_g determined by this method are in agreement with the T_g obtained from calorimetric studies, and they are equal to 335.6 and 342.5 K for ezetimibe−Aeroperl 300 and ezetimibe−Neusilin US2, respectively.

The literature reports suggest that also the $\tau_{\alpha'}(T)$ dependence may reveal VFT type behavior.[51] Because in our case the temperature dependence of $\tau_{\alpha'}$ could be determined only in a very short temperature range (see open symbols in Figure 6), we were not able to parametrize this dependence in both examined systems using the VFT equation. Therefore, the quasi linear temperature dependences of α' relaxation time of ezetimibe confined in 30 and 5 nm pores has been described by the Arrhenius law:

$$\tau_{\alpha'}(T) = \tau_\infty \exp\left(\frac{\Delta E}{k_B T}\right) \quad (5)$$

where τ_∞ is pre-exponential factor, ΔE is the activation energy for concerned relaxation process, and k is the Boltzmann constant. Based on this equation, the activation energies of the α'-processes of ezetimibe incorporated in the examined porous materials have been calculated. The values of $\Delta E_{\alpha'}$ are equal to 243 ± 5 kJ/mol and 210 ± 40 kJ/mol for ezetimibe−Neusilin US2 and ezetimibe−Aeroperl 300, respectively.

The important observation is that during heating from the glassy state the ezetimibe confined in 30 nm pores begins to crystallize at a temperature equal to 361 K, while the drug recrystallization was not observed in case of the drug confined in smaller pores, which have a diameter equal to 5 nm. The mentioned crystallization onset is visible in Figure 4a as a drastic drop in the apparent dielectric strength of α-relaxation ($\Delta\varepsilon_\alpha$). Such a drop in the $\Delta\varepsilon_\alpha$ reflects devitrification of the sample, because the increase in the crystalline fraction leads to a reduction in the number of reorienting dipoles contributing to the α-relaxation ($\Delta\varepsilon_\alpha \sim N\mu^2$). For better visualization, the recrystallization progress of ezetimibe inside the 30 nm pores is additionally presented in Figure 7.

As can be seen, the apparent $\Delta\varepsilon_\alpha$ of ezetimibe−Aeroperl 300 drastically decreases with time (during heating of the sample), while such a severe drop in the $\Delta\varepsilon_\alpha$ cannot be observed in the case of ezetimibe confined in smaller pores−where devitrification does not occur. This result shows that the pore size may have an impact on the physical stability of the amorphous ezetimibe drug.

Physical Stability Studies of Amorphous Ezetimibe inside the Nanopores. As we have shown in a previous paper, the amorphous ezetimibe drug is physically unstable and consequently quickly begins to crystallize (after 21 days) when

Table 2. Comparison of the Values of T_g Obtained from DSC and BDS and Fitting Parameters from the VFT Equation for Bulk EZB and for Host/Guest Systems of Ezetimibe−Aeroperl 300 or Neusilin US2

		VFT params				
system	pore size [nm]	log τ_0	T_0 [K]	$B = DT_0$	$T_{g(BDS)}$ [K]	$T_{g(DSC)}$ [K]
ezetimibe−Neusilin US2	5	−13.5 ± 0.1	288.7 ± 1.1	1926.3 ± 46.6	342.5	343.1
ezetimibe−Aeroperl 300	30	−14.4 ± 0.4	285.9 ± 1.8	1840.1 ± 107.7	335.6	337.2
ezetimibe, bulk		−18.5 ± 0.6	259.5 ± 2.4	3483.0 ± 209.8	333.1	336.4

DOI: 10.1021/acs.molpharmaceut.5b00903
Mol. Pharmaceutics 2016, 13, 1308−1316

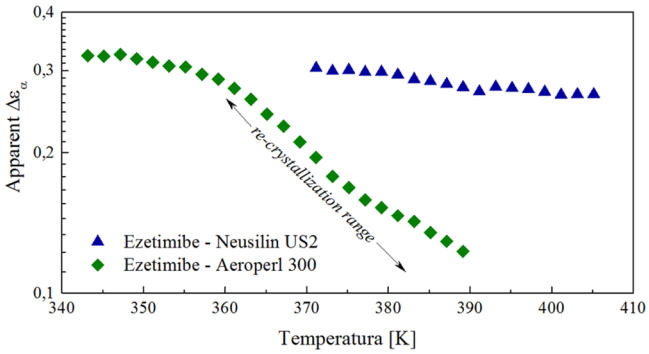

Figure 7. Temperature dependence of the apparent dielectric strength $\Delta\varepsilon_\alpha$ of structural relaxation for supercooled ezetimibe incorporated into pores of Aeroperl 300 (green diamonsa) and Neusilin US2 (blue triangles).

stored at room temperature.[25] The results presented in the previous section suggest that this transformation may be suppressed when the drug is confined to small enough pores. To confirm that the pore size has indeed a huge impact on the physical stability of amorphous ezetimibe, we examined the crystallization tendency of this drug incorporated into the pores of Aeroperl 300 and Neusilin US2 in two ways. On the one hand, to obtain the results as quickly as possible, we drastically changed the storage condition of the samples (T = 398 K) and by using DSC technique we measured the isothermal kinetics of the sample's crystallization. On the other hand, to keep the experiment conditions as close as possible to those employed during the standard storage conditions of pharmaceuticals, we left the samples for a long period of time at T = 300 K and after this time we measured it using XRD.

From the isothermal cold crystallization trace obtained by DSC, the relative degree of crystallinity $X(t)$ has been estimated by using the following formula:

$$X(t) = \frac{X_c(t)}{X_c(t_\infty)} = \frac{\int_0^t \frac{dH(t)}{dt}\,dt}{\int_0^\infty \frac{dH(t)}{dt}\,dt} = \frac{\Delta H_t}{\Delta H_\infty} \quad (6)$$

where t_0 and t_∞ represent the times at which the crystallization process begins and ends, respectively, while dH denotes the enthalpy of crystallization that is released during an infinitesimal time dt. Figure 8a shows the time dependences of X for ezetimibe−Aeroperl 300 as well as for ezetimibe−Neusilin US2 systems.

As can be seen, the ezetimibe inside pores of Aeroperl 300 (stored at T = 398 K) begins to crystallize after 1 h, while this drug incorporated into the smaller pores of Neusilin US2 even after 20 h is still physically stable. A very interesting fact is that the devitrification of ezetimibe inside 30 nm pores can be divided into two stages. In the first step ezetimibe forms crystal faster, while noticeable difference in the kinetics of the crystal formation may be observed after ∼6 h. The reason for such behavior may be explained by the existence of two groups of ezetimibe's molecules: core and interfacial. At the beginning, the faster fraction of molecules (core molecules) is involved in the crystal growth, and after this stage the second group of molecules (interfacial molecules) begin to participate in the crystal formation. It should be noted that, just after conducting the experiments of isothermal crystallization of confined ezetimibe, the DSC thermograms of the samples have been recorded (see Figure 8b). These measurements indicate that

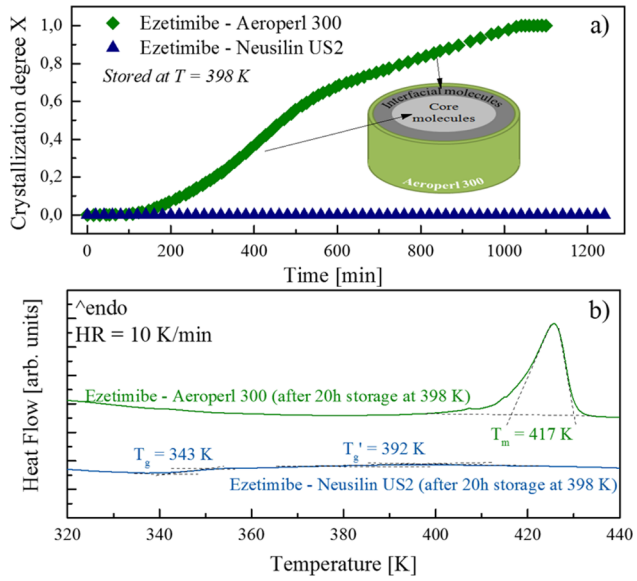

Figure 8. (a) Crystallization degree X of ezetimibe inside pores of Aeroperl 300 (green points) and Neusilin US2 (blue points) as a function of time from crystallization process occurring at 398 K. (b) DSC thermograms of ezetimibe−Aeroperl 300 (green line) and ezetimibe−Neusilin US2 (blue line) systems measured just after 20 h storage at 398 K.

ezetimibe inside pores of Aeroperl 300 indeed forms the crystal, while devitrification of ezetimibe did not begin when the drug was incorporated into the smaller pores of Neusilin US2.

It should be pointed out that the crystal of ezetimibe that has been formed inside Aeroperl's pores is characterized by a lower melting temperature than bulk ezetimibe. The T_m of bulk ezetimibe is equal to 436 K, while after incorporation inside 30 nm pores, the melting temperature of ezetimibe was equal to 417 K. The size effect on melting point has been studied for a large variety of materials: from small molecules and metal particles up to polymers. It is worth noting that, if the pore size is known, it is possible to theoretically predict the value of melting temperature by using the Gibbs−Thomson equation:[38,39]

$$T_m(d) = T_m\left(\frac{1 - 4\sigma_{cl}}{d\Delta H_m \rho_c}\right) \quad (7)$$

where σ_{cl} is the surface energy (tension) of solid−liquid interface (for ezetimibe σ_{cl} = 0.0547 N/m[52]), T_m is the melting point of bulk material, $T_m(d)$ is the melting point of crystals within a constant pore diameter of size d, ΔH_m is the bulk enthalpy of fusion, and ρ_c is the density of the solid. The melting point value of the ezetimibe's small crystals that has been predicted by using presented above equation is equal to 425 K. The little discrepancy, which can be observed between the theoretically calculated and experimentally evaluated values of T_m, may be caused by pore size distribution of measured host systems.

As it has been mentioned, the crystallization tendency of examined systems has been also checked by using the XRD technique. In this experiment systems were store at T = 300 K for a long period of time. The X-ray diffraction pattern of ezetimibe incorporated into 30 nm pores, and stored for 5 months, exhibits sharp Bragg peaks indicating the presence of the crystalline phase of the drug (see Figure 9). On the other

DOI: 10.1021/acs.molpharmaceut.5b00903
Mol. Pharmaceutics 2016, 13, 1308−1316

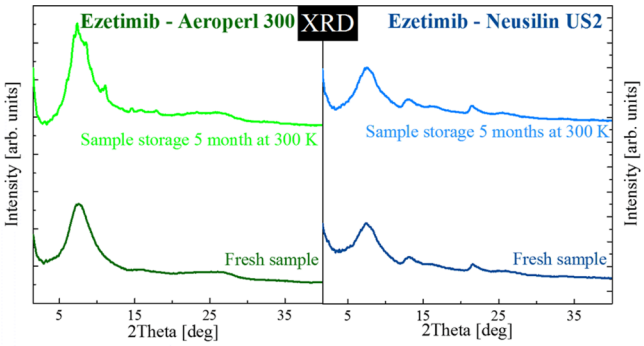

Figure 9. X-ray diffraction patterns for freshly prepared (lower XRD patterns) and stored (storage for 5 months at 300 K) samples of amorphous ezetimibe−Aeroperl 300 and ezetimibe−Neusilin US2.

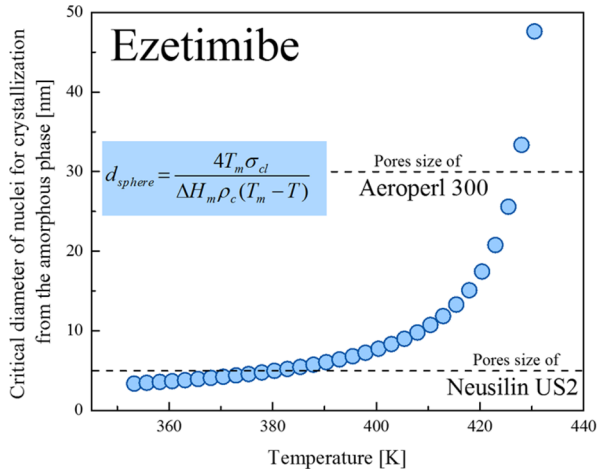

Figure 10. Calculated from eq 8, temperature dependence of critical diameter of nuclei for crystallization of ezetimibe drug from the amorphous phase.

hand, a broad amorphous halo, suggesting that there is no long-range three-dimentional molecular order, can be observed in the case of an ezetimibe−Neusilin US2 system stored for the same period of time.

Both DSC and XRD experiments show that the physical stability of amorphous ezetimibe may be significantly improved after incorporation of the drug into 5 nm pores. The reason for such behavior is probably 3-fold. First, the molecular dynamics of ezetimibe incorporated into pores of Neusilin is significantly slower in comparison with the molecular mobility of ezetimibe inside Aeroperl pores or the bulk drug. It is well-known that the system becomes more stable if its molecular dynamics slows down. Second, inside smaller pores the fraction of interfacial molecules is greater and, consequently, a larger part of ezetimibe molecules is immobilized. Third, the critical size of ezetimibe nuclei can be slightly bigger than Neusilin US2 pores size (>5 nm). Therefore, the sample would be unable to form the crystal in such small pores.

To verify whether the stability improvement of amorphous ezetimibe results from the use of suitably small pores, the critical size of nuclei d needed for ezetimibe crystal formation has been estimated. For this purpose, we used the following formula:

$$d = \frac{4T_m\sigma_{cl}}{\Delta H_m \rho_c (T_m - T)} \quad (8)$$

where σ_{cl} is the surface tension of solid liquid interface, T_m is the melting point of bulk material, ΔH_m is the bulk enthalpy of fusion, and ρ_c is the density of the solid.

As can be seen in the Figure 10, the critical diameter of ezetimibe's nuclei has almost the same size as pores of Neusilin US2. This result indicates that the pore size of the guest system can also have an impact on the enhancement of physical stability of ezetimibe in this host/guest system. Due to the Neusilin pore size being the same as or smaller than the critical size of the drug nuclei, ezetimibe may be not able to form the crystal. This property makes the examined system very interesting from a pharmaceutical point of view.

CONCLUSIONS

In this paper the guest/host systems of ezetimibe−Aeroperl 300 as well as ezetimibe−Neusilin US2 were investigated using X-ray diffraction, differential scanning calorimetry, and broad-band dielectric spectroscopy. The XRD experiment indicates that the drug loaded inside the 5 and 30 nm pores was indeed in the amorphous form. The decrease in intensity of the low angle diffraction peak after adding ezetimibe to the porous materials can be ascribed to the successful loading of the drug inside the pores. Thermal analysis of the examined systems shows that, with the pore size reduction, the glass transition temperature of the system is shifted to higher temperatures.

The influence of confinement on the molecular mobility of the ezetimibe drug in small pores was investigated over a broad frequency and temperature range using BDS. This experiment revealed the presence of two distinguishable phases of the loaded pharmaceutical. The first connected to the surface−liquid interface while the second is associated with the molecules of the inner pore volume (core molecules). Interestingly, during heating from the glassy state, the ezetimibe confined in 30 nm pores began to crystallize, while an absence of drug recrystallization was observed after filling the smaller (5 nm) pores. Long-term studies of physical stability have confirmed that ezetimibe incorporated into 5 nm pores is much more physically stable than inside 30 nm pores. During all of our measurements we did not observe any recrystallization of the ezetimibe−Neusilin US2 guest/host system. Consequently, our studies have shown that by using commercial porous systems with small pores (such as Neusilin US2) it is possible to stabilize amorphous drugs, which have a high tendency to crystallization in bulk systems. We found that the reason for the significant stabilization of ezetimibe incorporated into pores of Neusilin US2 can be 3-fold. First, after the incorporation of ezetimibe inside porous matrix the molecular dynamics of the drug significantly slows down. Second, inside small pores a lot of the drug's molecules are immobilized by the host system's surface layer. Third, the critical size of ezetimibe nuclei is slightly larger than the Neusilin US2 pore size. Therefore, the sample is unable to form the crystal in such small pores.

AUTHOR INFORMATION

Corresponding Author

*E-mail: jknapik@us.edu.pl.

Notes

The authors declare no competing financial interest.

DOI: 10.1021/acs.molpharmaceut.5b00903
Mol. Pharmaceutics 2016, 13, 1308−1316

■ ACKNOWLEDGMENTS

The authors J.K., Z.W., K.G. and M.P. are grateful for the financial support received within the Project No. 2015/16/W/NZ7/00404 (SYMFONIA 3) from the National Science Centre, Poland. The authors wishes to express their thanks to E. Mc Court, Queen's University of Belfast, for critical reading of the manuscript.

■ REFERENCES

(1) Li B., Luo X., Deng B., Wang J., McComb D. W., Shi Y., Gaensler K. M. L., Tan X., Dunn A. L., Kerlin B. A., Dong Y., An Orthogonal Array Optimization of Lipid-like Nanoparticles for mRNA Delivery in Vivo, *Nano Lett.* **2015**, *3*, DOI: 809910.1021/acs.nanolett.5b03528.

(2) Moreno, E.; Schwartz, J.; Larrea, E.; Conde, I.; Font, M.; Sanmartín, C.; Irache, J. M.; Espuelas, S. Assessment of β-lapachone loaded in lecithin-chitosan nanoparticles for the topical treatment of cutaneous leishmaniasis in L. major infected BALB/c mice. *Nanomedicine* **2015**, *11*, 2003−2012.

(3) Piao, Y.; Burns, A.; Kim, J.; Wiesner, U.; Hyeon, T. Designed Fabrication of Silica-Based Nanostructured Particle Systems for Nanomedicine Applications. *Adv. Funct. Mater.* **2008**, *18*, 3745−3758.

(4) Rocha, J.; Carlos, L. D.; Almeida Paz, F. A.; Ananias, D. Luminescent multifunctional lanthanides-based metal−organic Framework. *Chem. Soc. Rev.* **2011**, *40*, 926−940.

(5) Vallet-Regi, M.; Rámila, A.; del Real, R. P.; Pérez-Pariente, J. A New Property of MCM-41: Drug Delivery System. *Chem. Mater.* **2001**, *13*, 308−311.

(6) Wang, Y.; Zhao, Q.; Han, N.; Bai, L.; Li, J.; Liu, J.; Che, E.; Hu, L.; Zhang, Q.; Jiang, T.; Wang, S. Mesoporous silica nanoparticles in drug delivery and biomedical applications. *Nanomedicine* **2015**, *11*, 313−327.

(7) Semete, B.; Booysen, L.; Lemmer, Y.; Kalombo, L.; Katata, L.; Verschoor, J.; Swai, H. S. In vivo evaluation of the biodistribution and safety of PLGA nanoparticles as drug delivery systems. *Nanomedicine* **2010**, *6*, 662−671.

(8) Qu, F.; Zhu, G.; Huang, S.; Li, S.; Sun, J.; Zhang, D.; Qiu, S. Controlled release of Captopril by regulating the pore size and morphology of ordered mesoporous silica. *Microporous Mesoporous Mater.* **2006**, *92*, 1−9.

(9) Nunes, C. D.; Vaz, P. D.; Fernandes, A. C.; Ferreira, P.; Romao, C.; Jose, M.; Calhorda. Loading and delivery of sertraline using inorganic micro and mesoporous materials. *Eur. J. Pharm. Biopharm.* **2007**, *66*, 357−365.

(10) Vallet-Regi, M.; Balas, F.; Arcos, D. Mesoporous Materials for Drug Delivery. *Angew. Chem., Int. Ed.* **2007**, *46*, 7548−7558.

(11) Torchilin, V. P. Targeted Pharmaceutical Nanocarriers for Cancer Therapy and Imaging. *Nat. Rev. Drug Discovery* **2005**, *4*, 145−160.

(12) Nishio, K.; Kōga, J.; Yamaguchi, T.; Yonezawa, F. Molecular dynamics study on the stability of amorphous Ar inside a nanopore. *J. Non-Cryst. Solids* **2007**, *353*, 3550−3554.

(13) Zhang, P.; Forsgren, J.; Strømme, M. Stabilisation of amorphous ibuprofen in Upsalite, a mesoporous magnesium carbonate, as an approach to increasing the aqueous solubility of poorly soluble drugs. *Int. J. Pharm.* **2014**, *472*, 185−191.

(14) Qian, K. K.; Bogner, R. H. Application of Mesoporous Silicon Dioxide and Silicate in Oral Amorphous Drug Delivery Systems. *J. Pharm. Sci.* **2012**, *101*, 444−463.

(15) Klafter, J, Drake, J. M., 1989. *Molecular dynamics in restricted geometries*. 1st ed. Wiley, New York City, NY.

(16) Jackson, C. L.; McKenna, G. B. Vitrification and crystallization of organic liquids confined to nanoscale pores. *Chem. Mater.* **1996**, *8* (8), 2128−2137.

(17) Bhardwaj, S. P.; Suryanarayanan, R. Molecular mobility as an effective predictor of the physical stability of amorphous trehalose. *Mol. Pharmaceutics* **2012**, *9* (11), 3209−3217.

(18) Wojnarowska, Z.; Grzybowska, K.; Hawelek, L.; Dulski, M.; Wrzalik, R.; Gruszka, I.; Paluch, M.; Pienkowska, K.; Sawicki, W.; Bujak, P.; Paluch, K. J.; Tajber, L.; Markowski, J. Molecular Dynamics, Physical Stability and Solubility Advantage from Amorphous Indapamide Drug. *Mol. Pharmaceutics* **2013**, *10* (10), 3612−3627.

(19) Kolodziejczyk, K.; Paluch, M.; Grzybowska, K.; Grzybowski, A.; Wojnarowska, Z.; Hawelek, L.; Ziolo, J. D. Relaxation Dynamics and Crystallization Study of Sildenafil in the Liquid and Glassy States. *Mol. Pharmaceutics* **2013**, *10* (6), 2270−2282.

(20) Kothari, K.; Ragoonanan, V.; Suryanarayanan, R. Influence of Molecular Mobility on the Physical Stability of Amorphous Pharmaceuticals in the Supercooled and Glassy States. *Mol. Pharmaceutics* **2014**, *11*, 3048−3055.

(21) Wojnarowska, Z.; Grzybowska, K.; Adrjanowicz, K.; Kaminski, K.; Paluch, M.; Hawelek, L.; Wrzalik, R.; Dulski, M.; Sawicki, W.; Mazgalski, J.; Tukalska, A.; Bieg, T. Study of the Amorphous Glibenclamide Drug: Analysis of the Molecular Dynamics of Quenched and Cryomilled Material. *Mol. Pharmaceutics* **2010**, *7*, 1692−1707.

(22) Jia, L. Nanoparticle formulation increases oral bioavailability of poorly soluble drugs: approaches, experimental evidences and theory. *Curr. Nanosci.* **2005**, *1*, 237−243.

(23) Bhugra, C.; Pikal, M. Role of thermodynamic, molecular, and kinetic factor in crystallization from amorphous state. *J. Pharm. Sci.* **2008**, *97*, 1329−1349.

(24) Yoshioka, M.; Hancock, B. C.; Zografi, G. Crystallization of indomethacin from the amorphous state below and above its glass transition temperature. *J. Pharm. Sci.* **1994**, *83*, 1700.

(25) Knapik, J.; Wojnarowska, Z.; Grzybowska, K.; Hawelek, L.; Sawicki, W.; Wlodarski, K.; Markowski, J.; Paluch, M. Physical Stability of the Amorphous Anticholesterol Agent (Ezetimibe): The Role of Molecular Mobility. *Mol. Pharmaceutics* **2014**, *11*, 4280−4290.

(26) Knapik, J.; Wojnarowska, Z.; Grzybowska, K.; Jurkiewicz, K.; Tajber, L.; Paluch, M. Molecular Dynamics and Physical Stability of Coamorphous Ezetimib and Indapamide Mixtures. *Mol. Pharmaceutics* **2015**, *12*, 3610−9.

(27) Yang, X.; Ong, T. C.; Michaelis, V. K.; Heng, S.; Huang, J.; Griffin, R. G.; Myerson, A. S. Formation of organic molecular nanocrystals under rigid confinement with analysis by solid state NMR. *CrystEngComm* **2014**, *16*, 9345−9352.

(28) Gumaste, S. G.; Dalrymple, D. M.; Serajuddin, T. M. Development of Solid SEDDS, V: Compaction and Drug Release Properties of Tablets Prepared by Adsorbing Lipid-Based Formulations onto Neusilin® US2. *Pharm. Res.* **2013**, *30*, 3186−3199.

(29) Bras, A. R.; Fonseca, I. M.; Dionísio, M.; Schonhals, A.; Affouard, F.; Correia, N. T. Influence of Nanoscale Confinement on the Molecular Mobility of Ibuprofen. *J. Phys. Chem. C* **2014**, *118*, 13857−13868.

(30) Fuji Chemical Industry Co., LTD.. Neusilin® The Extraordinary Excipient for Oral Dosage Forms. *Technical Newsletter* **2007**, *12*, 1−4, http://www.neusilin.com/multicms/neusilin/pdf/news/29/2_neusilin_newsletter_nov07.pdf.

(31) Evionik Industries AG, Aeroperl 300, *product information* 2011, *11*, 1−2 (http://kanchanrasayan.com/pdf/PI%20AEROPERL%20300-Pharma.pdf).

(32) Kazakevich, I. Merck & Co., Porous Incoganic Excipients as Carriers for Amorphous Solid Dispersions. *AAPS 2014 San Diego* **2014**, *12*, 1−27.

(33) Krupa, A.; Szlek, J.; Jany, B. R.; Jachowicz, R. Preformulation Studies on Solid Self-Emulsifying Systems in Powder Form Containing Magnesium Aluminometasilicate as Porous Carrier. *AAPS PharmSciTech* **2015**, *16* (3), 623−635.

(34) Meer Tarique Ali Sadique A., Release modification designs for poorly water soluble drugs, Chapter II: Solubility Modulation of Bicalutamide Using Porous Silica, PhD thesis - Department of Pharmaceutical Sciences and Technology Institute of Chemical Technology, Mumbai Maharashtra, India, 2015. (http://shodhganga.inflibnet.ac.in/bitstream/10603/42012/11/11_chapter%202.pdf).

(35) Son, W.-J.; Choi, J.-S.; Ahn, W.-S. Adsorptive removal of carbon dioxide using olyethyleneimine-loaded mesoporous silica materials. *Microporous Mesoporous Mater.* **2008**, *113*, 31−40.

DOI: 10.1021/acs.molpharmaceut.5b00903
Mol. Pharmaceutics 2016, 13, 1308−1316

(36) Lavenn, C.; Albrieux, F.; Tuel, A.; Demessence, A. Synthesis, characterization and optical properties of an amino-functionalized gold thiolate cluster: Au10(SPh-pNH2)10. *J. Colloid Interface Sci.* **2014**, *418*, 234−239.
(37) Trofymluk, O.; Levchenko, A. A.; Navrotsky, A. Interfacial effects on vitrification of confined glass-forming liquids. *J. Chem. Phys.* **2005**, *123*, 194509.
(38) Alcoutlabi, M.; McKenna, G. B. Effects of confinement on material behaviour at the nanometre size scale. *J. Phys.: Condens. Matter* **2005**, *17*, R461−R524.
(39) Jackson, C. L.; McKenna, G. B. The melting behavior of organic materials confined in porous solids. *J. Chem. Phys.* **1990**, *93* (12), 9002−9011.
(40) Fragiadakis, D.; Dou, S.; Colby, R. H.; Runt, J. Molecular mobility and Li+ conduction in polyester copolymer ionomers based on poly(ethylene oxide). *J. Chem. Phys.* **2009**, *130*, 064907.
(41) Fragiadakis, D.; Dou, S.; Colby, R. H.; Runt, J. Molecular mobility, ion mobility, and mobile ion concentration in poly (ethylene oxide)-based polyurethane ionomers. *Macromolecules* **2008**, *41*, 5723−5728.
(42) Mel'nichenko, Y. B.; Schüller, J.; Richert, R.; Ewen, B.; Loong, C. K. Dynamics of dydrogen-bonded liquids confined to mesopores: A dielectric and neutron spectroscopy study. *J. Chem. Phys.* **1995**, *103* (6), 2016−2024.
(43) Schuller, J.; Richert, R.; Fischer, E. W. Dielectric relaxation of liquids at the surface of a porous glass. *Phys. Rev. B: Condens. Matter Mater. Phys.* **1995**, *52* (21), 15232−15238.
(44) Havriliak, S.; Negami, S. A complex plane representation of dielectric and mechanical relaxation processes in some polymers. *Polymer* **1967**, *8* (4), 161.
(45) Suzuki, Y.; Duran, H.; Steinhart, M.; Butt, H. J.; Floudas, G. Homogeneous crystallization and local dynamics of poly(ethylene oxide) (PEO) confined to nanoporous alumina. *Soft Matter* **2013**, *9*, 2621.
(46) Suzuki, Y.; Duran, H.; Akram, W.; Steinhart, M.; Floudas, G.; Butt, H. J. Multiple nucleation events and local dynamics of poly- (3-caprolactone) (PCL) confined to nanoporous alumina. *Soft Matter* **2013**, *9*, 9189.
(47) Suzuki, Y.; Steinhart, M.; Graf, R.; Butt, H. J.; Floudas, G. Dynamics of Ice/Water Confined in Nanoporous Alumina. *J. Phys. Chem. B* **2015**, *119* (46), 14814−14820.
(48) Vogel, H. Das Temperaturabhangigkeitgesetz der Viskosität von Flüssigkeiten. *J. Phys. Z.* **1921**, *22*, 645−646.
(49) Fulcher, G. S. Analysis of Recent Measurements of the Viscosity of Glasses. *J. Am. Ceram. Soc.* **1925**, *8*, 339−355.
(50) Tammann, G.; Hesse, W. Die Abhängigkeit der Viscosität von der Temperatur bie unterkühlten Flüssigkeiten. *Z. Anorg. Allg. Chem.* **1926**, *156*, 245−257.
(51) Bras, A. R.; Merino, E. G.; Neves, P. D.; Fonseca, I. M.; Dionísio, M.; Schonhals, A.; Correia, N. T. Amorphous Ibuprofen Confined in Nanostructured Silica Materials: A Dynamical Approach. *J. Phys. Chem. C* **2011**, *115*, 4616−4623.
(52) Patel, K. M.; Shah, D. H.; Patel, J. B.; Patel, J. S.; Garg, C. S.; Sen, D. J. Chemistry of four membered heterocylic ezetimibe as lipid lowering agent. *Int. J. Drug Dev. Res.* **2011**, *2* (3), 104−110.

DOI: 10.1021/acs.molpharmaceut.5b00903
Mol. Pharmaceutics 2016, 13, 1308−1316

Dr Żaneta Wojnarowska
Instytut Fizyki
Uniwersytet Śląski
Zakład Biofizyki i Fizyki Molekularnej
ul. 75 Pulku Piechoty 1A, 41-500 Chorzów

Chorzów, 02.05.2016r.

OŚWIADCZENIE

Oświadczam, że w pracy:

Knapik J., Wojnarowska Z., Grzybowska K., Jurkiewicz K., Stankiewicz A., Paluch M. *Stabilization of the Amorphous Ezetimib Drug by Confining Its Dimension.* Mol. Pharmaceuticals 2016, 13, 1308–1316

mój udział polegał na udziale w dyskusji otrzymanych wyników.

Z. Wojnarowska
.....

Podpis

Dr Katarzyna Grzybowska
Instytut Fizyki
Uniwersytet Śląski
Zakład Biofizyki i Fizyki Molekularnej
ul. 75 Pułku Piechoty 1A, 41-500 Chorzów

Chorzów, 02.05.2016r.

OŚWIADCZENIE

Oświadczam, że w pracy:

Knapik J., Wojnarowska Z., Grzybowska K., Jurkiewicz K., Stankiewicz A., Paluch M. *Stabilization of the Amorphous Ezetimib Drug by Confining Its Dimension.* Mol. Pharmaceuticals 2016, 13, 1308–1316

mój udział polegał na weryfikacji przeprowadzonych analiz, dyskusji otrzymanych wyników oraz korekcji tekstu manuskrytptu.

Katarzyna Grzybowska
.....

Podpis

mgr Karolina Jurkiewicz
Instytut Fizyki
Uniwersytet Śląski
Zakład Biofizyki i Fizyki Molekularnej
ul. 75 Pułku Piechoty 1A, 41-500 Chorzów

Chorzów, 02.05.2016r.

OŚWIADCZENIE

Oświadczam, że w pracy:

Knapik J., Wojnarowska Z., Grzybowska K., Jurkiewicz K., Stankiewicz A., Paluch M. *Stabilization of the Amorphous Ezetimib Drug by Confining Its Dimension.* Mol. Pharmaceuticals 2016, 13, 1308–1316

mój udział polegał na wykonaniu pomiarów XRD.

Karolina Jurkiewicz

Podpis

Prof. zw. dr hab. Marian Paluch
Instytut Fizyki
Uniwersytet Śląski
Zakład Biofizyki i Fizyki Molekularnej
ul. 75 Pułku Piechoty 1A, 41-500 Chorzów

Chorzów, 02.05.2016r.

OŚWIADCZENIE

Oświadczam, że w pracy:

Knapik J., Wojnarowska Z., Grzybowska K., Jurkiewicz K., Stankiewicz A., Paluch M. *Stabilization of the Amorphous Ezetimib Drug by Confining Its Dimension.* Mol. Pharmaceuticals 2016, 13, 1308–1316

mój udział polegał na uczestnictwie w dyskusji wyników oraz korekcji manuskryptu.

.....

Podpis

4 PODSUMOWANIE

Niniejszą rozprawę doktorską stanowi seria trzech artykułów naukowych dotyczących badań nad fizyczną stabilnością amorficznej formy ezetimibu. Punktem wyjścia dla przeprowadzonych eksperymentów była chęć polepszenia rozpuszczalności krystalicznego ezetimibu w wodzie poprzez przekształcenie go do formy amorficznej. Eksperymentalnie udowodniono, że w warunkach standardowego przechowania leków, to znaczy w temperaturze równej 298 K, amorficzny ezetimib zaczyna re-krystalizować już po dwóch tygodniach od momentu witryfikacji. Ponadto w pracy pokazano, że czas fizycznej stabilności badanego leku przeciw cholestrolowego można przewidzieć przy pomocy metody polegającej na konstrukcji tzw. master plotów. Oznacza to, że skala czasowa relaksacji strukturalnej ezetimibu koreluje się z jego fizyczną stabilnością. Ze względu na fakt, że ezetimib w formie amorficznej nie spełnia minimalnego czasu stabilności wymaganego od farmaceutyków przed wprowadzeniem ich na rynek, dużą uwagę poświęcono poprawie jego fizycznej stabilności.

Wykazano, iż mieszając ezetimib z polimerem o nazwie Soluplus można spowolnić dynamikę molekularną badanego leku, co w konsekwencji hamuje jego re-krystalizację. Przewidziano, że kompozycja zawierająca w swoim składnie ezetimib oraz masowo 20% wspomnianego polimeru powinna być fizycznie stabilna przez minimum 4 lata od momentu amorfizacji, jeśli jest przechowywana w temperaturze 298 K. Badania rozpuszczalności wykazały, że testowana amorficzna mieszanina ezetimibu i Soluplus'u dodatkowo charakteryzuje się ponad sześciokrotnie lepszą rozpuszczalnością w wodnie w porównaniu do obecnie dostępnej na rynku krystalicznej formy ezetimibu.

Pokazano, że również substancja o znacznie mniejszej od polimeru masie molowej, jaką jest inny lek o nazwie indapamid, jest w stanie efektywnie stabilizować ezetimib. Badania przeprowadzone przy pomocy skaningowej kalorymetrii różnicowej, szerokopasmowej spektroskopii dielektrycznej oraz dyfrakcji rentgenowskiej dowiodły, że imponujący efekt stabilizacji ezetimibu jest widoczny przy zastosowaniu nawet niewielkiej ilości indapamidu (8.8%). Pomiary FTIR oraz DSC potwierdziły, że molekuły ezetimibu i indapamidu w stanie amorficznym nie oddziałują w specyficzny sposób ze sobą (nie tworzą się wiązania wodorowe pomiędzy wspomnianymi molekułami). Oznacza to, że w badanej podwójnie amorficznej mieszaninie dwóch leków efekt antyplastufikujacy wywierany przez indapamid jest główną przyczyną odpowiedzialną za stabilizację ezetimibu.

Przeprowadzone eksperymenty dowiodły również, że amorficzna forma ezetimibu może zostać ustabilizowana przy pomocy komercyjnie stosowanego w przemyśle farmaceutycznym

porowatego materiału o nazwie Neusilin US2. Jak wykazano, wspomniany stabilizacyjny efekt związany jest bezpośrednio z zastosowaniem materiału o odpowiednio małych porach. Materiał posiadający pory o wielkości podobnej do krytycznej średnicy zarodka krystalizacji badanego leku przeciw cholesterolowego jest w stanie całkowicie zahamować proces re-krystalizacji, ponieważ ograniczony przestrzennie do roziarów nano lek nie jest w stanie wytworzyć zarodka krystalizacji. Eksperymentalnie potwierdzono, że podczas przechowywania ezetimibu wypełniającego nanopory o promieniu większym od krytycznego promienienia nukleacji ezetimibu, badany amorficzny lek bez najmniejszego problemu powraca do swojej krystalicznej formy.

5 BIBLIOGRAFIA

[1] Chmiel-Polec Z.; Cybulska I. Smoking and other risk factors of cardiovascular disease, connected with arteriosclerosis among youth. Przegl Lek 2008, 65, 437–45.

[2] Hokanson, J. E.; Austin, M. A. Plasma Triglyceride Level is a Risk Factor for Cardiovascular Disease Independent of High-Density Lipoprotein Cholesterol Level: A Metaanalysis of Population-Based Prospective Studies. J. Cardiovasc. Risk 1996, 3, 213−219.

[3] Gordon, D. J.; Probstfield, J. L.; Garrison, R. J.; Neaton, J. D.; Castelli, W. P.; Knoke, J. D.; Jacobs, D. R., Jr; Bangdiwala, S.; Tyroler, H. A. High-density lipoprotein cholesterol and cardiovascular disease. Four prospective American studies. Circulation 1989, 79, 8−15.

[4] Garcia-Calvoa, M.; Lisnocka, J. M.; Bulla, H. G.; Hawesc, B. E.; Burnettc, D. A.; Braunc, M. P.; Cronac, J. H.; Davis, H. R.; Deanc, D. C.; Detmersc, P. A.; Grazianoc, M. P.; Hughesa, M.; MacIntyrec, D. E.; Ogawac, A.; O'Neillc, K. O.; Iyerc, S. P. N.; Shevellc, D. E.; Smithc, M. M.; Tangc, Y. S.; Makarewiczc, A. M.; Ujjainwallac, F.; Altmannc, S. W.; Chapmanc, K. T.; Thornberrya, N. A. The target of ezetimibe is Niemann−Pick C1-Like 1 (NPC1L1). Proc. Natl. Acad. Sci. U.S.A. 2004, 102, 8132−8137.

[5] Taylor, A. J.; Villines, T. C.; Stanek, E. J.; Devine, P. J.; Griffen, L.; Miller, M.; Weissman, N. J.; Turco, M. Extended-release niacin or ezetimibe and carotid intima-media thickness. N. Engl J. Med. 2009, 361 (22), 2113−2122.

[6] Drugbank Version 4.5. *DrugBank: Ezetimibe* http://www.drugbank.ca/drugs/DB00973, 03.05.2016r.

[7] Patel, K. M.; Shah, D. H.; Patel, J. B.; Patel, J. S.; Garg, C. S.; Sen, D. J. Chemistry of four membered heterocylic ezetimibe as lipid lowering agent. Int. J. Drug Dev. Res. 2011, 2 (3), 104−110.

[8] Hancock, B. C.; Parks, M. What is the true solubility advantage for amorphous pharmaceuticals? Pharm. Res. 2000, 17, 397.

[9] Craig, D. Q. M.; Royall, P. G.; Kett, V.; Hopton, M. The relevance of the amorphous state to pharmaceutical dosage forms: glassy drugs and freeze dried systems. Int. J. Pharm. 1999, 179, 179−207.

[10] Williams, H. D.; Trevaskis, N. L.; Charman, S. A.; Shanker, R. M.; Charman, W. N.; Pouton, C. W.; Porter, C. J. H. Strategies to Address Low Drug Solubility in Discovery and Development. Pharm. Rev. 2013, 65, 315−499.

[11] Kaminski, K.; Adrjanowicz, K.; Wojnarowska, Z.; Grzybowska, K.; Hawelek, L.; Paluch, M.; Zakowiecki, D.; Mazgalski, J. Molecular dynamics of the cryomilled base and hydrochloride ziprasidones by means of dielectric spectroscopy. J. Pharm. Sci. 2011, 10, 22479.
[12] Zallen R., Fizyka ciał amorficznych, PWN, Warszawa (1994)
[13] Martino P.; Palmieri G. F.; Martelli S. Chem. Pharm. Bull. 2008, 48, 8, 1105–1108
[14] Yoshioka, M.; Hancock, B. C.; Zografi, G. Crystallization of indomethacin from the amorphous state below and above its glass transition temperature. J. Pharm. Sci. 1994, 83, 1700.
[15] Saleki-Gerhardt, A.; Zografi, G. Nonisothermal and Isothermal Crystallization of Sucrose from the Amorphous State. Pharm. Res. 1994, 11, 1166.
[16] Zhou, D.; Geoff, G.; Zhang, Z.; Law, D.; Grant, D.; Schmitt, E. A. Thermodynamics, molecular mobility and crystallization kinetics of amorphous griseofulvin. Mol. Pharmaceutics 2008, 5, 927.
[17] Bhugra, C.; Pikal, M. Role of thermodynamic, molecular, and kinetic factor in crystallization from amorphous state. J. Pharm. Sci. 2008, 97, 1329−1349.
[18] Priemel, P. A.; Laitinen, R.; Barthold, S.; Grohganz, H.; Lehto, V.-P.; Rades, T.; Strachan, C. J. Inhibition of surface crystallisation of amorphous indomethacin particles in physical drug−polymer mixtures. Int. J. Pharm. 2013, 456, 301−306.
[19]Bhugra, C.; Pikal, M. J. Role of thermodynamic, molecular, and kinetic factors in crystallization from the amorphous state. J. Pharm. Sci. 2008, 97, 1329−1349.
[20] Crowley, K.; Zografi, G. Cryogenic grinding of indomethacin polymorphs and solvates: assessment of amorphous phase formation and amorphous phase physical stability. J. Pharm. Sci. 2002, 91, 492.
[21] Wojnarowska, Z.; Grzybowska, K.; Adrjanowicz, K.; Kaminski, K.; Paluch, M.; Hawelek, L.; Wrzalik, R.; Dulski, M.; Sawicki, W.; Mazgalski, J.; Tukalska, A.; Bieg, T. Study of the Amorphous Glibenclamide Drug: Analysis of the Molecular Dynamics of Quenched and Cryomilled Material. Mol. Pharmaceutics 2010, 7, 1692−1707.
[22] Wojnarowska, Z.; Wlodarczyk, P.; Kaminski, K.; Grzybowska, K.; Hawelek, L.; Paluch, M. On the Kinetics of Tautomerism In Drugs-New Application of Broadband Dielectric Spectroscopy. J. Chem. Phys. 2010, 133, 094507.
[23] Hancock, B. C.; Shamblin, S. L.; Zografi, G. Molecular mobility of amorphous pharmaceutical solids below their glass transition temperatures. Pharm. Res. 1995, 12, 799.
[24] Yoshioka, S.; Aso, Y. Correlations between molecular mobility and chemical stability during storage of amorphous pharmaceuticals. J. Pharm. Sci. 1007, 96, 960.

[25] Shamblin, S. L.; Tang, X.; Chang, L.; Hancock, B. C.; Pikal, M. J. Characterization of the time scales of molecular motion in pharmaceutically important glasses. J. Phys. Chem. B 1999, 103, 4113−4121.

[26] Van Eerdenbrugh, B.; Taylor, L. S. Small Scale Screening To Determine the Ability of Different Polymers To Inhibit Drug Crystallization upon Rapid Solvent Evaporation. Mol. Pharmaceutics 2010, 7 (4), 1328−1337.

[27] Taylor, T. S.; Zografi, G. Pharm. Res. 1997, 14 (12), 1691−1698.

[28] Miyazaki, T.; Yoshioka, S.; Aso, Y. Physical Stability of Amorphous Acetanilide Derivatives Improved by Polymer Excipients. Chem. Pharm. Bull. 2006, 54 (8), 1207−1210.

[29] Matsumoto, T.; Zografi, G. Physical Properties of Solid Molecular Dispersions of Indomethacin with Poly(Vinylpyrrolidone) and Poly-(Vinylpyrrolidone-Co-Vinyl-Acetate) in Relation to Indomethacin Crystallization. Pharm. Res. 1999, 16 (11), 1722−1728.

[30] Serajuddin, A. T. Solid dispersion of poorly water-soluble drugs: early promises, subsequent problems, and recent breakthroughs. J. Pharm. Sci. 1999, 88 (10), 1058−66.

[31] Kothari, K.; Ragoonanan, V.; Suryanarayanan, R. The Role of Drug−Polymer Hydrogen Bonding Interactions on the Molecular Mobility and Physical Stability of Nifedipine Solid Dispersions. Mol. Pharmaceutics 2015, 12, 162−170.

[32] Gupta, P.; Thilagavathi, R.; Chakraborti, A. K.; Bansal, A. K. Role of Molecular Interaction in Stability of Celecoxib-PVP Amorphous Systems. Mol. Pharmaceutics 2005, 2 (5), 384−391.

[33] Laitinen, R.; Lobmann, K.; Strachan, C. J.; Grohganz, H.; Rades, T. Emerging trends in the stabilization of amorphous drugs. Int. J. Pharm. 2013, 453, 65−79.

[34] Grzybowska, K.; Paluch, M.; Wlodarczyk, P.; Grzybowski, A.; Kaminski, K.; Hawelek, L.; Zakowiecki, D.; Kasprzycka, A.; Jankowska - Sumara, I. Enhancement of amorphous celecoxib stability by mixing it
with octaacetylmaltose: the molecular dynamics study. Mol. Pharmaceutics 2012, 9 (4), 894−904.

[35] Löbmann, K.; Strachan, C.; Grohganz, H.; Rades, T.; Korhonen, O.; Laitinen, R. Co-amorphous simvastatin and glipizide combinations show improved physical stability without evidence of intermolecular interactions. Eur. J. Pharm. Biopharm. 2012, 81 (1), 159−69.

[36] Chieng, N.; Aaltonen, J.; Saville, D.; Rades, T. Physical characterization and stability of amorphous indomethacin and ranitidine hydrochloride binary systems prepared by mechanical activation. Eur. J. Pharm. Biopharm. 2009, 71 (1), 47−54.

[37] Kaminska, E.; Adrjanowicz, K.; Tarnacka, M.; Kolodziejczyk, K.; Dulski, M.; Mapesa, E. U.; Zakowiecki, D.; Hawelek, L.; Kaczmarczyk-Sedlak, I.; Kaminski, K. Impact of inter- and

intramolecular interactions on the physical stability of indomethacin dispersed in acetylated saccharides. Mol. Pharmaceutics 2014, 11 (8), 2935−2947.

[38] Lobmann, K.; Laitinen, R.; Grohganz, H.; Gordon, C.; Strachan, C.; Rades, T. Coamorphous Drug Systems: Enhanced Physical Stability and Dissolution Rate of Indomethacin and Naproxen. Mol. Pharmaceutics 2011, 8, 1919−1928.

[39] Nishio, K.; Kōga, J.; Yamaguchi, T.; Yonezawa, F. Molecular dynamics study on the stability of amorphous Ar inside a nanopore. J. Non-Cryst. Solids 2007, 353, 3550−3554.

[40] Zhang, P.; Forsgren, J.; Strømme, M. Stabilisation of amorphous ibuprofen in Upsalite, a mesoporous magnesium carbonate, as an approach to increasing the aqueous solubility of poorly soluble drugs.
Int. J. Pharm. 2014, 472, 185−191.

[41] Jackson, C. L.; McKenna, G. B. Vitrification and crystallization of organic liquids confined to nanoscale pores. Chem. Mater. 1996, 8 (8), 2128−2137.

[42] Qian, K. K.; Bogner, R. H. Application of Mesoporous Silicon Dioxide and Silicate in Oral Amorphous Drug Delivery Systems. J. Pharm. Sci. 2012, 101, 444−463.

[43] Klafter, J, Drake, J. M., 1989. Molecular dynamics in restricted geometries. 1st ed. Wiley, New York City, NY.

[44] Kolodziejczyk, K.; Paluch, M.; Grzybowska, K.; Grzybowski, A.; Wojnarowska, Z.; Hawelek, L.; Ziolo, J. D. Relaxation Dynamics and Crystallization Study of Sildenafil in the Liquid and Glassy States. Mol. Pharmaceutics 2013, 10 (6), 2270−2282.

[45] Hodge, I. M. Effects of annealing and prior history on enthalpy relaxation in glassy polymers. 6. Adam−Gibbs formulation of nonlinearity. Macromolecules 1987, 20, 2897.